



**TÉCNICO**  
LISBOA

**Thermal and Thermal-Mechanical Analysis  
of Thermo-Active Pile Foundations**

**Rui Manuel Freitas Assunção**

Thesis to obtain the Master of Science Degree in  
**Civil Engineering**

Supervisor: Prof. Peter John Bourne-Webb

**Examination Committee**

Chairperson: Prof. Jaime Alberto dos Santos

Supervisor: Prof. Peter John Bourne-Webb

Member of Committee: Prof. Teresa Maria Bodas de Araújo Freitas

**March 2014**



# Abstract

Thermo-active foundations make use of shallow geothermal energy to heat or cool buildings. By making use of this green and renewable energy form, this technology can significantly reduce building energy and maintenance costs in the long term and reduce carbon dioxide emissions. However, a complete understanding of the thermal-mechanical behaviour of such foundations has not yet been achieved which has been a major obstacle to the uptake and the industrial development of this technology. A thermal and thermal-mechanical numerical study of a thermal active pile was performed in this thesis using the finite element software Abaqus. The thermal analysis focused on some of the modelling aspects of the problem such as the simulation of the heating of the pile and definition of the ground surface temperature. The thermal-mechanical analysis studied the effect, in terms of thermally induced stresses in the pile, of the relationship between soil and concrete coefficients of thermal expansion, of the ground surface temperature and of the pile length to diameter ratio. The relationship between soil and concrete coefficient of thermal expansion coefficients was found to have a key role in the observed behaviour of the pile affecting both the direction (compression/tension) and the magnitude of the developed thermally induced stresses in the pile. The ground surface temperature showed an important effect when the soil was more thermally expansive than concrete, leading to considerable further stress changes in the pile. An increase in the pile length to diameter ratio also led to an increase of the thermally induced stresses in the pile.

## Keywords

Foundation pile; thermal-mechanical; geothermal energy; finite elements.



# Resumo

As fundações termoativas usam energia geotérmica superficial para aquecer e arrefecer edifícios. Através do uso desta energia renovável e amiga do ambiente, esta tecnologia permite reduzir significativamente os custos de aquecimento/arrefecimento de um edifício a longo prazo e as suas emissões de dióxido de carbono. No entanto, um entendimento completo do comportamento termomecânico destas fundações ainda não foi alcançado, o que tem sido um dos maiores obstáculos ao desenvolvimento industrial desta tecnologia. Um estudo numérico térmico e termomecânico de uma estaca termoativa foi realizado nesta tese através do uso do software de elementos finitos Abaqus. A análise térmica focou-se em alguns aspetos de modelação do problema como a simulação do aquecimento da estaca termoativa e a correta definição da temperatura da superfície do solo. A análise termomecânica estudou o efeito, em termos de esforços induzidos termicamente na estaca, da relação entre os coeficientes de expansão térmica do solo e do betão, da temperatura da superfície do solo e da relação entre o diâmetro e o comprimento da estaca. Os resultados mostraram que a relação entre o coeficiente de expansão térmica do solo e do betão desempenha um papel fundamental no comportamento da estaca, afetando tanto a direção como a magnitude dos esforços termicamente induzidos. Quando o solo tem maior coeficiente de expansão térmica que o betão, a temperatura da superfície do solo exibiu um efeito importante na estaca, levando a consideráveis alterações de esforços na mesma. Um aumento da relação comprimento/diâmetro da estaca conduziu a um aumento dos esforços termicamente induzidos na mesma.

## Palavras-chave

Estaca; termomecânica; energia geotérmica; elementos finitos.



# Table of Contents

Abstract .....	iii
Resumo .....	iv
Table of Contents .....	vii
List of Figures .....	ix
List of Tables .....	xii
List of Acronyms .....	xiii
List of Symbols .....	xiv
1 Introduction .....	1
1.1 Overview.....	2
1.2 Motivation and Contents .....	3
1.3 Structure of the Thesis.....	4
2 Geothermal Energy and Heat Pump Systems .....	5
2.1 Shallow Geothermal Energy and its Use.....	6
2.2 Ground Source Heat Pump Systems .....	7
2.2.1 Introduction .....	7
2.2.2 Efficiency of the GSHP Systems .....	9
3 Heat Transfer Mechanisms.....	11
3.1 Heat Transfer Mechanisms.....	12
3.1.1 Conduction.....	12
3.1.2 Convection.....	13
3.1.3 Radiation.....	13
3.2 Heat Transfer in Soils .....	13
3.2.1 Thermal Conduction in Soils and Concrete .....	14
3.2.2 Thermal Expansion in Soils and Concrete .....	16
3.3 Heat Transfer in Thermo-Active Piles.....	17
4 The Effect of Heating and Cooling of a Pile .....	19
4.1 Thermally Induced Deformation – General Principles .....	20
4.1.1 Free Body Response (No Restraint) .....	20

4.1.2	Perfectly Restrained Body .....	21
4.1.3	Partially Restrained Body .....	21
4.2	Experimental Observations of the Effect of Heating and Cooling a Pile.....	23
4.2.1	École Polytechnique Fédérale de Lausanne .....	23
4.2.2	Lambeth College, London .....	27
4.3	Numerical Analysis of the Effect of Heating and Cooling a Pile .....	29
4.3.1	Bodas Freitas et al., 2013 and Cruz Silva, 2012 .....	29
4.3.2	Di Donna et al., 2013.....	31
4.3.3	Suryatriyastuti et al., 2013 .....	34
5	Thermal Analysis .....	39
5.1	Introduction.....	40
5.2	Thermal Load through the Pile.....	40
5.2.1	Axisymmetric Thermal Model .....	41
5.2.2	2D Thermal Model .....	47
5.3	Thermal Loss through the Ground-Floor Slab and Ground Surface Temperature 51	
5.3.1	Numerical Model Implementation .....	51
5.3.2	Analysis Methodologies and Objectives .....	53
5.3.3	Results and Discussion .....	53
6	Thermal-Mechanical Analyses .....	57
6.1	Introduction.....	58
6.2	Numerical Model Implementation.....	58
6.2.1	Materials and material behaviour .....	58
6.2.2	Geometry, Mesh, Boundary Conditions and Initial Conditions .....	59
6.2.3	Pile-Soil Interface Behaviour .....	61
6.2.4	Model Validation .....	62
6.3	Analysis Methodology and Objectives.....	64
6.4	Results and Discussion.....	66
6.4.1	Baseline Analysis.....	66
6.4.2	Parameter Study.....	69
7	Conclusions .....	81
7.1	Conclusions and Results Summary .....	82
7.2	Future Developments.....	83
	References .....	85



# List of Figures

Figure 1-1. Number of energy piles installed in Austria between 1984 and 2004 (Brandl, 2006).	2
Figure 2-1. Ground temperature at depth in Europe and tropics (Brandl, 2006).	6
Figure 2-2. Various types of ground heat exchangers (Amis, 2011).	7
Figure 2-3. Scheme of a ground source heat pump system with energy piles as ground heat exchangers (Brandl, 2006).	8
Figure 2-4. Heat pump and its interactions with the primary and secondary circuits (Bourne-Webb, 2014).	8
Figure 3-1. Predominant heat transfer mechanisms by grain size and degree of saturation (Loveridge 2012, redrawn from Farouki, 1986).	14
Figure 3-2. Soil thermal conductivity values as a function of moisture content (ASHRAE Fundamentals, 2009).	15
Figure 3-3. Thermal volumetric strain of Kaolin clay during drained heating (Cekerevac & Laloui (2004)).	17
Figure 3-4. Thermo-active pile heat transfer: a) plan of thermal pile components; b) temperature differences (Powrie & Loveridge, 2013).	18
Figure 4-1. Thermal response of a non-restrained pile (free body): a) heating; b) cooling (Bourne-Webb, et al., 2013).	20
Figure 4-2. Thermal response of a perfectly restrained pile: a) heating; b) cooling (Bourne-Webb, et al., 2013).	21
Figure 4-3. Thermal response of a pile laterally restrained: (a) heating; (b) cooling (Bourne-Webb, et al., 2013).	22
Figure 4-4. Thermal response of a pile laterally and end restrained: (a) heating; (b) cooling (Bourne-Webb, et al., 2013).	22
Figure 4-5. Combined mechanical and thermal load effects on a partially restrained pile. Dash-dotted lines represent the effect of stronger thermal load or pile restraint. (a) Mechanical load only; (b) combined mechanical load and heating; (c) combined mechanical load and cooling; (Bourne-Webb, et al., 2013).	23
Figure 4-6. Soil stratigraphy and location of measurement instruments (Laloui et al., 2006).	24
Figure 4-7. Test pile configuration (Laloui et al., 2006).	24
Figure 4-8. Thermo-mechanical loading history (Laloui et al., 2006).	25
Figure 4-9. Temperature values imposed in the pile (Laloui et al., 2006).	26
Figure 4-10. Thermal vertical stresses under a thermal load of 13.4°C (Laloui et al., 2006).	26
Figure 4-11. Thermo-mechanical vertical stresses in the pile: (a) experimental results; (b) numerical simulations).	27
Figure 4-12. Observed response of the Lambeth College main pile test: (a) end of heating; (b) end of cooling (Bourne-Webb et al., 2013).	28
Figure 4-13. Steady-state temperature field as function of surface thermal boundary condition (contour interval: 2°C) (Bodas Freitas et al., 2013).	29
Figure 4-14. Change in pile axial stress due to temperature change of +30°C (Bodas Freitas et al., 2013).	30
Figure 4-15. Change in pile-soil interface shear stress due to temperature change of +30°C (Bodas Freitas et al., 2013).	30
Figure 4-16. Numerical model: geometry, mesh and boundary conditions (Di Donna et al., 2013).	31

Figure 4-17. Thermally induced displacement of the foundation (Di Donna et al., 2013). .....	32
Figure 4-18. Effects of heating on the axial stress in Pile 2 (Di Donna et al., 2013). .....	33
Figure 4-19. Effects of heating and cooling on the axial stress in Pile 2 (Di Donna et al., 2013). .....	33
Figure 4-20. Ground temperature profile under climatic effect (Suryatriyastuti et al., 2013). ....	34
Figure 4-21. Ground temperature profile in the winter mode: (a) the initial conditions. (b) at the end of the thermal load (Suryatriyastuti et al., 2013). .....	35
Figure 4-22. Thermally induced mechanical behaviour of the pile at winter and summer mode: ... (a) thermal axial force (b) thermal axial displacement (Suryatriyastuti et al., 2013). .....	35
Figure 4-23. Cyclic variation in the pile head displacement (Suryatriyastuti et al., 2013). .....	36
Figure 4-24. Thermally induced normal force at the beginning and at the end of the thermal cycles (Suryatriyastuti et al., 2013). .....	37
Figure 5-1. Usual thermo-active pile construction details: (a) absorber pipes fixed to a pile reinforcement; (b) absorber pipes installed in the centre of the pile (Powrie & Loveridge, 2013). .....	40
Figure 5-2. Axisymmetric thermal model: finite element mesh and thermal boundary conditions. ....	42
Figure 5-3. Modes of heating: (a) centreline heating; (b) edge heating; (c) full body heating. ...	43
Figure 5-4. Model temperature field at steady state for the full body heating case and for the base case thermal conductivity values. ....	44
Figure 5-5. Radial temperature profiles at a 5m depth. ....	45
Figure 5-6. Radial temperature profiles at a 5 m depth (zoomed closer to the pile). ....	45
Figure 5-7. Radial temperature profiles at a 5m depth with centreline heating. ....	46
Figure 5-8. Radial temperature profiles at a 5m depth with edge heating. ....	46
Figure 5-9. Influence of the interface thermal conductance value. ....	47
Figure 5-10. 2D Thermal Model: finite element mesh, geometry and thermal boundary conditions. ....	48
Figure 5-11. Pile ring configuration. ....	48
Figure 5-12. Pile pipe configuration. ....	49
Figure 5-13. Temperature fields through time for the two pile configurations (the bold black lines represent the pile-soil interface). ....	50
Figure 5-14. Pile-soil interface temperature profiles around pile circumference through time and at the steady state. ....	51
Figure 5-15. 30m Slab numerical model: mesh and thermal boundary conditions. ....	52
Figure 5-16. 30 m Slab model temperature field for an outside temperature of 0°C. ....	53
Figure 5-17. 30 m Slab model temperature field for an outside temperature of 25°C. ....	54
Figure 5-18. Horizontal temperature profile below the 15m slab. ....	55
Figure 5-19. Horizontal temperature profile below the 30m slab. ....	55
Figure 6-1. Mesh and boundary conditions of the thermal-mechanical model for the baseline analysis. ....	60
Figure 6-2. Interface elements constitutive model: total slip versus shear stress. ....	62
Figure 6-3. Pile load-settlement curve. ....	63
Figure 6-4. Mobilized pile-soil interface shear stress. ....	63
Figure 6-5. Stresses in the pile and in the pile-soil interface. ....	66
Figure 6-6. Pile vertical displacement. ....	67
Figure 6-7. Thermally induced stresses (heating and cooling thermal loads). ....	68
Figure 6-8. Thermally induced stresses for three cases of soil and concrete thermal expansion values. ....	71
Figure 6-9. Thermally induced vertical displacements in the pile for three cases of soil and concrete thermal expansion values. ....	71

Figure 6-10. Thermally induced stresses for three different ground surface temperatures. .... 72

Figure 6-11. Thermally induced vertical displacements for three different ground surface temperatures..... 73

Figure 6-12. Thermally induced stresses for three different pile lengths. .... 74

Figure 6-13. Maximum thermally induced axial stress in the pile as a function of the ground surface temperature (15m pile)..... 75

Figure 6-14. Maximum thermally induced axial stress in the pile as a function of the ground surface temperature (30m pile)..... 75

Figure 6-15. Maximum thermally induced axial stress in the pile as a function of the ground surface temperature (45m pile)..... 76

Figure 6-16. Maximum thermally induced axial stress in the pile as a function of the ground surface temperature (soil half as thermally expansive as concrete). .... 77

Figure 6-17. Maximum thermally induced axial stress in the pile as a function of the ground surface temperature (soil two times more thermally expansive than concrete). 77

Figure 6-18. Maximum thermally induced axial stress in the pile as a function of the ground surface temperature (soil four times more thermally expansive than concrete). .... 78

Figure 6-19. Maximum thermally induced axial stress on the pile as a function of the ratio between soil and concrete thermal expansion coefficients (30m Pile). .... 79

# List of Tables

Table 3-1. Usual thermal conductivity values of substances common in soils (Rees et al., 2000).....	15
Table 5-1. Soil and concrete thermo-physical properties used in the base analysis. ....	41
Table 6-1. Soil and concrete mechanical properties. ....	59
Table 6-2. Parameter changes applied to the model. ....	64

# List of Acronyms

BC	Boundary Condition
COP	Coefficient of Performance
CTE	Coefficient of Thermal Expansion
GSHP	Ground Source Heat Pump
OCR	Over Consolidation Ratio
SPF	Seasonal Performance Factor

# List of Symbols

- $\alpha$  - Linear coefficient of thermal expansion ( $m/m/K$ )
- $\beta$  - Volumetric coefficient of thermal expansion ( $m^3/m^3/K$ )
- $\tau$  - Shear stress (kPa)
- $\nu$  - Poisson's ratio
- $\varepsilon_T$  - Thermal strain
- $\rho$  - Density ( $Kg/m^3$ )
- $\sigma$  - Stefan Boltzmann constant ( $5.670373(21)\times 10^{-8} W/m^2K^4$ )
- A - Area ( $m^2$ )
- c - Specific heat capacity ( $J/Kg.K$ )
- d - Diameter (m)
- D - Thermal diffusivity ( $m^2/s$ )
- E - Young Modulus (MPa)
- h - Heat transfer coefficient ( $W/m^2.K$ )
- k - Thermal conductivity ( $W/m.K$ )
- $k_c$  - Concrete thermal conductivity ( $W/m.K$ )
- $k_s$  - Soil thermal expansion ( $W/m.K$ )
- K - Coefficient of lateral stress
- L - Length (m)
- $L_0$  - Initial length (m)
- $N_c$  - Bearing capacity factor
- $q_s$  - Shaft shear resistance (kN)
- Q - Rate of heat transfer ( $W$ )
- P - Axial load (kN)
- R - Radius, radial coordinate (m)
- T - Temperature ( $^{\circ}C$  or  $K$ )







# Chapter 1

## Introduction

This chapter gives a brief introduction to thermo-active foundations; how they function and how they fit in the current state of civil construction and the World's ongoing demand for green and efficient energy usage. The motivation and the objectives behind this work are also presented and at the end of the chapter, the thesis structure is outlined.

## 1.1 Overview

The World's energy consumption is rising due to population growth and the overall improvement of living standards, at the same time, fossil fuels are becoming less reliable due to negative environmental impacts, overuse of natural energy resources, rising prices and political instability in some of the major production countries. This reality has led to a drive towards urban sustainability as we seek to meet our energy demands through the use of renewable energies.

The majority of a building's energy consumption is used to maintain a comfortable environmental temperature within it. A sustainable building design can critically decrease this energy consumption by a combination of two main aspects: the use of renewable energies to meet most of the building's energy demands and a good thermal design that minimizes these demands by reducing heat transfer between the building and its exterior.

Geothermal energy contained in the subsurface of the Earth has been found to have a great potential as a directly usable and renewable energy. Shallow geothermal energy can be extracted from trench collectors and borehole heat exchangers, or through foundation elements, which when used for this purpose are also referred to as thermo-active foundations or energy foundations. Among these options, the use of foundation elements as ground heat exchangers has been rising in the past years. For instance, in Austria, the number of energy foundation piles installed grew almost exponentially between 1998 and 2004 (Figure 1-1).

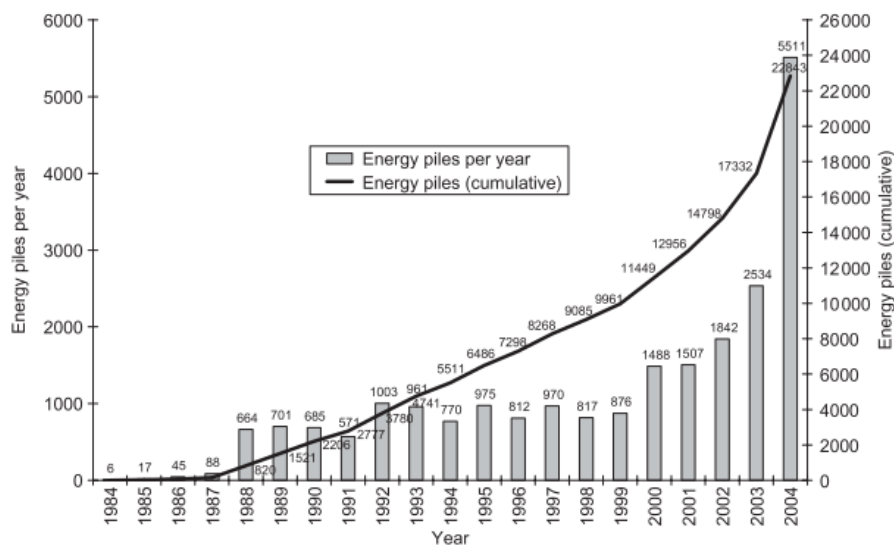


**Figure 1-1. Number of energy piles installed in Austria between 1984 and 2004 (Brandl, 2006).**

By using foundation elements, which are already required for structural reasons, as ground heat exchangers, a considerable initial cost saving is achieved when compared to the construction of a separate system for the sole purpose of ground heat exchanging.

Concrete is also a favourable material for exchanging heat with the ground due to its high thermal conductivity and thermal storage capacity. Among the foundation elements, piles make the best ground heat exchangers as they maximize the surface area of concrete in contact with the soil and extend to greater depths than shallow foundations where the soil temperature is less affected by the exterior air temperature, allowing better heat extraction.

Heat is extracted or injected into the ground by the circulation of a fluid through polyethylene pipes installed inside these foundation elements. Ground heat exchangers such as energy piles are generally used in conjugation with a heat pump, which is referred to as a ground-coupled heat pump system. The heat pump is required to adjust the temperature levels extracted from the ground to more suitable levels, depending on the building's heating or cooling needs. The energy obtained via a ground-coupled heat pump system can be used in conventional air-conditioning systems and other low-temperature heating systems such as floor and wall heating. Data from existing applications report that the use of energy piles can save up to two thirds of a building's conventional heating and cooling costs (Brandl, 2006), and lead to a reduction in CO<sub>2</sub> emissions of up to 50% (Laloui et al., 2006).

While energy piles have increasingly been used in recent years, a full understanding of their thermal-mechanical behaviour has yet to be achieved due to the complexity of the problem and a lack of published quantitative evidence regarding their thermal-mechanical behaviour. In fact, energy piles show a very complex behaviour as the strain and stresses induced by the temperature changes in the pile will depend on both the concrete and soil thermal and mechanical properties which, in the case of the latter, often vary with depth. Temperature changes can also affect the soil properties and possibly the behaviour of the pile-soil interface.

Thermally induced stresses in the pile can potentially reduce the design safety margin when compared to a conventional pile design which does not take into consideration the thermal load. Current thermal pile design often neglects the effect of the thermal load while published evidence points to the possibility of considerable additional stresses and strains in the pile due to the thermal load. The lack of a complete understanding of the effect of the thermal load in the structural behaviour of the pile has been a major obstacle to the uptake and to the industrial development of this technology as it is difficult to demonstrate to clients that besides being an economically viable and green technology, it is also safe.

## 1.2 Motivation and Contents

This work aims to fill some gaps regarding the understanding of the thermal-mechanical behaviour of energy piles and contribute, in conjugation with other ongoing and past investigations, to the ultimate goal of gaining a complete understanding of the effects of the thermal load on a foundation element. In order to achieve these goals, systematic thermal and a thermal-mechanical numerical analysis of an energy pile was performed and the results are reported and discussed in this thesis.

Besides contributing to a better understanding of the energy pile problem from a purely thermal point of view, some of the aspects investigated in the thermal analysis helped to define some of the

characteristics of the thermal-mechanical model such as the ground surface temperature and how heat was applied to the pile. The following aspects were investigated in the thermal analysis:

- The simulation of the pile thermal load in a numerical model;
- The effect of soil and concrete thermal conductivity values in the temperature fields obtained;
- Ground surface temperature immediately below the ground floor slab of a modern building.

In the thermal-mechanical analysis, the effects of the thermal load in the mechanical behaviour of the pile were studied. Specifically, the following aspects were investigated:

- The influence of the ground surface temperature;
- The effect of differing relative values for the concrete and the soil coefficient of thermal expansion;
- The influence of the pile length and therefore the length to diameter ratio.

## 1.3 Structure of the Thesis

This thesis is composed of seven main chapters which are ordered as follows:

1. Introduction;
2. Ground Source Energy and Heat Pump Systems;
3. Heat Transfer Mechanisms;
4. The Effect of Heating and Cooling a Pile;
5. Thermal Analysis;
6. Thermal-Mechanical Analysis;
7. Conclusions and Recommendations for Future Work.

In Chapter 1, a general overview of thermo-active foundations technology has been presented. Chapters 2, 3 and 4 constitute the literature review of the thesis, where an overview of thermal pile behaviour is given as well as the theoretical concepts necessary to understand it. In Chapters 5 and 6, the thermal and thermal-mechanical analysis respectively are presented. The numerical models used to perform these analyses are described and then the results are detailed and discussed. Finally, in Chapter 7, a summary of the most pertinent results is presented, conclusions are drawn and recommendations for future developments are made

# **Chapter 2**

## **Geothermal Energy and Heat Pump Systems**

This chapter provides an overview of geothermal energy, and how it can be extracted and efficiently used to heat or cool a building through the use of ground source heat pump (GSHP) systems.

## 2.1 Shallow Geothermal Energy and its Use

Geothermal energy is the energy stored as heat in the ground. Ground heat exchangers, such as energy piles, allow heat exchange between the ground and an energy consuming entity such as buildings.

In most regions of the world, ground temperature is not affected by climatic and daily temperature changes below a depth of about 10 m to 15 m (Figure 2-1). Due to this constancy in ground temperature, heat can be extracted or injected in the ground using a ground heat exchanger system.

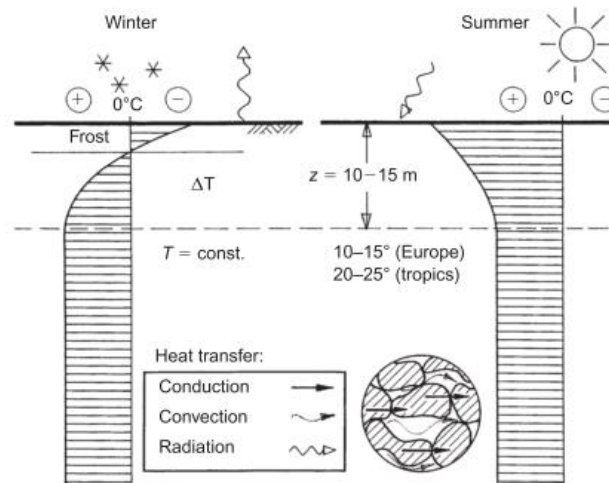


**Figure 2-1. Ground temperature at depth in Europe and tropics (Brandl, 2006).**

There are two main types of ground source heat exchangers, open and closed systems, they are, however, all based on the same principle: the use of a circulating fluid, generally water, to extract or inject heat into the ground.

In open systems, water is directly extracted/injected into aquifers. Two wells are generally required, one to extract the ground water and another to re-inject it into the same aquifer.

In closed systems, a fluid, generally a water/ glycol mix, circulates inside plastic tubes, called absorber pipes, which can be placed directly into boreholes or cast inside foundation elements such as piles. As the fluid circulates inside these pipes, it will exchange heat with the ground, to provide heating during the winter and cooling during the summer. Figure 2-2 illustrates the types of ground heat exchangers previously mentioned.

The use of concrete foundation piles as heat exchangers has seen an increase in usage during the past years. As previously mentioned, by taking advantage of these necessary structural elements, we avoid the construction of boreholes for the sole purpose of heat exchanging which will lead to a reduction in the initial capital cost of the system.

With the development of more efficient technology and the overall increase in knowledge about the subject, geothermal energy is increasingly becoming a reliable source of sustainable and green energy.

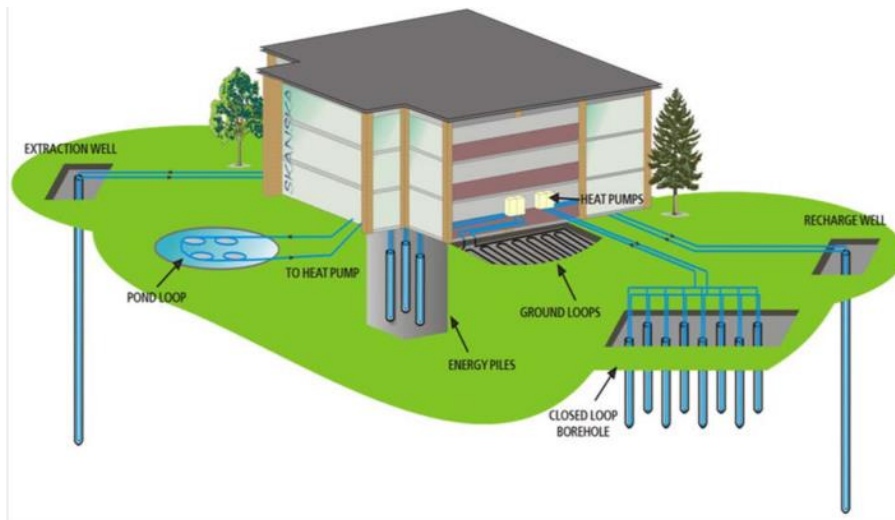


**Figure 2-2. Various types of ground heat exchangers (Amis, 2011).**

## 2.2 Ground Source Heat Pump Systems

### 2.2.1 Introduction

Ground source energy heat pump (GSHP) systems allow the extraction of heat from the ground at a relatively low temperature which is then increased by a heat pump and used in a heating delivery system. These systems can be reversible, meaning they can also be used for cooling.

Heat pump systems are constituted by a number of components which can be sub-divided into the primary circuit, heat pump and the secondary circuit (Figure 2-3).

The primary circuit contains the absorber pipes which can be placed inside earth-contact concrete elements or directly into boreholes, their respective connecting lines, a circulation pump and the header block which connects the ground heat exchanger to the heat pump. A heat exchange fluid, generally a water/glycol solution, is pumped through these absorber pipes using a circulation pump, which will allow energy exchange between the heat pump and the ground.

As previously mentioned, the heat pump is responsible for raising the temperature levels of the pumped fluid to more usable values at the cost of a small amount of electrical energy, it also makes the connection between the primary and secondary circuits as shown in Figure 2-4.

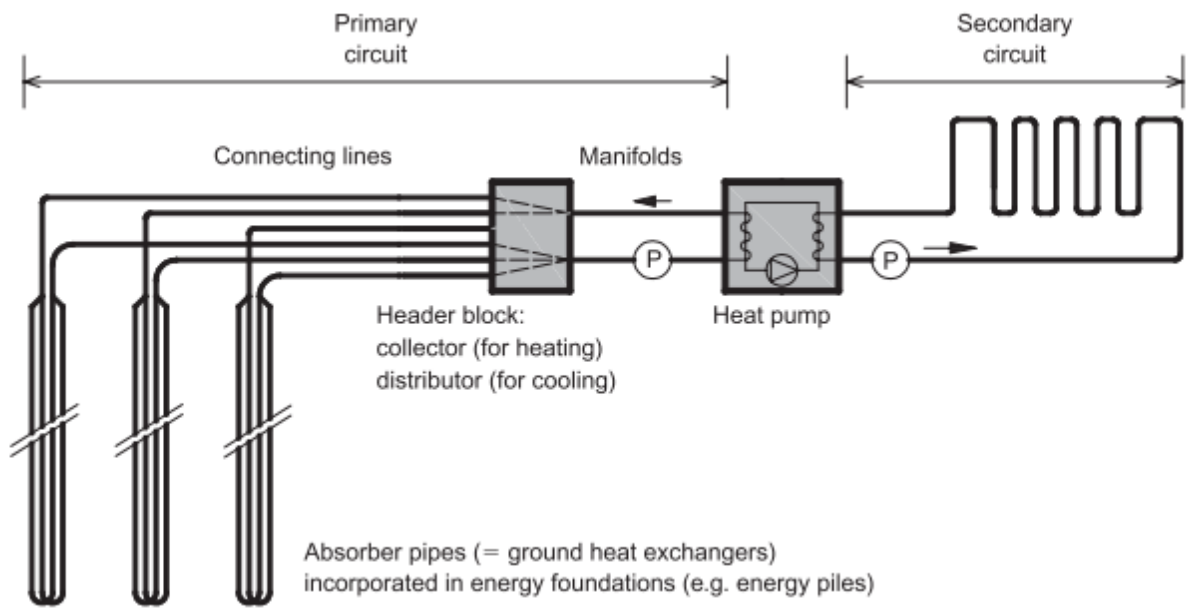


Figure 2-3. Scheme of a ground source heat pump system with energy piles as ground heat exchangers (Brandl, 2006).

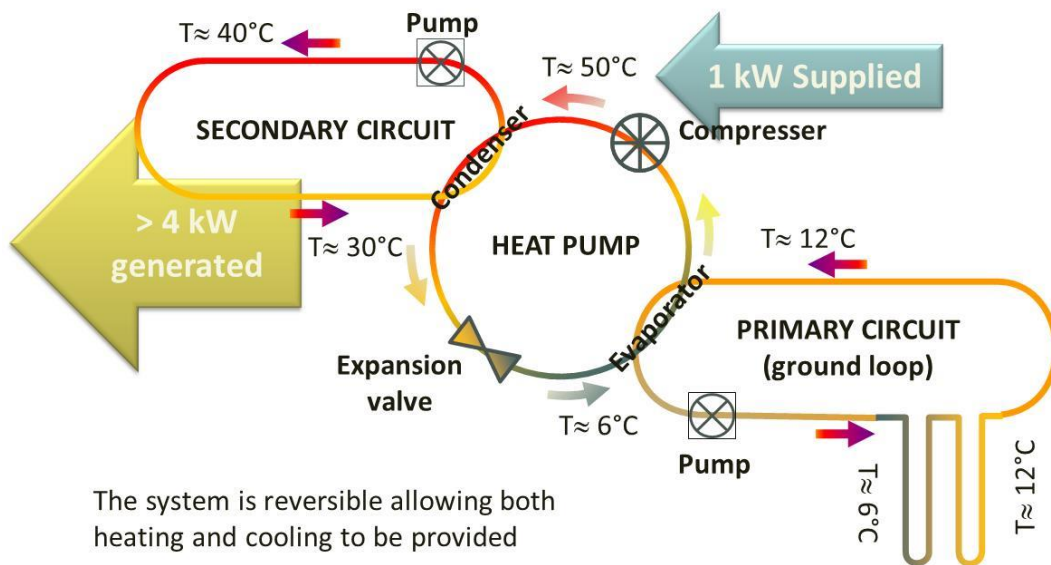


Figure 2-4. Heat pump and its interactions with the primary and secondary circuits (Bourne-Webb, 2014).

Heat pumps integrate a compression-expansion circuit through which circulates a refrigerant. Refrigerants are chemical substances used in heat cycles which present a reversible phase transition from a liquid to a gas, and a low boiling point. In heating mode, using heat extracted from the ground, water circulating through the primary circuit heats the refrigerant which due to its low boiling point



vaporizes reaching the compressor in a gaseous phase. The compressor increases the pressure of the refrigerant and, as the Boyle's Law states, when the pressure of a gas is increased at constant volume, its temperature also increases. After this process, the refrigerant will be at a usable temperature, typically between 30°C and 45°C, and it heats the water circulating through the secondary circuit which is then responsible for distributing the heat through the building. At the end of the cycle, the refrigerant goes through an expansion valve which lowers its temperature leading to its condensation and the start of a new cycle. As previously mentioned, heat pump systems, can either be unidirectional allowing either heating or cooling only or be bidirectional allowing the system to be reversible, meaning it can be changed from cooling to heating and vice-versa, as desired.

The last component of the GSHP system, the secondary circuit, includes a circulation pump, the distribution pipes and the heating/air conditioning delivery system responsible for heating or cooling the building.

## 2.2.2 Efficiency of the GSHP Systems

In order to increase the efficiency of the heat pump, the difference between extracted and actually used temperature must be as low as possible, as this will minimize the input of electrical energy necessary. To do so, when heating, low temperature delivery systems, such as underfloor heating which only requires a heating delivery of 30°C to 45°C, should be adopted. When cooling, the same principle of minimizing the difference between extracted and usable temperatures should also be taken into consideration.

The efficiency of a heat pump can be quantified by the coefficient of performance (COP) which is defined by:

$$COP = \frac{\text{energy output after heat pump}}{\text{energy input for operation}} \quad (\text{Equation 2-1})$$

The energy input for operation includes the energy required to operate the heat pump and the circulation pumps. Naturally, the higher the COP value the more efficient is the heat pump. For economic reasons, a value of  $COP \geq 4$  should be achieved (Brandl, 2006). To achieve this value, the usable temperature in the secondary circuit when heating should not exceed 45°C and the extraction temperature in the absorber pipes should not fall below zero to 5°C.

The overall performance of the ground source energy heat pump system can be quantified by the seasonal performance factor (SPF) which is identical to the heat pump COP but includes the remaining components of the system, including the secondary circuit.

The SPF is defined by:

$$SPF = \frac{\text{usable energy output of the energy system}}{\text{energy input of the energy system}} \quad (\text{Equation 2-2})$$

GSHP systems usually have an SPF value of 3.5 to 4, meaning, we can generally achieve an energy output at least 3.5 times higher than our electrical energy input.

Ground source energy may save up to two-thirds of the conventional heating costs of a building by taking advantage of clean and renewable geothermal energy (Brandl, 2006). With worldwide building regulations tending to minimize new construction's energy consumption or even aiming for zero-net energy buildings, ground source energy systems are an efficient and cost-effective way to help achieve this goal. While the capital costs of these systems are high, maintenance and operating costs are low meaning that in the long term they will not only repay the initial investment but lead to considerable cost savings.

# Chapter 3

## Heat Transfer Mechanisms

This chapter gives an overview of the three main heat transfer mechanisms (conduction, convection and radiation). Amongst these three mechanisms, thermal conduction will be particularly discussed as it is the main mechanism of heat transfer in soils.

## 3.1 Heat Transfer Mechanisms

Each body has a certain amount of internal energy which is related to the random movement of its atomic particles (i.e. kinetic and potential energy) and to its specific phase (i.e. liquid, solid, gas); this internal energy is commonly referred to as thermal energy. Temperature is the average value of a body's particles thermal energy. The transfer of thermal energy is defined as heat and is measured in Joules (J). Heat flow can occur due to phase changes, which is not considered in this thesis, or by three distinct mechanisms: conduction, convection and radiation, as follows:

### 3.1.1 Conduction

If there is a temperature gradient within a body, heat will flow from the higher temperature region to the lower temperature region due to molecular motion and interaction, as adjacent atoms vibrate against each other or as electrons move from one atom to another. This phenomenon is known as thermal conduction which only occurs within a body or between two bodies that are in contact.

Conduction is defined at a steady state if the rate of heat transfer doesn't change with time, meaning that the amount of heat entering any section of the body is equal to the amount of heat coming out. At steady state, experience has shown that conductive heat transfer can be expressed by the Fourier's law which, in one dimension, takes the form:

$$\frac{Q}{A} = -k \frac{dT}{dx} \quad (\text{Equation 3-1})$$

According to the Fourier's law, the rate of heat transfer through a material,  $Q/A$ , is proportional to the magnitude of the temperature gradient,  $dT/dx$ , and opposite to it in sign. The constant of proportionality,  $k$  ( $W/mK$ ), is called the thermal conductivity and reflects the ability of a certain material to conduct heat. An overview of soil and concrete thermal conductivity is given in Section 3.2.1.

During conductive heat flow, if temperatures are changing in time and thus the temperature gradients are not constant, conduction is in a transient state. In a transient state, Equation 3-1 no longer applies and the mathematical analysis of the problem is more complex, often requiring numerical solutions or approximation theories. In a transient state, conductive heat transfer can be described by the heat diffusion equation:

$$\frac{d^2T}{dx^2} = \frac{\rho c}{k} \frac{dT}{dt} = \frac{1}{D} \frac{dT}{dt} \quad (\text{Equation 3-2})$$

Where  $\rho$  ( $kg/m^3$ ) is the density, and  $c$  ( $J/kg.K$ ) the specific heat capacity of the material; i.e. the amount of energy per unit mass required to raise the temperature of a body by one degree. The thermal diffusivity,  $D$  ( $\frac{m^2}{s}$ ) =  $k/\rho c$ , is a measure of how quickly a material responds to temperature changes.

### 3.1.2 Convection

Convection is the process of heat transfer through the movement of a fluid or a gas. In general, it can be seen as the heat transferred between a surface and a moving fluid at a different temperature. For instance, convective heat transfer can take place in permeable soils as a result of seepage flow. If the soil particles and the water are at different temperatures, convective heat transfer will take place. Convection can be described by the Newton's law of cooling:

$$\frac{Q}{A} = h(T - T_f) \quad (\text{Equation 3-3})$$

Where  $h$  ( $W/m^2K$ ) is the heat transfer coefficient. This parameter depends on the properties of the fluid, for example its viscosity, density, specific heat capacity, as well as on the properties of the surface such as its roughness and the interface geometry.  $T$  and  $T_f$  represent respectively the temperature of the fluid and the surface over which it is flowing.

### 3.1.3 Radiation

All bodies emit energy constantly through electromagnetic radiation. The intensity of this energy flux depends on the body's temperature and the nature of its surface. For instance, if we sit in front of a fire most of the heat we feel is transferred to us by radiation. The Stefan Boltzmann law describes the amount of energy radiated from a black body in relation to its absolute temperature:

$$\frac{Q}{A} = \sigma T^4 \quad (\text{Equation 3-4})$$

Where  $\sigma$  is a constant of proportionality named the Stefan-Boltzmann constant and has the value of  $5.670373(21) \times 10^{-8} W/m^2K^4$  and  $T$  is the absolute temperature in Kelvin, K. As most bodies are not black bodies and are not isolated, the exact calculation of its radiated heat is hard to measure and will be lower than the one idealized by Stefan-Boltzmann's law. When determining the radiated heat of a non-black body, the result obtained from Equation 3-4 is usually multiplied by an emissivity factor, which for the case of concrete usually has a value between 0.85 and 0.94 ([http://www.engineeringtoolbox.com/emissivity-coefficients-d\\_447.html](http://www.engineeringtoolbox.com/emissivity-coefficients-d_447.html), accessed 09 February 2014).

## 3.2 Heat Transfer in Soils

Even though all of the three heat transfer mechanisms previously mentioned can take place in a soil medium, thermal conduction is generally the dominant process, while convection and radiation usually have negligible or small effects. However, some particular cases exist, for instance if the soil presents a high degree of saturation and a large grain size, convection may become important as we should expect a significant percolation of water through the soil particles. In unsaturated soils, moisture migration due to evaporation and subsequent condensation may be an important process as well since it induces phase changes in the soil and therefore affects its thermal properties, particularly, by changing

its degree of saturation. Figure 3-1, illustrates the previous statements, indicating some of the cases, according to the degree of saturation and grain size of the soil, when convective or radiative heat transfer as well as moisture migration become more important.

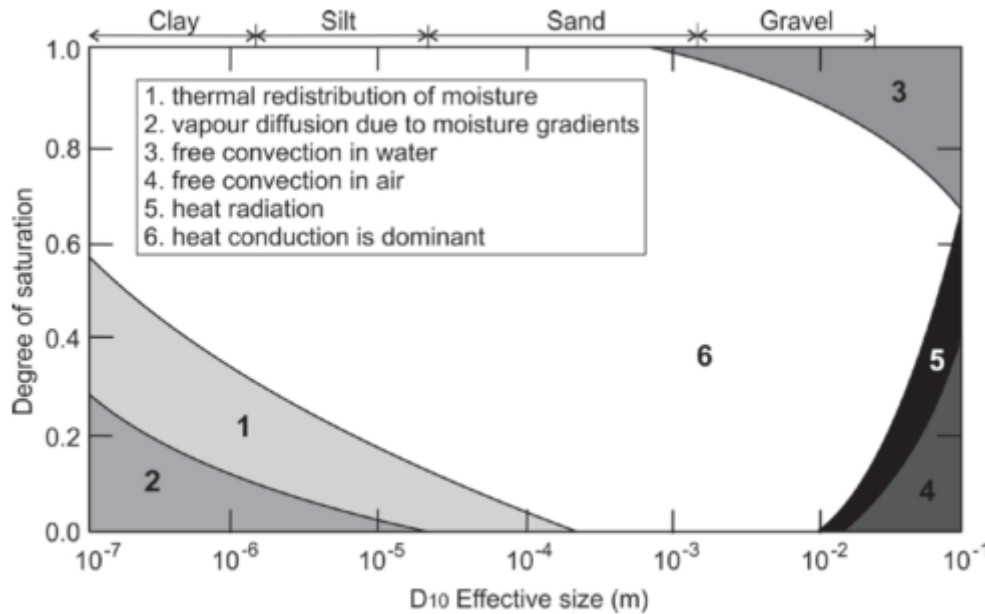


**Figure 3-1. Predominant heat transfer mechanisms by grain size and degree of saturation (Loveridge 2012, redrawn from Farouki, 1986).**

Being the predominant process of heat transfer through soils, thermal conduction will be the focus of the following section and the only thermal heat transfer process taken into consideration in the thermal and thermal-mechanical analyses performed in Chapters 5 and 6.

### 3.2.1 Thermal Conduction in Soils and Concrete

Heat conduction takes place in all the soil constituents, i.e. the soil particles, pore water, and pore air. As previously mentioned, the thermal conductivity, usually denoted as  $k$  ( $W/mK$ ), is a proportionality factor relating the rate at which heat is transferred by conduction to a temperature gradient.

The thermal conductivity of soils is a difficult parameter to measure or estimate as it depends on a vast number of factors such as water content, mineral composition, porosity, density and temperature. For instance, saturated soils with a high content of quartz will generally have a high thermal conductivity as quartz is a highly conductive mineral and the thermal conductivity of water is one order of magnitude higher than that of air. Frozen soils also present higher thermal conductivity than when unfrozen because ice has a thermal conductivity about four times higher than water. Table 3-1, indicates typical thermal conductivity values of common soil constituents:

Substance	Thermal conductivity (W/mK)
Quartz	8.79
Clay Minerals	2.93
Organic Matter	0.25
Water	0.57
Ice	2.18
Air	0.025

**Table 3-1. Usual thermal conductivity values of substances common in soils (Rees et al., 2000).**

Regarding the effects of temperature on the thermal conductivity of soils, Hiraiwa et al (2000) measured the thermal conductivity of two different soils as a function of temperature (zero to 75°C). Results showed that, in general, thermal conductivity increased with temperature. This increase in soil thermal conductivity due to the temperature increase (zero to 75°C) was up to 0.75 W/mK, depending also on the water content and the specific type of soil analysed.

Given the high dependence of thermal conductivity on the soil characteristics, it is to be expected that a wide variety of thermal conductivity values are found in the literature and are being used in numerical simulations. Typical thermal conductivity values of soils lie in a range from about 0.5 W/mK to 3 W/mK (Figure 3-2).

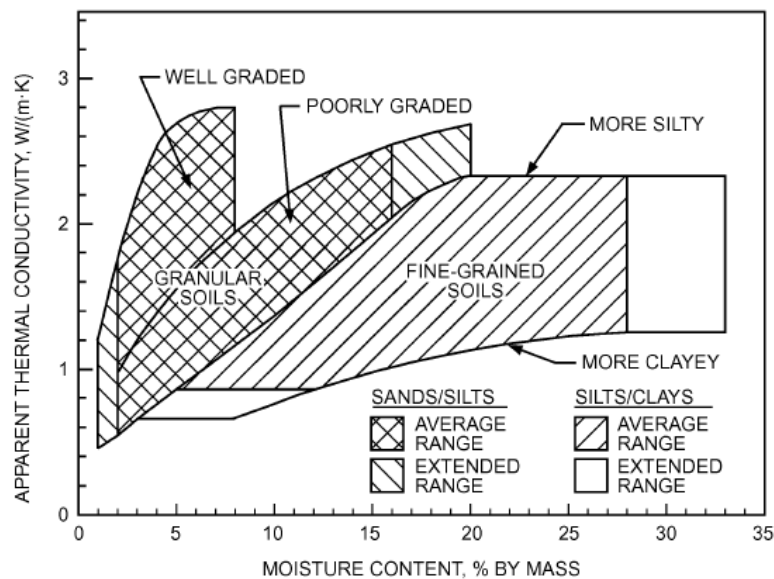


**Figure 3-2. Soil thermal conductivity values as a function of moisture content (ASHRAE Fundamentals, 2009).**

Like soil, concrete is constituted by different materials/substances which present different chemical and physical properties. As a composite material, concrete's thermal conductivity will be a function of the thermal and physical properties of its constituents such as cement, aggregates and additives. The density, moisture content and temperature of the concrete will also affect its thermal conductivity. Depending on these factors, the thermal conductivity of concrete can vary between  $1 \text{ W/mK}$  and  $4 \text{ W/mK}$ . For instance, Neville (1995), reports typical thermal conductivity values of saturated concrete between  $1.4 \text{ W/mK}$  and  $3.6 \text{ W/mK}$ .

It is apparent that the thermal conductivity for both soil and concrete has a wide range values. In Section 5.2.1, as part of the thermal analysis, the effect of varying the thermal conductivity of the concrete and the soil between  $1 \text{ W/mK}$  and  $3 \text{ W/mK}$ , in terms of developed temperature fields in the model, will be investigated.

### 3.2.2 Thermal Expansion in Soils and Concrete

The coefficient of thermal expansion (CTE) describes the tendency of a material to change in volume when subjected to a temperature change and it is defined as the fractional increase in length per unit rise in temperature. Most materials increase in volume when heated due to the increased thermal vibration of their atoms which results in an increase in the average separation distance of adjacent atoms, however, this is not the case for soils, which can also present a contractive behaviour when heated.

Thermal strains in soils due to thermal loading are the result of thermal expansion/contraction of the soil particles and pore water, which due to their different thermal expansion coefficients results in the build-up of excess pore pressures, and the rearrangement of the solid skeleton of the soil. Many past studies (Cekerevac & Lalou, 2004, Sultan et al., 2004 and Baldi et al., 1988) report a great influence of the over consolidation ratio (OCR) on the thermal volume changes of clays. When heated, normal and lightly over consolidated clays present a plastic contractive behaviour while high OC clays an elastically expansive behaviour which increases with OCR and is followed by plastic contraction as illustrated in Figure 3-3. This means that clays can present positive or negative thermal expansion coefficients depending mainly on their OCR values but also on their mineralogical properties and the temperature magnitudes they are subjected to.

As with most construction materials and unlike soil, concrete always presents a positive coefficient of thermal expansion meaning that it will increase in volume when heated and reduce in volume when cooled. Aggregates are the main component of concrete and have a great influence over its thermal expansive behaviour. Different aggregate types will present different mineralogical content which will make them more or less thermal expansive, for instance, siliceous aggregates present high thermal expansion and consequently, concrete which contains these aggregates will generally also exhibit a high thermal expansion. Tatro (2006) reports values of concrete linear CTE between  $0.76\text{E-}5 \text{ m/m/K}$  and  $1.36\text{E-}5 \text{ m/m/K}$ , depending on the aggregate type used in its production. The water/cement ratio also influences the thermal expansion value of the concrete as it changes the thermal expansion of the cement past which constitutes 15 to 20% of its volume. In general, the coefficient of thermal expansion



of the concrete increases with a decrease in the water/cement ratio.

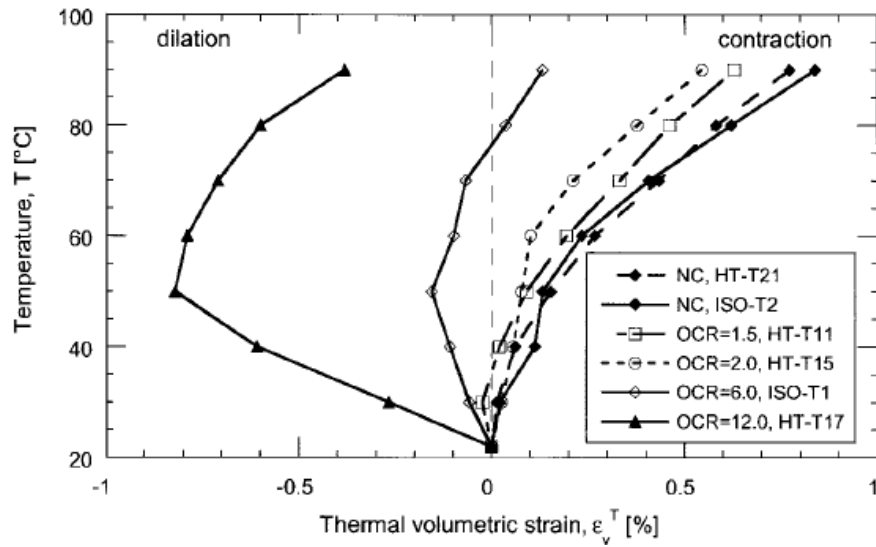


**Figure 3-3. Thermal volumetric strain of Kaolin clay during drained heating (Cekerevac & Laloui (2004)).**

### 3.3 Heat Transfer in Thermo-Active Piles

Two main heat transfer processes are observed in a thermo-active pile, convection and conduction. As water circulates inside the absorber pipes, it exchanges heat with the pipe walls by convection. Due to molecular vibration and interaction, the pipe walls exchange heat with concrete and this with the ground by conduction. As concrete, soil and plastic, which is usually the material used for the absorber pipes, will present different values of thermal conductivity and specific heat, the rate of heat flow will not be constant through these different materials. Figure 3-4 illustrates the process of heat transfer through thermo-active piles previously described, where  $\lambda$  represents thermal conductivity and  $T$  temperature.

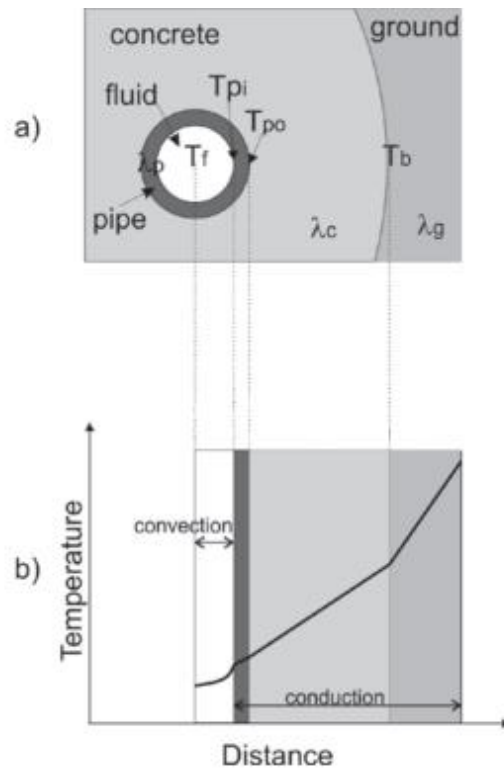


Figure 3-4. Thermo-active pile heat transfer: a) plan of thermal pile components; b) temperature differences (Powrie & Loveridge, 2013).

# Chapter 4

## The Effect of Heating and Cooling of a Pile

This chapter gives an overview of what is to be expected in terms of developed strains and stresses in a pile when it is subjected to a temperature change, as well as the base theory which describes their development. The results of prominent field studies and numerical analyses performed on thermo-active piles will then be analysed and compared to the theoretical base initially presented.

# 4.1 Thermally Induced Deformation – General Principles

When a body is subjected to a temperature change, it will attempt to expand if heated or contract if cooled. If the body is free to expand/contract it will change in volume without any development of additional stresses. However, if the body is partially or fully restrained thermally induced stresses will develop, whose magnitude will be proportional to the amount of restraint the body is subjected to.

The following sub-sections give an overview of what is to be expected in terms of thermally induced stresses on a pile which is subjected to three different restraint levels: no restraint (free body), perfect restraint and partial restraint.

## 4.1.1 Free Body Response (No Restraint)

When heated or cooled, a free body will expand or contract proportionally to its coefficient of linear thermal expansion,  $\alpha (m/m/K)$ , and to the applied change in temperature,  $\Delta T$ , as expressed by Equation 4-1, where  $\epsilon_{T-Free}$  represents the free thermal strain.

$$\epsilon_{T-Free} = \alpha \Delta T \quad \text{(Equation 4-1)}$$

The resulting geometry change, due to the thermal load can be written as:

$$\Delta L = L_0 \epsilon_{T-Free} \quad \text{(Equation 4-2)}$$

Since the body is free to expand/contract, it will change in geometry without mobilizing any additional stresses. Figure 4-1 illustrates the previous statement, considering a pile as the free body.

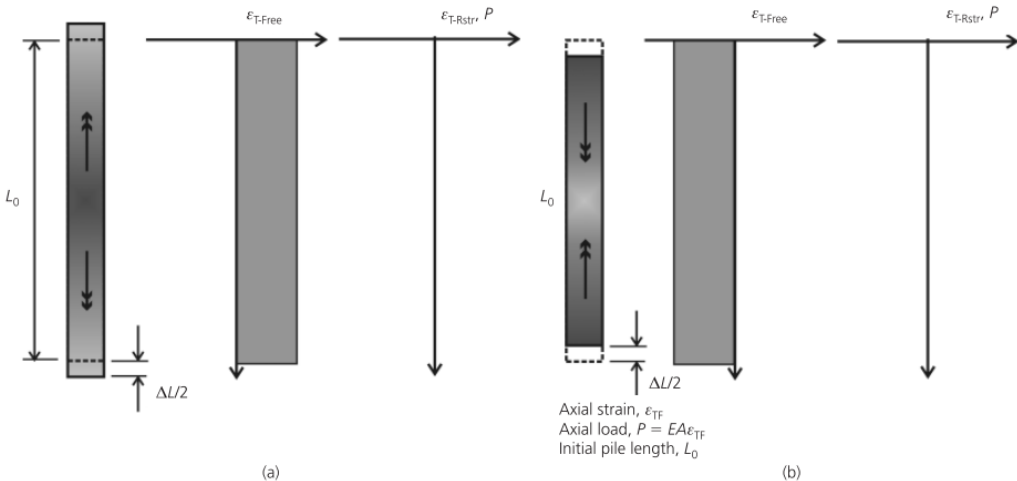


**Figure 4-1. Thermal response of a non-restrained pile (free body): a) heating; b) cooling (Bourne-Webb, et al., 2013).**

### 4.1.2 Perfectly Restrained Body

In contrast to the previous case, if the pile is perfectly restrained and its ends are not able to move, any applied thermal load will lead to additional axial load, uniform compressive stress if the pile is heated and uniform tensile stress if the pile is cooled. Considering the pile as a perfectly elastic and homogeneous material, the additional axial load,  $P$ , due to a temperature change will be proportional to the cross-sectional area,  $A$ , Young’s Modulus,  $E$ , and the equivalent strain due to the restraint,  $\epsilon_{T-Rstr}$ , which for the case of a perfectly restrained body is equal to  $\epsilon_{T-Free}$ .

$$P = EA\epsilon_{T-Rstr} \quad \text{(Equation 4-3)}$$

Figure 4-2 illustrates the case of a perfectly restrained pile subjected to thermal load.

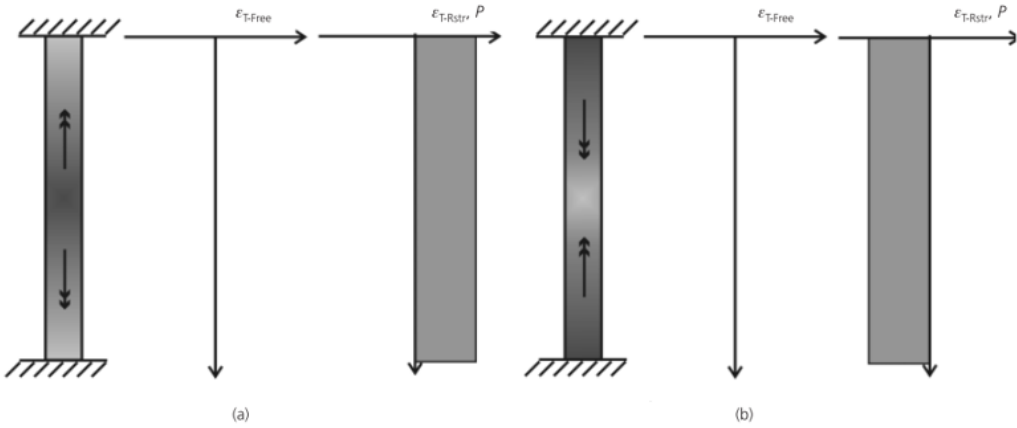


**Figure 4-2. Thermal response of a perfectly restrained pile: a) heating; b) cooling (Bourne-Webb, et al., 2013).**

### 4.1.3 Partially Restrained Body

The case of a pile partially restrained by surrounding soil and subject to thermal load is illustrated in Figure 4-3, admitting a rigid-perfectly plastic shaft resistance,  $q_s$ , zero base resistance and a non-thermally expansive soil ( $\alpha=0$ ). In this figure, it can be seen that thermally induced axial load is higher at mid-depth, the section where the strain restraint,  $\epsilon_{T-Rstr}$ , is higher, and reduces towards the ends of the pile where no restraint is applied. However, if the pile is not symmetrically restrained, the maximum stress will no longer occur at mid-depth and the load profile will vary accordingly. Naturally, the stiffer and stronger the soil is, the more restraint will be applied on the pile and consequently the higher the thermal induced axial and shear stresses will be. Because the top and bottom halves of the pile expand equally but in opposite directions, the resulting shear stress profile is antisymmetric.

The same case with the addition of end-restraints to the pile is illustrated in Figure 4-4. As the ends of the pile are no longer free to move, thermally induced stresses will no longer be null at these sections and will assume a value proportional to the restraint applied.

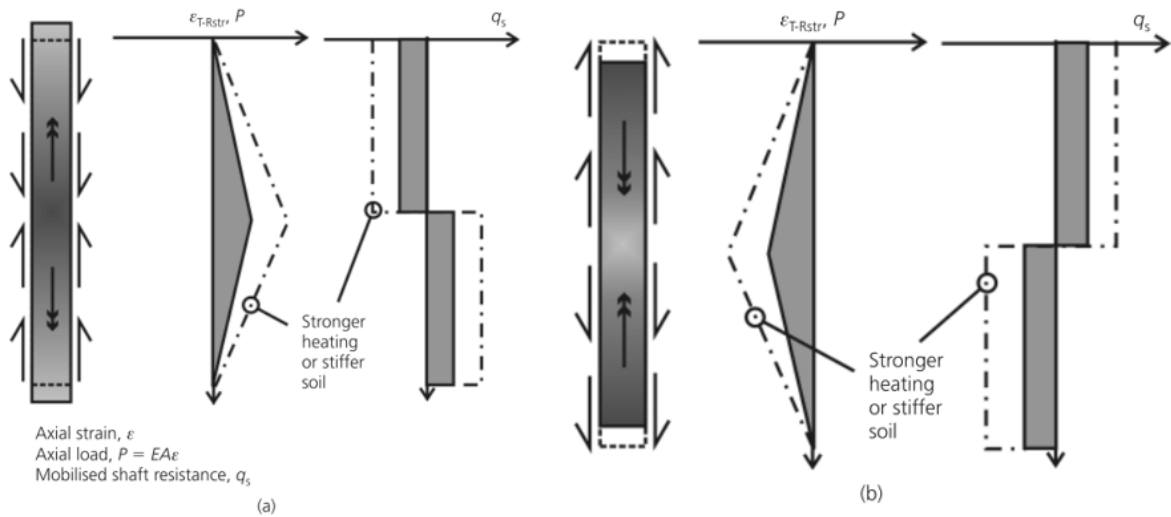


**Figure 4-3. Thermal response of a pile laterally restrained: (a) heating; (b) cooling (Bourne-Webb, et al., 2013).**

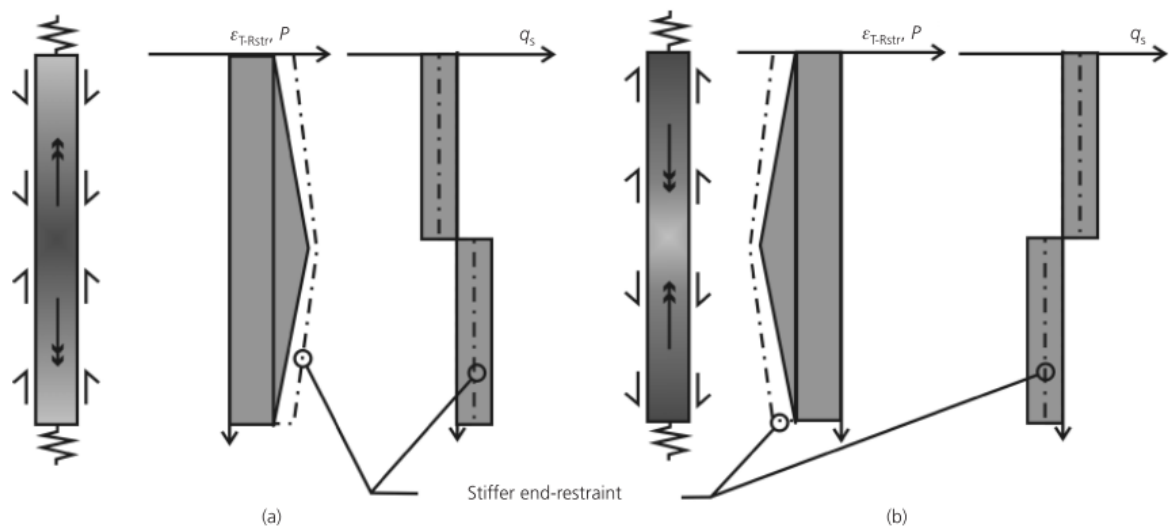


**Figure 4-4. Thermal response of a pile laterally and end restrained: (a) heating; (b) cooling (Bourne-Webb, et al., 2013).**

The typical response of a friction pile subjected to a mechanical load with no end-restraints considered is illustrated in Figure 4-5(a). Figure 4-5(b) and (c) illustrate the effects of a subsequent thermal load on the pile, heating and cooling respectively, which are the summation of the effects indicated in Figure 4-3 on the mechanical load transfer profile illustrated in Figure 4-5(a).

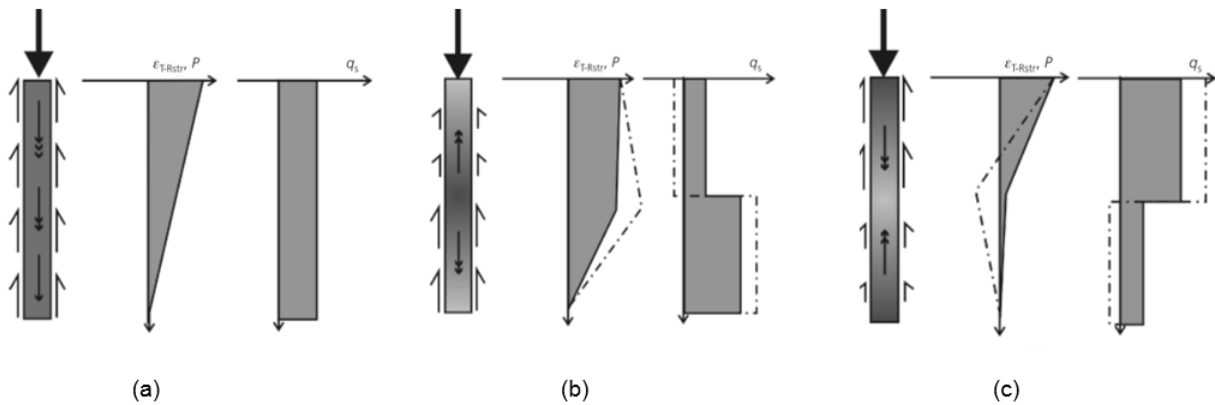


**Figure 4-5. Combined mechanical and thermal load effects on a partially restrained pile. Dash-dotted lines represent the effect of stronger thermal load or pile restraint. (a) Mechanical load only; (b) combined mechanical load and heating; (c) combined mechanical load and cooling; (Bourne-Webb, et al., 2013).**

While the concepts previously mentioned are very straight forward and easily understandable, in reality, the problem of a thermally loaded foundation pile is of great complexity. Soil is generally highly heterogeneous and therefore, the restraint it will induce in the pile will most likely change in depth. As the soil will also be heated/cooled together with the pile, it will also experience expansion/contraction, and the relationship between the concrete and soil thermal expansion values is likely to play a role in the resulting behaviour. A further look into thermal pile behaviour and an overview of past field experiments is now made.

## 4.2 Experimental Observations of the Effect of Heating and Cooling a Pile

In this section, the results of two tests performed on energy piles located in Lausanne, Switzerland and South London, United Kingdom are analysed. These tests were conducted with the aim of improving our knowledge regarding the impact of the thermal load on the geotechnical performance of pile foundations. The documentation of observational results is also important as these allow numerical models to be validated, i.e. to evaluate the ability of the models to recreate the behaviours we see in reality.

### 4.2.1 École Polytechnique Fédérale de Lausanne

The results of an in situ test carried on an energy pile at the École Polytechnique Fédérale de Lausanne (EPFL) in Switzerland, were reported by Laloui et al., (2006). The tested pile was located at the side of a 100 m long by 30 m wide building. The nominal pile diameter was 88 cm and its depth 25.8 m, the soil stratigraphy was complex and after various geotechnical investigations five different soil layers were identified (Figure 4-6). Over the top half of the pile, alluvial soil was identified while in the bottom half,

glacial moraine was found. The toe of the pile was socketed about 0.8 m into sandstone (molasses). These soils present different thermal and mechanical properties, for instance, the moraine was more thermally expansive and stronger than the alluvial soil. These different soil properties will considerably affect the thermally induced stresses, as the pile will not be equally restrained in depth and the restraint level will depend on the respective soil layer.

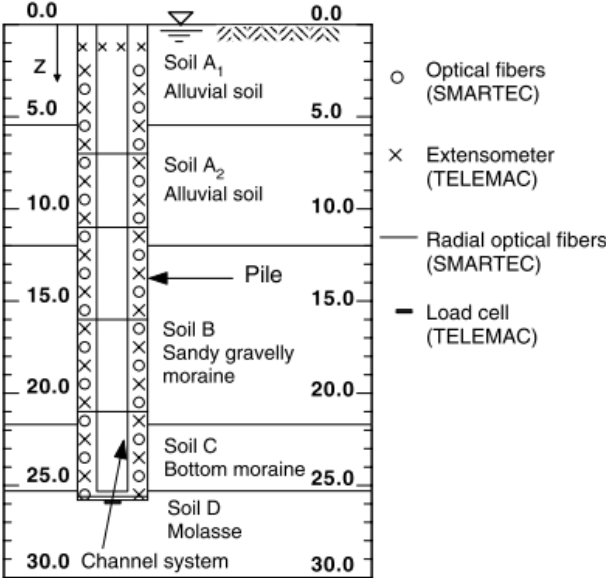


**Figure 4-6. Soil stratigraphy and location of measurement instruments (Laloui et al., 2006).**

U-shaped polyethylene tubes were placed vertically inside the pile to allow the circulation of the heat-carrying fluid as indicated in Figure 4-7. Strain and temperature measurements were provided by a total of 61 extensometers of various types and placed at various depths. In order to measure the load at the bottom of the pile, a load cell was also installed (Figure 4-6).

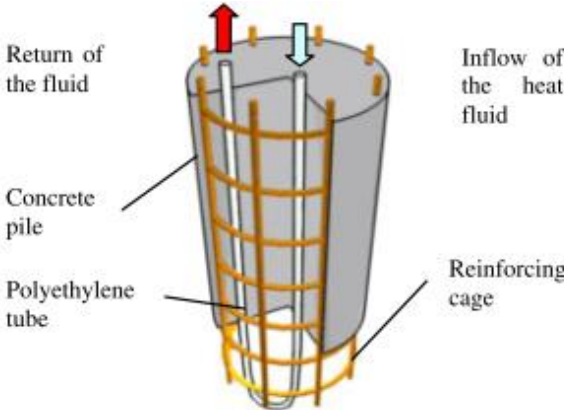


**Figure 4-7. Test pile configuration (Laloui et al., 2006).**

The testing period coincided with the construction of the building and each thermal load test was therefore undertaken with a different level of mechanical load provided by the dead weight of the structure at different stages of construction (Figure 4-8). The thermal load was induced by increasing the temperature of the water inside the polyethylene tubes. A thermal loading cycle was applied to the



pile at the end of the construction of each story. In addition to the measurements made during the casting of the pile (Test 0), a total of seven tests were carried out. The loading history of the pile can be seen in Figure 4-8; Test 1 was started in May 1998 and Test 7 completed in April 1999.

Test 1 differs from the subsequent tests since at this stage the restraint at the pile head was low as only the substructure of the building was in place at the time, while in the remaining tests, pile head restraint is considerably higher due to the construction of the building structure. Test 1 was also subjected to a higher thermal load ( $\Delta T = 21^{\circ}\text{C}$ ) than the following tests ( $\Delta T = 15^{\circ}\text{C}$ ). A finite element thermo-mechanical model of the test pile was also developed with the aim of recreating the observed experimental results.

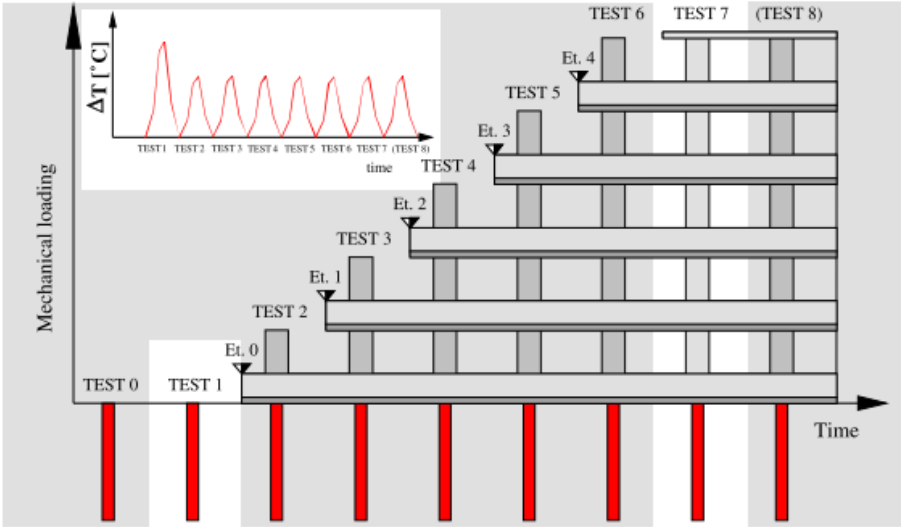


Figure 4-8. Thermo-mechanical loading history (Laloui et al., 2006).

**4.2.1.1 Thermally Induced Stresses (Test 1)**

As previously mentioned, during Test 1 no mechanical load other than the self-weight of the pile was applied and a heating-cooling cycle was imposed (12 days of heating then 16 days of natural cooling) as indicated by Figure 4-9. At this stage the restraint on the pile head was also diminished as only the substructure of the building was constructed. While the head of the pile was largely free to move, the pile was partially restrained along the pile shaft by the development of friction on the pile-soil interface and at the toe due to the presence of the sandstone. As the pile cannot expand freely, thermally induced stresses are expected to develop. Figure 4-10 illustrates the axial stress changes in the pile during Test 1 when it was subjected to a temperature increase of  $13.4^{\circ}\text{C}$ .

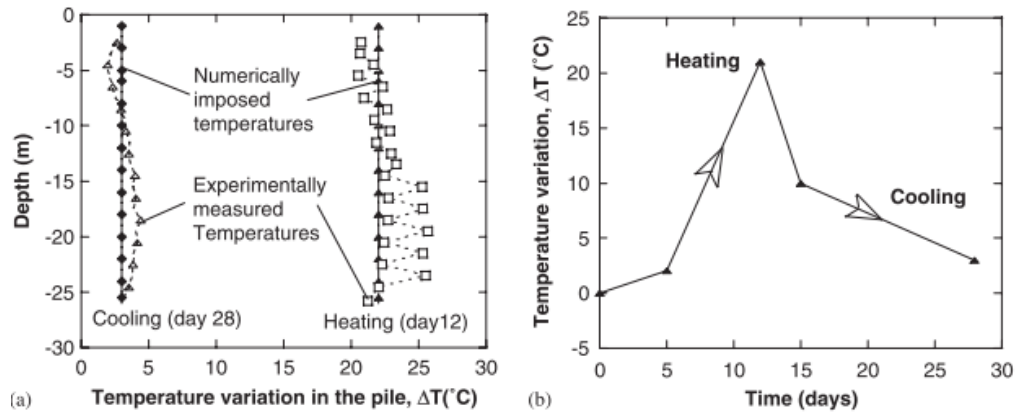


Figure 4-9. Temperature values imposed in the pile (Laloui et al., 2006).

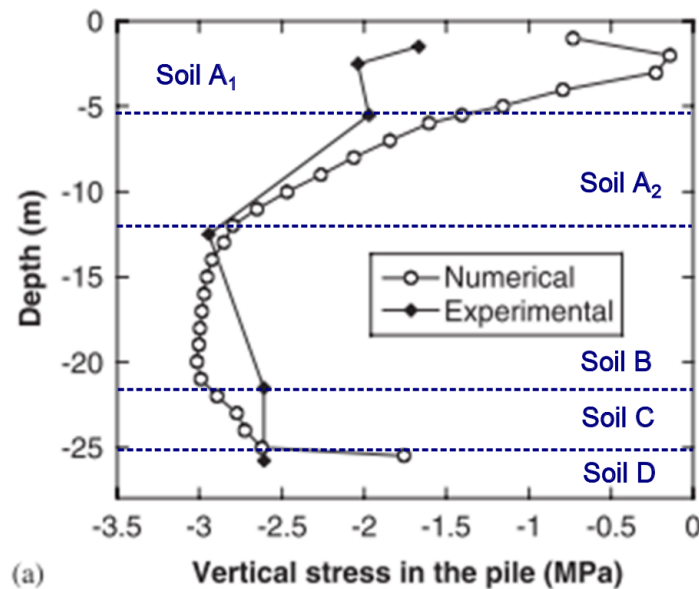
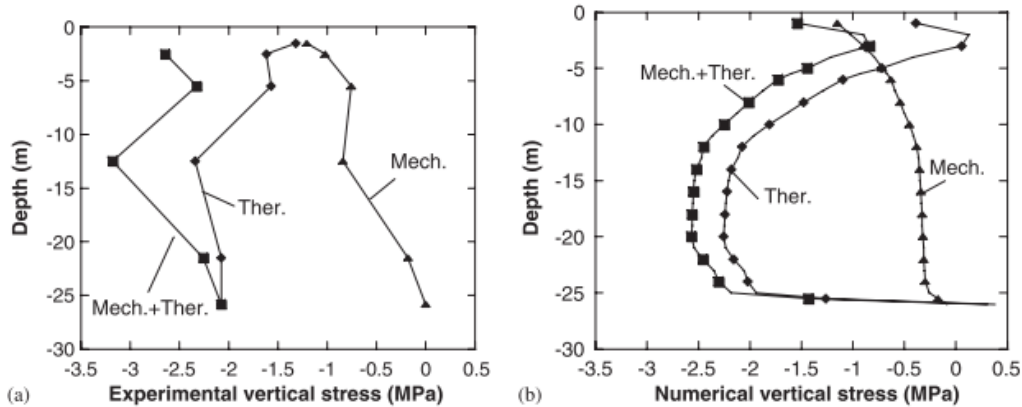


Figure 4-10. Thermal vertical stresses under a thermal load of 13.4°C (Laloui et al., 2006).

The heating thermal load led to the development of significant compressive stresses in the pile reaching a maximum value of about 3 MPa. It was also assessed that as the surrounding types of soil changed so did the stress levels, which can be seen in Figure 4-10, where the soil layers A, B, C and D can be identified. The thermal loading also led to a maximum uplift of the pile of about 4 mm.

#### 4.2.1.2 Thermal-mechanical behaviour of the pile (Test 7)

During test 7, the pile was under mechanical load due to the weight of the completed building which led to a vertical stress of about 1.3 MPa at the pile head, the load was carried entirely on the pile shaft with the toe carrying almost no load, "Mech." in Figure 4-11(a). The effect of the thermal load ( $\Delta T = +15^\circ\text{C}$ ) was quite significant as it led to a considerable compressive overstress of about 1.2 MPa at the pile head and 2 MPa at the toe ("Mech.+Ther", Figure 4-11(a)).



**Figure 4-11. Thermo-mechanical vertical stresses in the pile: (a) experimental results; (b) numerical simulations).**

Comparing the results from Figure 4-11 (a) to the ones idealized in Figure 4-5, the influence of the soil non-homogeneity over the thermally induced stresses can clearly be seen. Due to different resistance and thermal expansion properties, different soil types will induce different levels of restraint on the pile as they will mobilize different levels of interface shear stress and therefore lead to different thermally induced stresses.

The effect of the pile's end restraint can also be seen, in Figure 4-5 no end restraints are applied to the pile and therefore no thermal stresses develop in these sections. However, the pile in Figure 4-11 is restrained at its head due to the building structure above it and at its toe due to it being socketed in the sandstone. This restraint led to considerable thermally induced stress in these sections.

Laloui et al. (2006) concluded that the numerical model was found able to reproduce the complex behaviour of the energy pile and reproduced well the experimental results. However, comparing Figure 4-11(a) and (b), it can be observed that the previous statement is only true to some extent. Some flaws can be pointed in the numerical model results, especially the reproduction of the stresses induced by the mechanical load and the magnitude of the predicted thermal stresses at the pile's head which were considerably lower than those measured experimentally.

## 4.2.2 Lambeth College, London

Situated within the grounds of the Clapham Centre of Lambeth College in South London, this test pile was carried as part of a project which involves the construction of a new five-storey building. The observational results from this test pile were reported by Bourne-Webb et al., 2009. The new building is supported on bored pile foundations with 143 piles of 600 mm nominal diameter, which also incorporate heat exchange pipe loops for use in the ground-source heat-pump system. In order to better understand the impact of the thermal load over the pile's mechanical behaviour, a 23 m long, 600 mm diameter test pile was loaded to a nominal working load of 1200 kN and then subjected to cycles of heating (input temperature of +56°C) and cooling (input temperature of -6°C).

The shaded areas in Figure 4-12 (a) indicate the observed changes in axial load and mobilised shaft resistance due to the heating cycle. The heating led to a considerable increase in the pile's axial stress especially in the upper part of the pile. As the pile ends were not highly restrained, almost no additional thermal stresses were observed in these sections. Mobilised shaft resistance values were reversed over the upper part of the pile and showed an increase, relative to that under mechanical load only, in the remainder of the pile shaft.

The observed axial load and mobilised shaft resistance due to the cooling cycle are indicated in Figure 4-12 (b). As expected, tensile stresses were developed leading to a decrease in the pile's axial stress, especially at its bottom part. Mobilized shaft resistance was barely changed in the upper 6 m of the pile but then increases in the mid-part and reverses in the lower part of the pile.

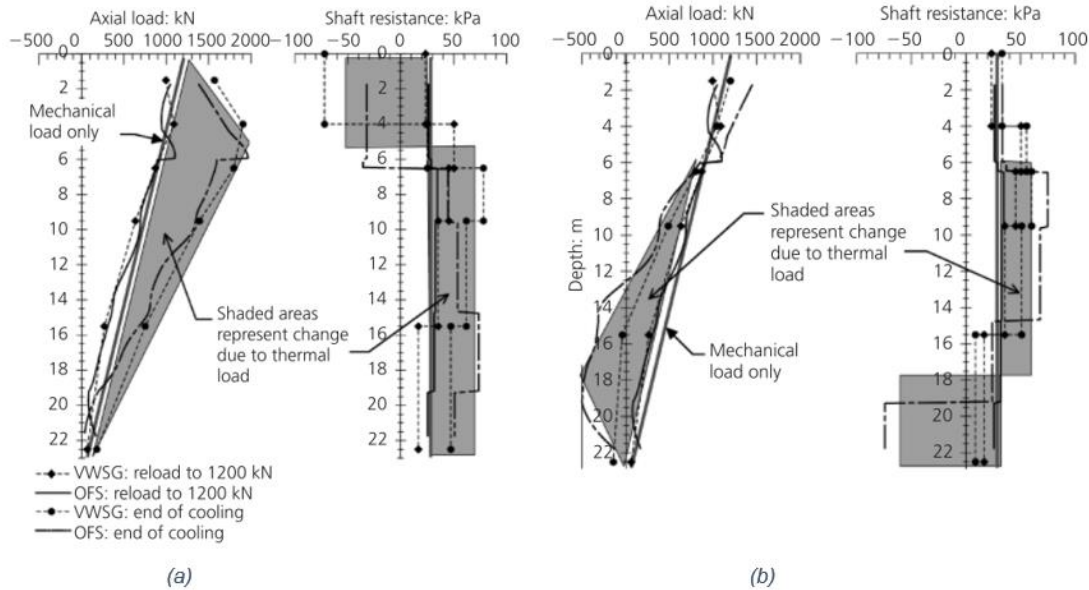


**Figure 4-12. Observed response of the Lambeth College main pile test: (a) end of heating; (b) end of cooling (Bourne-Webb et al., 2013).**

From the results shown in Figure 4-12, some asymmetry is clearly seen in the response of the pile. This is believed to be caused mainly by the details of the ground profile which comprised 5 m of fill and river terrace gravel on the upper part of the pile, and then stiff clay which stiffens with depth over the remainder of the pile depth. The construction of the pile, which features a larger diameter over the top 5 m through the fill and river terrace gravel (610 mm outside diameter), where casing was used to support the soil, than in the clay (550 mm auger diameter) can also contribute to this behaviour. Besides the observed asymmetry, the effect of the thermal load was found to be consistent with the descriptive mechanism illustrated in Figure 4-5.

## 4.3 Numerical Analysis of the Effect of Heating and Cooling a Pile

Few numerical studies have yet been published regarding the thermal-mechanical behaviour of energy piles. In this section, we will take a look at some of these studies and their respective findings and conclusions, some of which have been further investigated in this thesis.

### 4.3.1 Bodas Freitas et al., 2013 and Cruz Silva, 2012

Bodas Freitas et al. (2013) and Cruz Silva (2012), describe the development of an axisymmetric numerical model in the finite element software ADINA. A single pile with diameter of 1 m and length of 30 m was considered, the side and bottom boundaries of the finite element mesh were set at a distance of 60 m and 90 m respectively. Both the concrete making up the pile and the surrounding soil were considered as purely elastic materials with Young modulus of 30 GPa and 30 MPa respectively. Even though the soil Young modulus base value was 30 MPa an increase in this value to 60 MPa was also tested. The concrete coefficient of volumetric thermal expansion,  $\beta$ , was set to  $3.0E^{-5}K^{-1}$ , while three different values of the same parameter were tested for the soil: 0,  $1.5E^{-5}$  and  $6.0E^{-5}K^{-1}$ . The mechanical load applied to the pile (about 4.7 MN) was modelled by applying a boundary pressure of 6 MPa at the pile's head, and the thermal load, by the application of an increment of temperature  $\Delta T = +30^{\circ}C$  to all elements making up the pile, under steady state heat flow conditions.

The effect of the relationship between pile and soil coefficient of volumetric thermal expansion, the stiffness of the soil and the thermal boundary condition on the ground surface were assessed in this study. While a change in the thermal boundary condition on the ground surface won't affect the temperature of the pile, it will have a significant effect on the temperature of the surrounding soil (Figure 4-13), as the soil itself will contract or expand due to thermal load, this change will affect the pile-soil interaction.

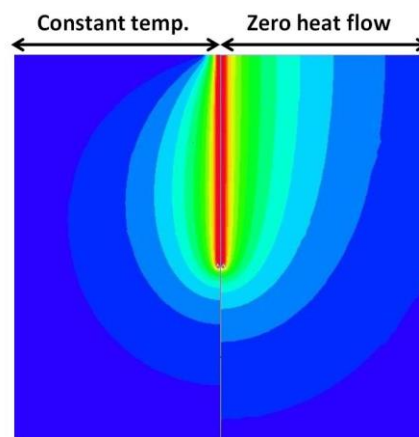


**Figure 4-13. Steady-state temperature field as function of surface thermal boundary condition (contour interval: 2°C) (Bodas Freitas et al., 2013).**

The results in terms of change in pile axial stress and pile-soil interface shear stress due to the thermal load of  $+30^{\circ}\text{C}$  are plotted in Figures 4-14 and 4-15 respectively.

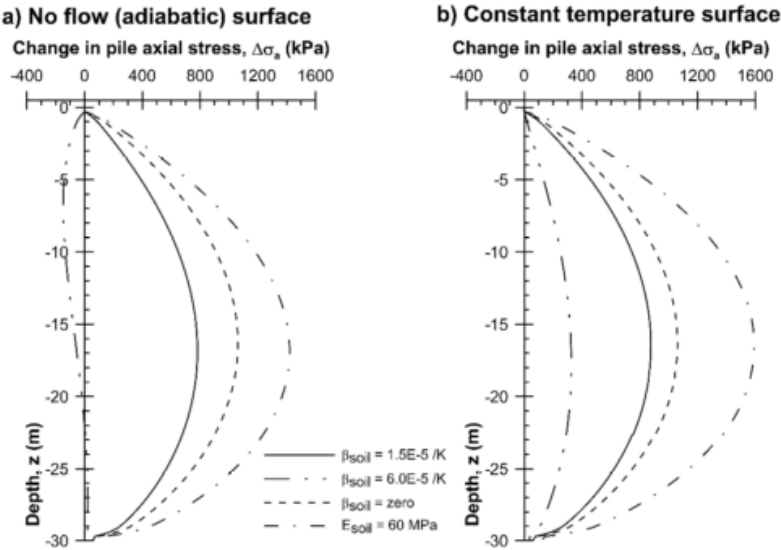


Figure 4-14. Change in pile axial stress due to temperature change of  $+30^{\circ}\text{C}$  (Bodas Freitas et al., 2013).

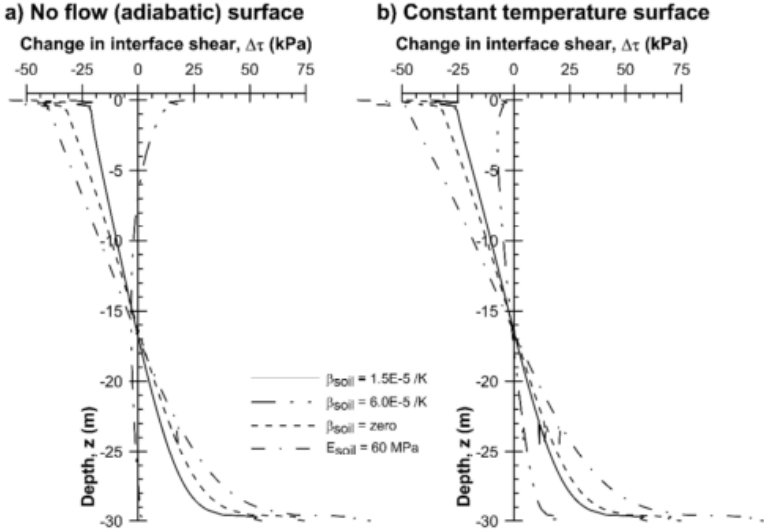


Figure 4-15. Change in pile-soil interface shear stress due to temperature change of  $+30^{\circ}\text{C}$  (Bodas Freitas et al., 2013).

From the above results, the following conclusions were made:

- Changing the soil coefficient of thermal expansion has a big impact on the resulting thermally induced stresses in the pile. When the soil was more expansive than the concrete ( $\beta_{soil} = 6E^{-5}K^{-1}$  and  $\beta_{concrete} = 3E^{-5}K^{-1}$ ) tensile axial stresses developed for the case of an adiabatic

surface, Figure 4-14 (a), while in the remaining cases (lower values of  $\beta_{\text{soil}}$  and constant temperature surface), heating led to compressive stresses;

- The applied ground surface thermal boundary condition impacts heavily the results if the soil is more thermally expansive than the concrete;
- An increase in soil Young modulus led to an increase in the thermally induced stresses, which was expected as a stiffer soil will impose more restraint on the pile.

Understanding in greater detail the relationship between the concrete and soil thermal expansion values, as well as the influence of the ground surface thermal boundary condition, is the main aim of this thesis and is further investigated in Chapters 5 and 6.

### 4.3.2 Di Donna et al., 2013

Di Donna et al. (2013) developed a numerical model with thermo-hydro-numerical coupling of a group of thermally-activated piles connected to a ground slab, which aimed to investigate the effects of cyclic temperature variations on the different aspects involved in the geotechnical design of thermally-activated pile foundations.

The foundation modelled comprised 150 piles with a diameter of 80 cm and a length of 20 m which were spaced 7 m apart in both directions. The slab was 110 m long and had a thickness of 0.5 m. Due to the symmetry of the problem and for simplicity reasons only, the numerical model was limited to 4 piles in 2D plane strain conditions (Figure 4-16). However, this simplification involves considering a circular pile as an infinite wall in the plane perpendicular to the one of the simulation. To account for this consideration, the pile axial stiffness was adjusted to an equivalent Young modulus, other parameters such as porosity and thermal conductivity were also adjusted to weighted average values. Because the deformation in the third direction is also prevented, the thermal expansion coefficient of the pile was also adjusted to the real one divided by  $(1+\nu)$ .

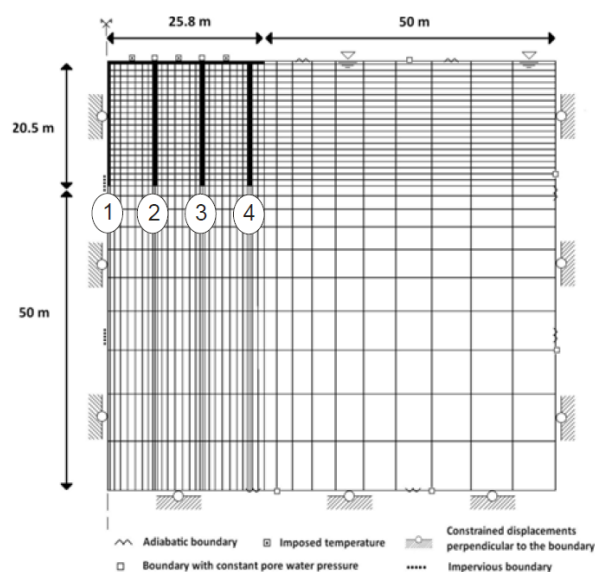


**Figure 4-16. Numerical model: geometry, mesh and boundary conditions (Di Donna et al., 2013).**

Both the concrete and the soil were considered as porous materials with a liquid and solid phase, and the whole medium was considered as fully saturated. The piles and slab are made of concrete which behaves thermo-elastically while the soil behaviour was simulated by a thermoelastic-thermoplastic constitutive model named ACMEG-T which allows for the consideration of thermal cyclic effects on the response of the material. Taking into consideration both the liquid and the solid phases, the soil presented a linear coefficient of thermal expansion of 3 m/m/K and the concrete 1.856 m/m/K, meaning that soil was approximately twice as thermally expansive as concrete. The pile-soil interface was set to behave according to the same ACMEG-T model with the same parameters as the soil but a lower angle of shearing resistance. Thermal loading of the piles was achieved by applying a heat flux in heating and cooling equivalent to 150 W/m along the pile.

The initial temperature of both soil and piles was set to 11°C while the temperature of the slab was fixed at 15°C throughout the computation which aimed to simulate a regulated temperature in the interior of the building. The remaining thermal boundary conditions of the model were set to be adiabatic.

Figure 4-17 shows the thermally induced displacements of the foundation through time due to the cyclic thermal load. Two phenomena were observed: One is cyclic vertical displacements of the foundation due to elastic dilative behaviour of the soil, which is reversible during cooling, and makes the foundation move upwards during heating and downwards during cooling. The other is an irreversible displacement induced by the cyclic thermal loading due to an increase in the soil pore water pressure during the heating phase and the following consolidation. The irreversible displacement induced a settlement of 0.3 cm (12% of the settlement induced by the mechanical load) while the elastic cyclic settlement had an amplitude of 0.6 cm. Because all the piles were heated and cooled equally no differential settlements were induced by the thermal load, however, according to the Di Donna et al. (2013), if thermal load is not equal to all piles potential differential cyclic settlements problems may occur.

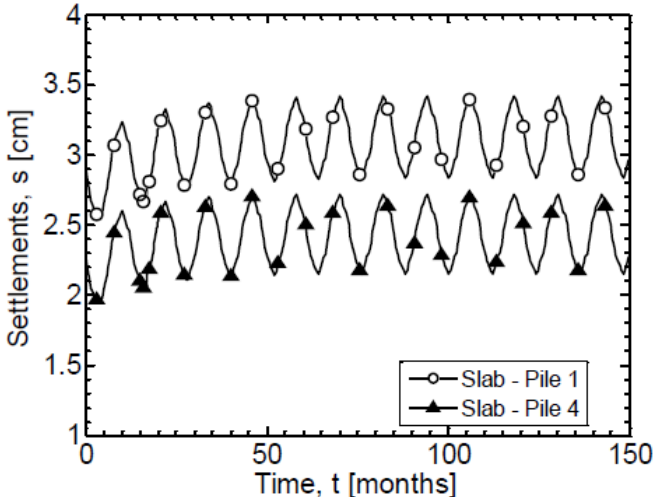


**Figure 4-17. Thermally induced displacement of the foundation (Di Donna et al., 2013).**

Figure 4-18 shows the evolution through time of the thermally induced vertical stresses in Pile 2 (Figure 4-16) at the end of a heating phase. As previously described in Section 4.1, pile heating led to an



increase of the pile compressive axial stress. These stresses were higher in the central part of the pile, which is its warmest zone, while the head and the tip have lower temperatures. In fact, when a heat flux is applied in a body, it will lead to higher temperature changes at its centre, which gradually decrease as we get closer to its edges. Because the temperature was higher in the pile centre region, more strain restraint takes place in this zone as the relative movement between pile and soil is higher. This effect leads to the higher thermally induced stresses observed in the central part of the pile.

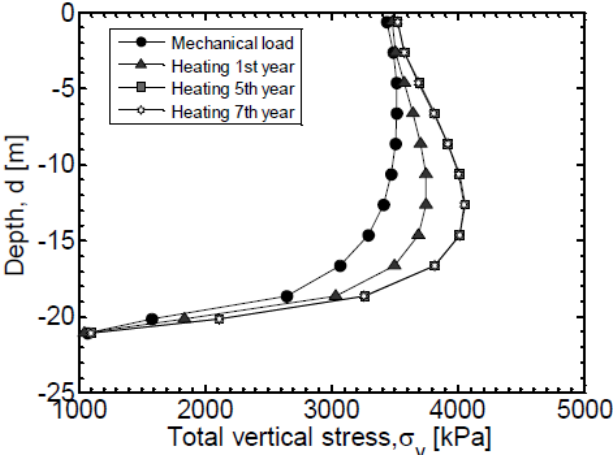


Figure 4-18. Effects of heating on the axial stress in Pile 2 (Di Donna et al., 2013).

Figure 4-19 shows the thermally induced vertical stresses in Pile 2 after the heating and cooling phases of the 5<sup>th</sup> year of analysis; beyond the 5<sup>th</sup> year the analysis predicted that the cyclic thermal effects in terms of pile axial stress stabilised, i.e. in Figure 4-18 the results for the 7<sup>th</sup> year plot on top of those for the 5<sup>th</sup> year. Because cooling leads to pile contraction, tensile thermal stresses developed during the cooling cycle leading to a decrease in the pile axial stress. The difference between the thermally induced stresses after the heating and cooling cycles seen in Figure 4-19 is believed to be caused by the soil downdrag i.e. additional pile friction caused by the downwards movement of the soil as it consolidates.

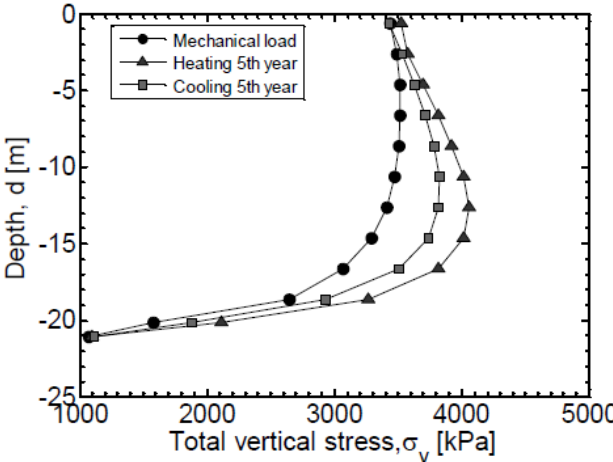


Figure 4-19. Effects of heating and cooling on the axial stress in Pile 2 (Di Donna et al., 2013).

While the thermal load led to considerable additional axial stresses in the piles, Di Donna et al. (2013) noted that these are still far away from reaching the structural ultimate state of the pile, as concrete is highly resistant to compression, and it is not likely that a cooling thermal load may induce high enough tensile stresses that these would surpass the compressive ones introduced by the mechanical load.

### 4.3.3 Suryatriyastuti et al., 2013

Suryatriyastuti et al., (2013), have developed a numerical model for a thermo-activate pile. The numerical analyses were divided in two parts: In the first part, the pile was subjected to a single thermal load and in the second part the pile was subjected to an external mechanical load and then cycles of mechanical strain equivalent to a thermal loading of  $\pm 10^\circ\text{C}$ .

The modelled pile had a diameter (d) of 60 cm and a length (L) of 15 m. The model boundary dimensions were set to ensure an adiabatic boundary condition, with a vertical dimension of 30 m (2L) and a horizontal dimension from the pile centreline of 15 m (25d). Both pile and soil were modelled as solid elements and behave as a linear thermo-elastic material. The concrete was considered three times more thermally expansive than soil.

#### 4.3.3.1 *Single pile under thermal load only*

In the single pile under thermal load analysis, the numerical model ran in two steps: Initially, the ground temperature was applied to the model according to the season of year in study (Figure 4-20). After the soil temperatures are set, the pile is heated by imposing a constant temperature at its centreline of  $5^\circ\text{C}$  during winter mode and  $25^\circ\text{C}$  during summer mode. Figure 4-21 shows the temperature profile before and after pile cooling is applied in winter mode.

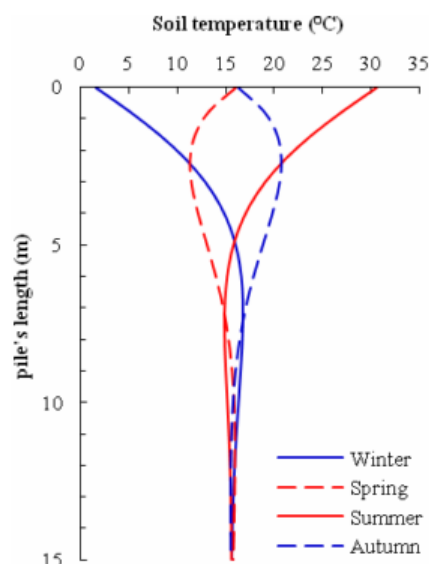


**Figure 4-20. Ground temperature profile under climatic effect (Suryatriyastuti et al., 2013).**

From Figure 4-21 it can be seen that because the ground surface and the right hand side boundary conditions of the model was defined as adiabatic, when the pile was cooled so was the hole soil mass

at the top of the model. This is however an unrealistic situation, in reality, the ground surface temperature will be imposed by the temperature of the overlying structure and the outside air temperature and should remain almost unchanged after the cooling thermal load is applied to the pile. The temperature profiles illustrated in Figure 4-13 are believed to better represent the effect of the pile heating in the surrounding soil temperature.

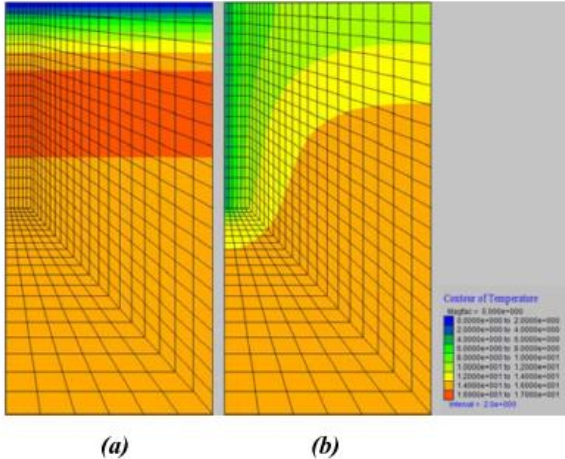


**Figure 4-21. Ground temperature profile in the winter mode: (a) the initial conditions. (b) at the end of the thermal load (Suryatriyastuti et al., 2013).**

Figure 4-22 (a) and (b) illustrate the thermally induced mechanical behaviour of the pile in terms of developed axial stress and axial displacement respectively. The heating thermal load led to pile expansion and the development of compressive stresses as part of this expansion is restrained by the surrounding soil, while the cooling thermal load led to the opposite behaviour. These results are in accordance to the theoretical ones previously described (Figure 4-3), with the difference that in this case the pile is partially restrained at its base by the soil, leading to non-symmetrical stress and displacement profiles.

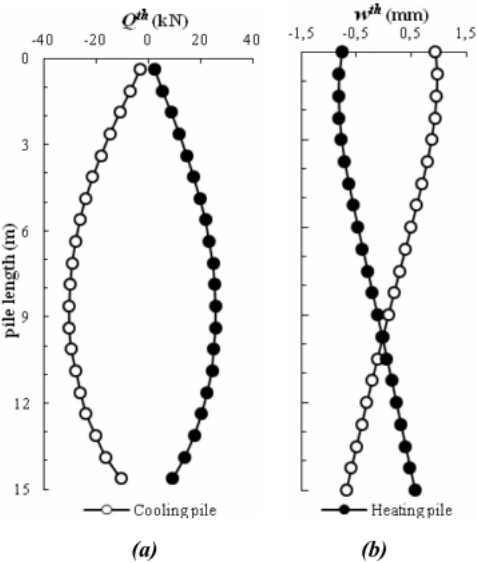


**Figure 4-22. Thermally induced mechanical behaviour of the pile at winter and summer mode: (a) thermal axial force (b) thermal axial displacement (Suryatriyastuti et al., 2013).**

### 4.3.3.2 Combined mechanical and cyclic thermal loading

In this analysis, the pile is initially mechanically and incrementally loaded up to 33% of its ultimate static load resistance. After the mechanical load is applied, cycles of mechanical strain equivalent to a thermal loading of  $\pm 10^\circ\text{C}$  were imposed on the pile. The magnitude of the strain cycles was calculated according to Equation 4-1 (free thermal strain) which admits that no restraint is applied to the pile. Some criticism can be made regarding this decision since by simulating the thermal load with additional strains in the pile and not actually by heating and cooling it, part of the thermal-mechanical interaction between the pile and soil is lost, and implies that the soil is unaffected by temperature change. A total of 24 cycles of strain were applied to the pile starting with strain equivalent to a cooling cycle and followed by strain equivalent to a heating cycle. Interface elements were introduced at the pile-soil contact zone following a constitutive interface law called Modjoin which is capable of modelling cyclic degradation phenomena.

Figure 4-23 shows the evolution of the pile head settlement due to the thermal cycles. The cooling thermal load led to contraction of the pile and therefore an increase in the pile head settlement while the opposite behaviour happened when a heating cycle took place. At the end of all the thermal cyclic loading, an additional plastic settlement of 3 mm (7% of the settlement induced by the mechanical load) was verified due to the degradation of the pile-soil interface resistance through the thermal cycles.

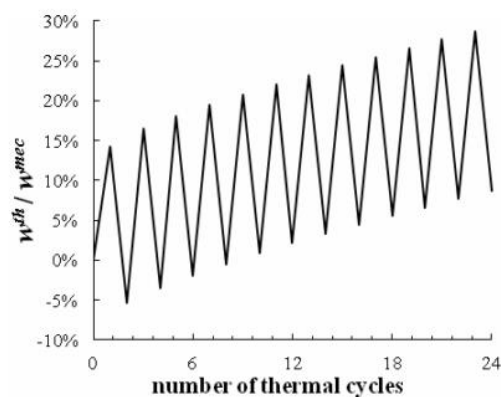
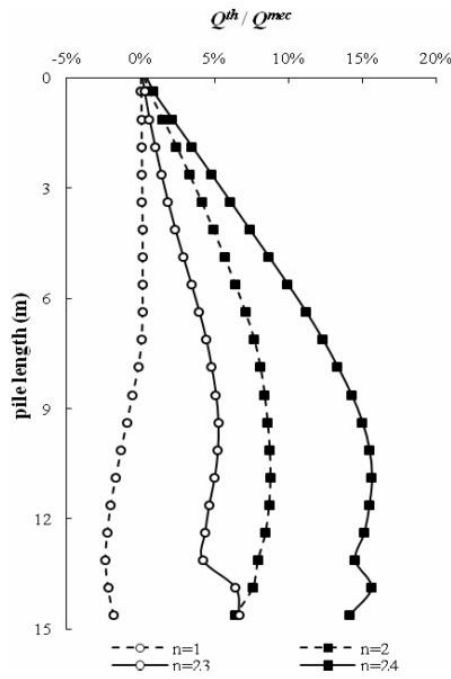


Figure 4-23. Cyclic variation in the pile head displacement (Suryatriyastuti et al., 2013).

Figure 4-24 illustrates the axial normal force on the pile at the beginning and at the end of the thermal cycles. It was observed that the variation in normal force increased more in heating cycles than in cooling ones, this happens because when the pile is expanding the pile-soil interface generated more restraint than when it contracts. At the end of the 24<sup>th</sup> cycle, a maximum normal force increase of 16% relative to the value induced by the mechanical load was predicted.



**Figure 4-24. Thermally induced normal force at the beginning and at the end of the thermal cycles (Suryatriyastuti et al., 2013).**

Suryatriyastuti et al. (2013) concluded that the cyclic degradation of the mechanical resistance of thermally activated piles is not negligible and should be taken into account in the geotechnical design of such piles. While this conclusion is true for the particular set of parameters used, no evidence of cyclic thermal degradation in thermo-active piles has yet been demonstrated in reality and the cyclic degradation reported in this study is probably a mere consequence of the constitutive law adopted for the interface.



# Chapter 5

## Thermal Analysis

In this chapter the results of a series of numerical thermal analyses are presented and discussed. These analyses were performed in order to better understand the pile-soil interaction problem from a purely thermal point of view, and to determine some of the thermal properties of the numerical thermal-mechanical model used in Chapter 6.

## 5.1 Introduction

In the analysis of the response of thermally activated pile foundations, a complex interaction resulting from the temperature field (and especially the surface temperature) and the thermal and mechanical properties of the pile and the soil, in particular the coefficient of thermal expansion, has been highlighted (Bodas Freitas et al. 2013, Cruz Silva, 2012).

In this section, and in order to better understand the first part of this interaction problem (i.e. the temperature field), the heat exchanger pile problem was studied from a purely thermal point of view and the following aspects were investigated:

- The simulation of the pile thermal load in a numerical model;
- The effect of soil and concrete thermal conductivity values;
- Heat loss through ground slabs and ground surface temperature.

Some of the findings and conclusions reported in this section are later implemented in a thermal-mechanical numerical model (Chapter 6) in order to investigate their influence in the thermo-mechanical response of a pile.

## 5.2 Thermal Load through the Pile

Thermal load on piles is often simulated in numerical models by applying a constant temperature increase or a heat flux to all elements or nodes constituting the pile. In reality, heat flows from absorber pipes which are either placed close to the centreline of the pile or close to the pile edge where the pipes are attached to the reinforcement cage. (Figure 5-1). This means that the temperature in the pile is not uniform and tends to be higher near the pipes, where the heat exchange fluid circulates, and reduces with distance from them.

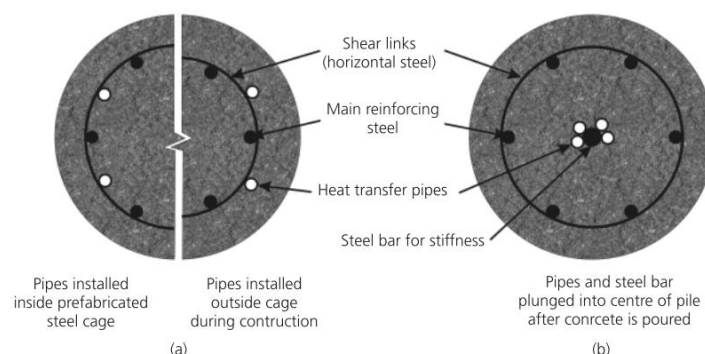


**Figure 5-1. Usual thermo-active pile construction details: (a) absorber pipes fixed to a pile reinforcement; (b) absorber pipes installed in the centre of the pile (Powrie & Loveridge, 2013).**



The main objectives of the analyses performed in this section are to assess how the heating of the pile is simulated affects the temperature field of the model and if the pile thermal load can be simplified by the application of constant temperature or a heat flux all over the pile or if the absorber pipe geometry should be modelled.

In order to look at the temperature fields both in depth and in plan, two finite element models were developed using the software Abaqus: one was axisymmetric and the other two-dimensional (2D). Alternatively it would also be possible to create a single 3D model but due to the added complexity that this required, the former option was preferred.

### 5.2.1 Axisymmetric Thermal Model

In many cases, piles are axisymmetric bodies and they can be numerically modelled by an axisymmetric 2D model. While presenting identical results, the use of an axisymmetric model instead of a 3D model presents a considerable advantage in terms of calculation time because the 3D model will require a much higher number of finite elements.

The pile has a diameter of 1 m and is 30 m deep, the bottom and side boundaries of the finite element model were set at a distance of 90 m (3L) and 60 m (2L) respectively. Bottom and side thermal boundaries were defined at a constant 12°C in accordance to Figure 2-1, while the top boundary was defined as having no heat flux (adiabatic) since in this study we don't want to take into consideration the effect of the outside temperature. All the elements in the model have an initial temperature of 12°C. The geometry, boundary conditions and mesh configuration of the model are indicated in Figure 5-2. Two different materials, concrete and soil, whose thermal properties are indicated in Table 5-1 were created. The pile is modelled with solid elements assigned the properties for concrete while the surrounding ground is modelled with solid elements assigned the properties for soil. Since only thermal conduction will take place in the model, no mechanical properties need to be specified.

	Soil	Concrete
<b>Thermal Conductivity ,k (W/m. K)</b>	1	2
<b>Specific Heat, c (J/kg. K)</b>	1220	940
<b>Density, ρ (kg/m<sup>3</sup>)</b>	1600	2450

**Table 5-1. Soil and concrete thermo-physical properties used in the base analysis.**

In Abaqus, in order for two bodies in contact to transfer heat by conduction, an interface thermal conductance value must be defined, which is a property that indicates the ability of an interface to conduct heat. As soil is a granular material and concrete has a rough surface, a perfect contact between these bodies is impossible to achieve and thermal resistance will develop in this interface mainly due to voids existing between the two surfaces. Interface thermal conductance is defined as the ratio between

the temperature drop at the interface and the average heat flow that crosses it. An interface thermal conductance value of  $25 \text{ W/m}^2$  was adopted for the current numerical model, the same value used in the thermal study of ground slab heat loss performed by Rees & Thomas (2009). This paper by Rees & Thomas was the only literature found which comments on soil-concrete interface thermal conductance, therefore, there is a clear lack of knowledge regarding this subject. The interface thermal conductance value of  $25 \text{ W/m}^2$  led to a temperature drop at the concrete-soil interface of about  $0.5^\circ\text{C}$ , when a temperature increase of  $15^\circ\text{C}$  was applied to the pile, which was found appropriate to represent soil-concrete interface thermal resistance. The sensitivity of the results to the interface thermal conductance was checked in Section 5.2.1.2 (Figure 5-9).

As thermal conduction analysis is considerably less complex than a mechanical or thermo mechanical pile analysis, coarser meshes can be used. The finite element mesh (Figure 5-2) was finer in the body of the pile and in the soil near it and coarsens as we get closer to the side and bottom boundaries of the model where the heat flux will be lower. A total of 864, 4 node heat transfer elements were used in the model.

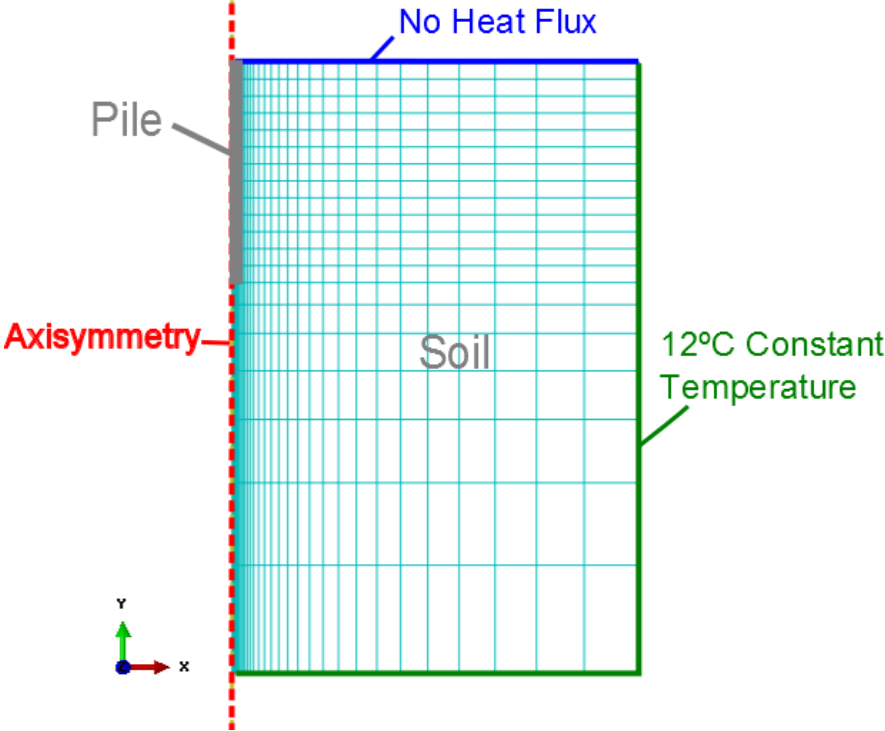


**Figure 5-2. Axisymmetric thermal model: finite element mesh and thermal boundary conditions.**

The model runs in two steps: an initial step where the boundary conditions and the initial temperature of all elements are applied followed by a heat transfer step where the heating of the pile occurs.

**5.2.1.1 Axisymmetric Thermal Analysis: methodologies and objectives**

The main objective of this model was to determine whether or not the way the heating of the pile is simulated significantly affects the temperature field close to it once a steady state is reached. Three modes of pile heating were simulated: centreline heating, edge heating and full body heating whose

characteristics are as follows:

- **Centreline Heating:** The pile is heated up to a constant temperature of  $30^{\circ}\text{C}$  ( $\Delta T = +18^{\circ}\text{C}$ ) on the centreline over its full length. (Figure 5-3 (a)). This heating mode aims to simulate the case where the absorber pipes are placed in the centre of the pile Figure 5-1 (b).
- **Edge Heating:** The pile is heated up to  $30^{\circ}\text{C}$  ( $\Delta T = +18^{\circ}\text{C}$ ) along a line which runs the depth of the pile and is located at a distance of  $0.375\text{ m}$  ( $0.75R$ ) from the pile centreline (Figure 5-3 (b)). This heating mode aims to simulate the case where the absorber pipes are attached to the reinforcement cage, close to the edge of the pile. Figure 5-1 (a).
- **Full Body Heating:** All elements making up the pile are heated to  $30^{\circ}\text{C}$  ( $\Delta T = +18^{\circ}\text{C}$ ) (Figure 5-3 (c)). This is the heating mode usually adopted in many published numerical studies of thermal active piles.

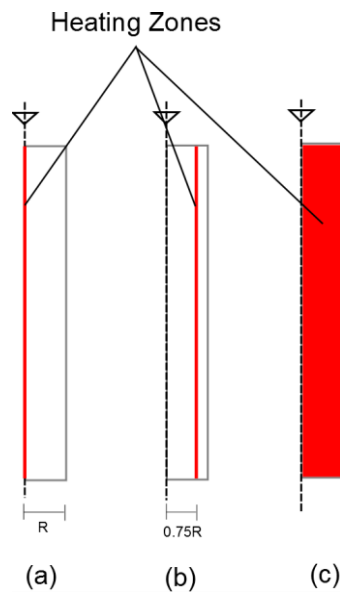


**Figure 5-3. Modes of heating: (a) centreline heating; (b) edge heating; (c) full body heating.**

In order to assess if the three heating modes previously described produce similar temperature fields or not, steady state analyses were run for each of these and the results compared.

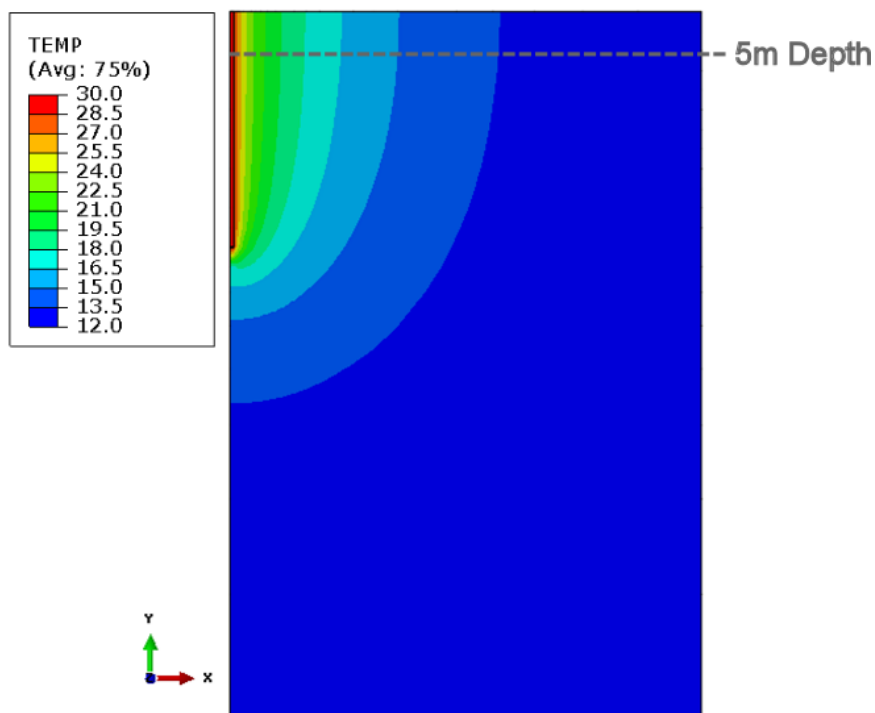
The second objective of the axisymmetric thermal study was to assess the influence of the values of thermal conductivity assumed for the soil and concrete on the temperature fields obtained. To do so, four steady state analyses were carried for each of the edge heating and centreline heating modes. In each of these four analyses, soil and concrete thermal conductivity values were varied as follows:

- **Base Case:** In the base case, soil and concrete thermal conductivity values were those indicated in Table 5-1 ( $k_c = 2\text{ W/m.K}$ ;  $k_s = 1\text{ W/m.K}$ ) and are the values that were used in the remaining thermal analysis performed in this thesis. In the base case concrete is twice as thermally conductive as soil.

- **Opposite case:** In this case, the thermal conductivity values from the base case were swapped meaning the thermal conductivity of the soil was twice that of the concrete ( $k_c = 1 \text{ W/m.K}$ ;  $k_s = 2 \text{ W/m.K}$ );
- **Soil three times more conductive:** In this case, the thermal conductivity of the soil was assumed to be three times more than that of the concrete ( $k_c = 1 \text{ W/m.K}$ ;  $k_s = 3 \text{ W/m.K}$ );
- **Concrete three times more conductive:** In this case, the thermal conductivity of the concrete was three times more than that of the soil ( $k_c = 3 \text{ W/m.K}$ ;  $k_s = 1 \text{ W/m.K}$ ).

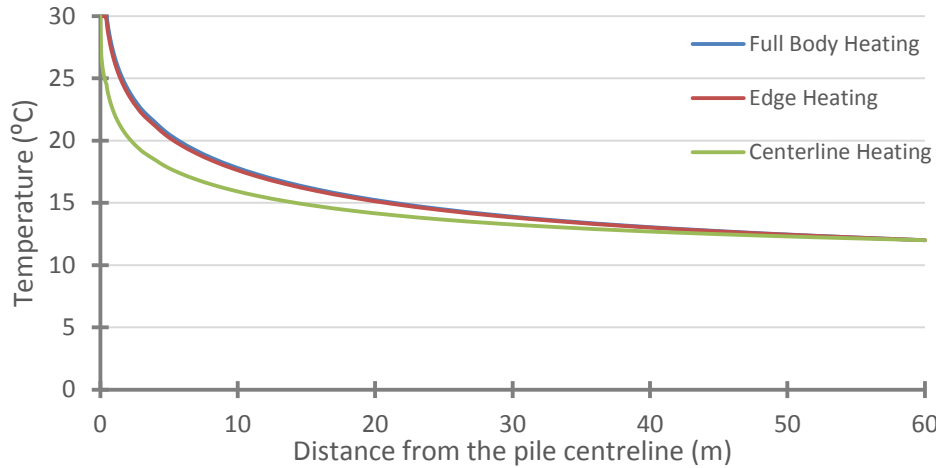
### 5.2.1.2 Axisymmetric Thermal Analysis: Results and Discussion

Figure 5-4 shows the temperature field predicted after a steady state was reached for the base case thermal conductivity values and for the case of full body heating, meaning that all the elements forming the pile were heated up to 30°C from the initial temperature of 12°C. As expected, temperatures decreased radially from the pile to the edges of the model where the temperature was kept constant at 12°C.



**Figure 5-4. Model temperature field at steady state for the full body heating case and for the base case thermal conductivity values.**

Figures 5-5 and 5-6 show the temperature profiles obtained along a horizontal line at a depth of 5m (dashed line in Figure 5-4) and for the three heating modes previously mentioned.



**Figure 5-5. Radial temperature profiles at a 5m depth.**

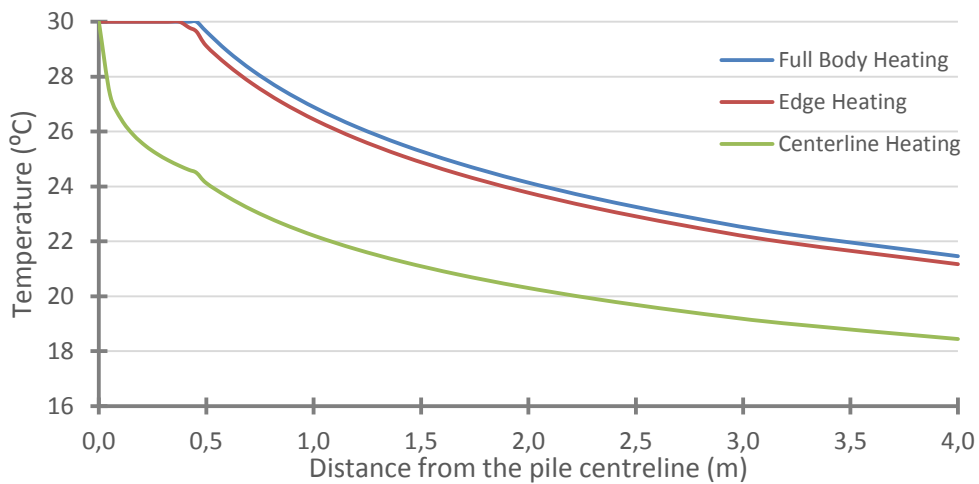


**Figure 5-6. Radial temperature profiles at a 5 m depth (zoomed closer to the pile).**

It can be seen from Figures 5-5 and 5-6 that while edge heating and full body heating led to similar temperature profiles, the difference between each being less than half a degree, centreline heating led to considerably lower temperatures; about 5°C at the pile-soil interface ( $R=0.5$  m) when compared to the other two heating cases.

It can be concluded from these results that if the thermal pile being modelled has its absorber pipes placed close to edge of the pile (Figure 5-1 (a)), full body heating, which is often used in numerical simulations, will produce similar results to edge heating and is therefore a reasonable approximation. However, if the absorber pipes are placed along the centreline of the pile (Figure 5-1 (b)), pile heating should not be simulated as a full body heating and centreline heating should be adopted.

Figures 5-7 and 5-8 show the temperature profiles obtained alongside a horizontal line at a depth of 5 m for the four combinations of thermal conductivity values previously mentioned and for centreline heating and edge heating modes respectively. The profiles shown are only for the first 4 m radially of the model which include the pile section (0 to 0.5 m) and 3.5 m of surrounding soil. In these figures,  $k_c$  and  $k_s$  represent the thermal conductivity of concrete and soil respectively.

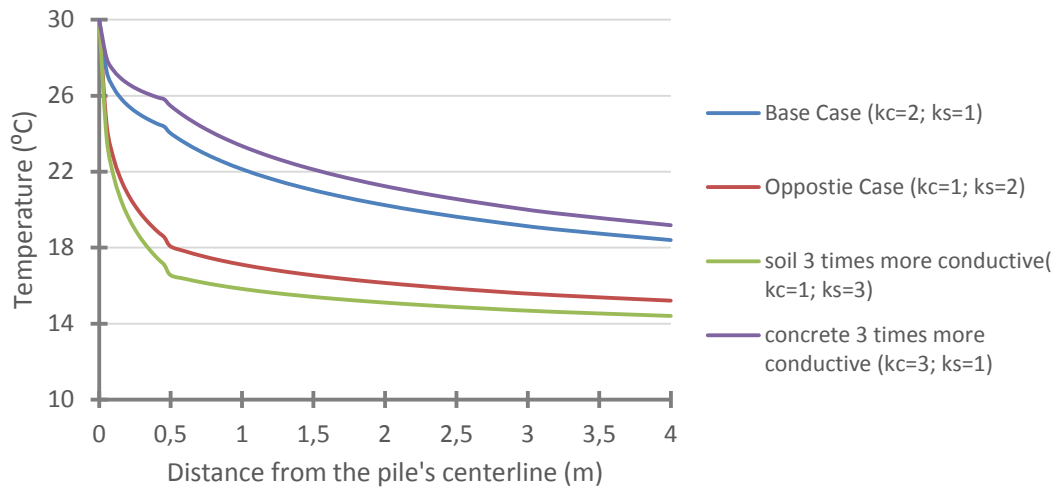


**Figure 5-7. Radial temperature profiles at a 5m depth with centreline heating.**

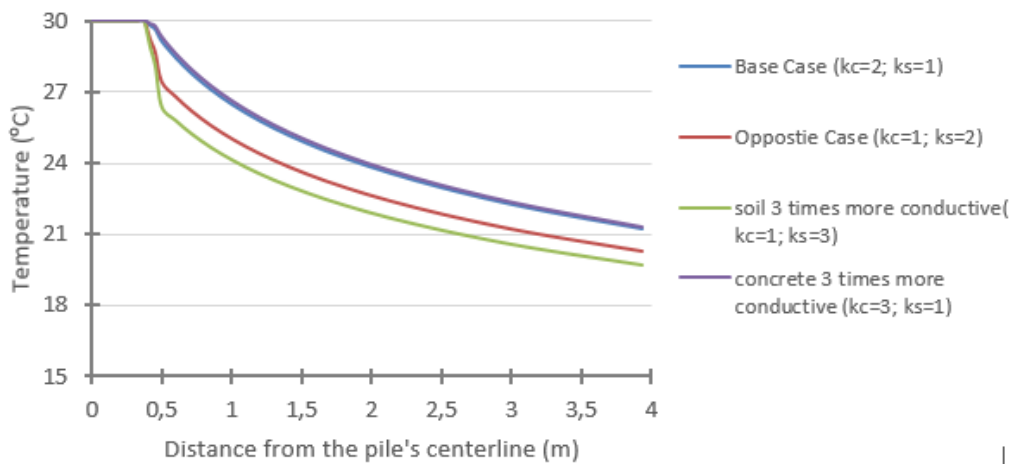


**Figure 5-8. Radial temperature profiles at a 5m depth with edge heating.**

From Figures 5-7 and 5-8 the following conclusions can be taken:

- The influence of both soil and concrete thermal conductivity was more significant for the centreline heating case (Figure 5-7) than for the edge heating case (Figure 5-8). These results were expected since with centreline heating, heat flows from the centre of the pile and has to be thermally conducted through the concrete pile and into the soil while in case of edge heating, only the concrete cover to the reinforcement cage will affect the thermal flow and the pile body will be at a fairly constant temperature. Therefore, with full body heating and edge heating the pile will play a lesser role in the overall heat transfer process.
- An increase in concrete thermal conductivity will lead to higher temperatures overall as it will be able to transfer heat from the heating source in the pile into the remaining elements of the pile and into the soil more quickly. When the soil thermal conductivity is increased, the opposite happens and lower temperatures were obtained due to the soil being able to transfer heat from

the model's boundaries faster, which are at a constant 12°C, and the model reaches a steady state at lower temperatures.

As previously mentioned, in order for two bodies in contact to transfer heat by conduction an interface thermal conductance value must be defined, which indicates the ability of the interface to conduct heat. In order to evaluate the sensitivity of the results to this parameter, the temperature profiles at a depth of 5m and for different thermal conductance values were plotted (Figure 5-9). In this figure the thermal properties of both soil and concrete are those of the base case (Table 5-1) and the pile heating method was edge heating.

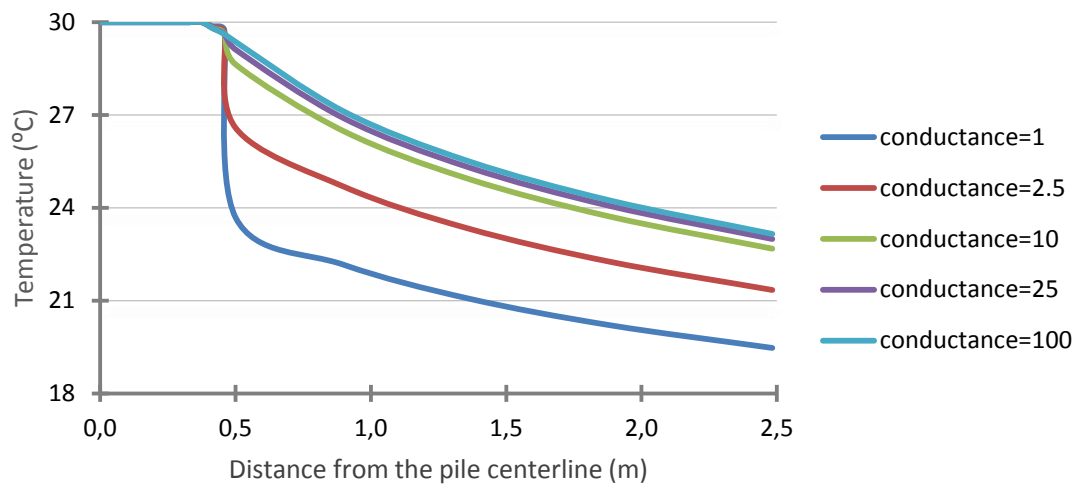


**Figure 5-9. Influence of the interface thermal conductance value.**

From Figure 5-9 it can be seen that the thermal conductance value of 25 W/m<sup>2</sup>, which was adopted for the thermal and thermal-mechanical analyses, leads to a temperature drop at the interface of about 0.5°C when the pile is heated from 15°C to 30°C. As expected, because the heat flux that reaches the interface is constant in each of these cases, the temperature drop at the interface was proportional to the thermal conductance value defined.

## 5.2.2 2D Thermal Model

As previously mentioned, a 2D thermal model was also developed in order to see temperature profiles in plan since the previous axisymmetric model only allowed us to see temperature profiles in depth. In the 2D thermal model, we take advantage of the bi-directional symmetry of the problem and only one fourth of the pile and the surrounding soil is modelled. As in the axisymmetric model, the pile diameter is 1 m and the side boundary of the model was set at a distance of 60 m. The geometry, boundary conditions and mesh configuration of the model are indicated in Figure 5-10. The initial temperature of all elements is set to 12°C. The same materials and their associated thermal properties described in Table 5-1 were used.

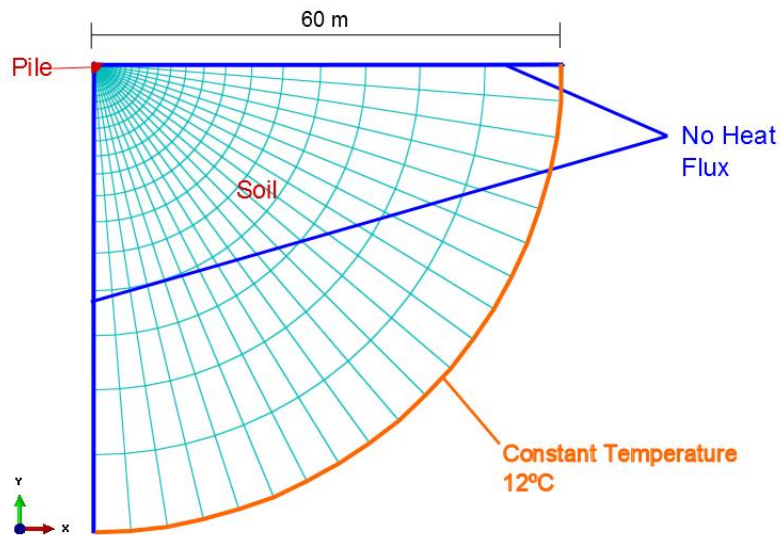


**Figure 5-10. 2D Thermal Model: finite element mesh, geometry and thermal boundary conditions.**

Two different pile configurations were considered:

- **Ring Configuration:** In this configuration the pile is heated along a circular line located at a distance of  $0.75R$  from the pile centre (Figure 5-11). This case corresponds to what is modelled when “edge heating” is used in an axisymmetric model (Figure 5-3 (b)).

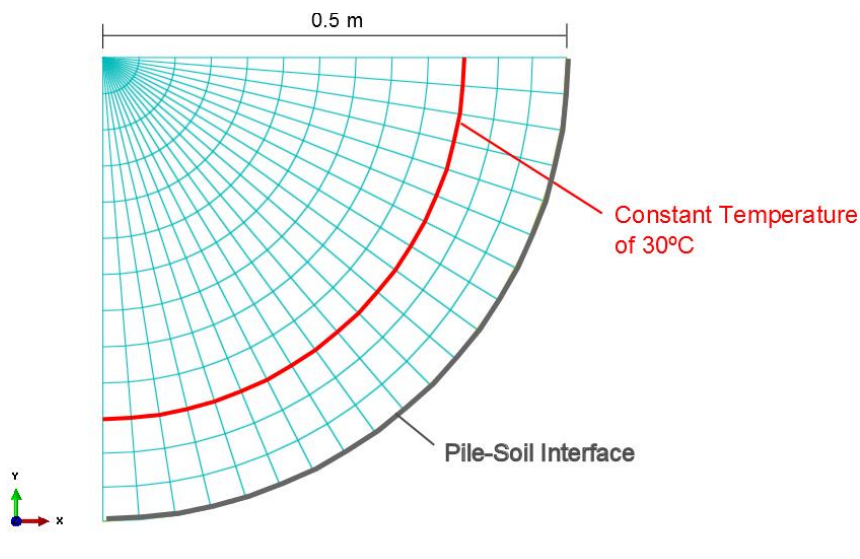


**Figure 5-11. Pile ring configuration.**

- **Pipe Configuration:** With this configuration, the aim is to model what really happens in a thermo-active pile. As the hot water circulates through the pipes of the pile, the pipe walls will heat and this heat will transfer by conduction to the pile and soil. A standard thermal pile



configuration was modelled (Figure 5-12), where the 1 m diameter pile contains 4 pairs of pipes. The pipe diameter is 0.038 m and they are placed at a distance of 0.39 m from the pile centre (approximating the position of the tubes when attached to the inside of a reinforcement cage).

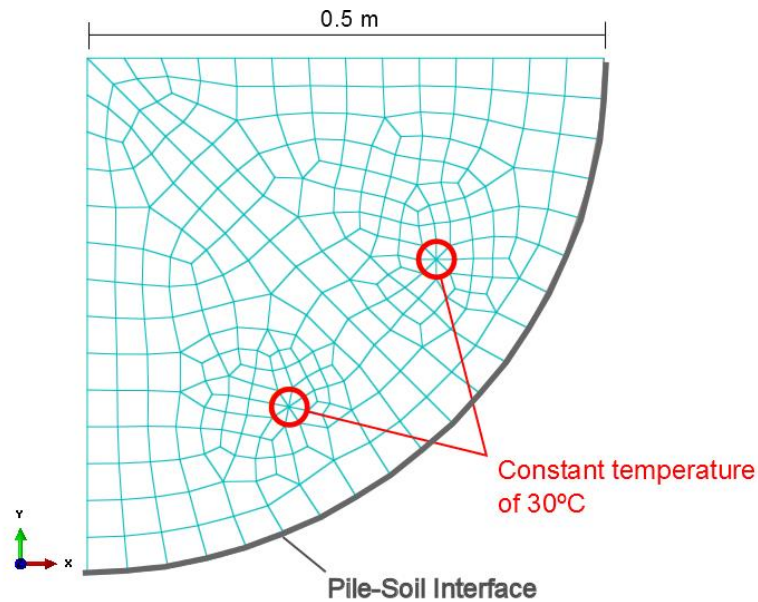


**Figure 5-12. Pile pipe configuration.**

The model runs in two steps: an initial step where the boundary conditions and the initial temperature of all elements are applied followed by a heat transfer step where the heating of the pile occurs.

### **5.2.2.1 2D Thermal Analysis: methodologies and objectives**

The aim of these analyses was to determine whether or not the thermo-active pile problem can be simplified and studied with an axisymmetric model where heating in the ring configuration will take place or if the pipe layout should be modelled which would require the development of a 3D a model. Both steady state and transient analyses were performed for the two configurations previously described, circular and pipe layout and the resulting temperature fields compared. The initial temperatures of all elements is 12°C while the temperature of the red zones indicated in Figures 5-11 and 5-12 were raised to a constant temperature of 30°C ( $\Delta T = +18^{\circ}C$ ) in order to simulate the thermal load on the pile.

### **5.2.2.2 2D Thermal Analysis: results and discussion**

The evolution with time of the temperature field in the pile and the surrounding soil is shown in Figure 5-13. Figure 5-14 shows the evolution of the temperature at the pile-soil interface until a steady state is reached. The temperature at the pile-soil interface is important as it is the relationship between the temperature of the pile and the surrounding soil together with their respective thermal expansion values

that are expected to dictate the thermo-mechanical response of the pile-soil system.

The transient analysis highlights a considerable difference in terms of temperature levels in the pile and surrounding soil for the two configurations studied, especially during the first weeks of heating. The pipe configuration led to lower temperature levels in the pile than the ring configuration during the first weeks (Figure 5-13). However, the difference between the two cases diminishes as time passes and as we get closer to a steady state where similar temperature levels were displayed (Figure 5-14).

It can be concluded that for a steady state analysis of the thermal active pile problem, the definition of a pipe configuration is not necessary which means that the ring configuration, typically modelled in an axisymmetric study, is a good approximation of reality. However, if either a transient analysis is carried out, where the behaviour of the pile during the first weeks of functioning is the object of study or if the thermal load is changing with time, the pipe configuration should be adopted and a 3D model of the pile is therefore required.

It can also be observed from Figure 5-13 that the concrete heated faster than soil due to both its higher thermal conductivity and lower specific heat.

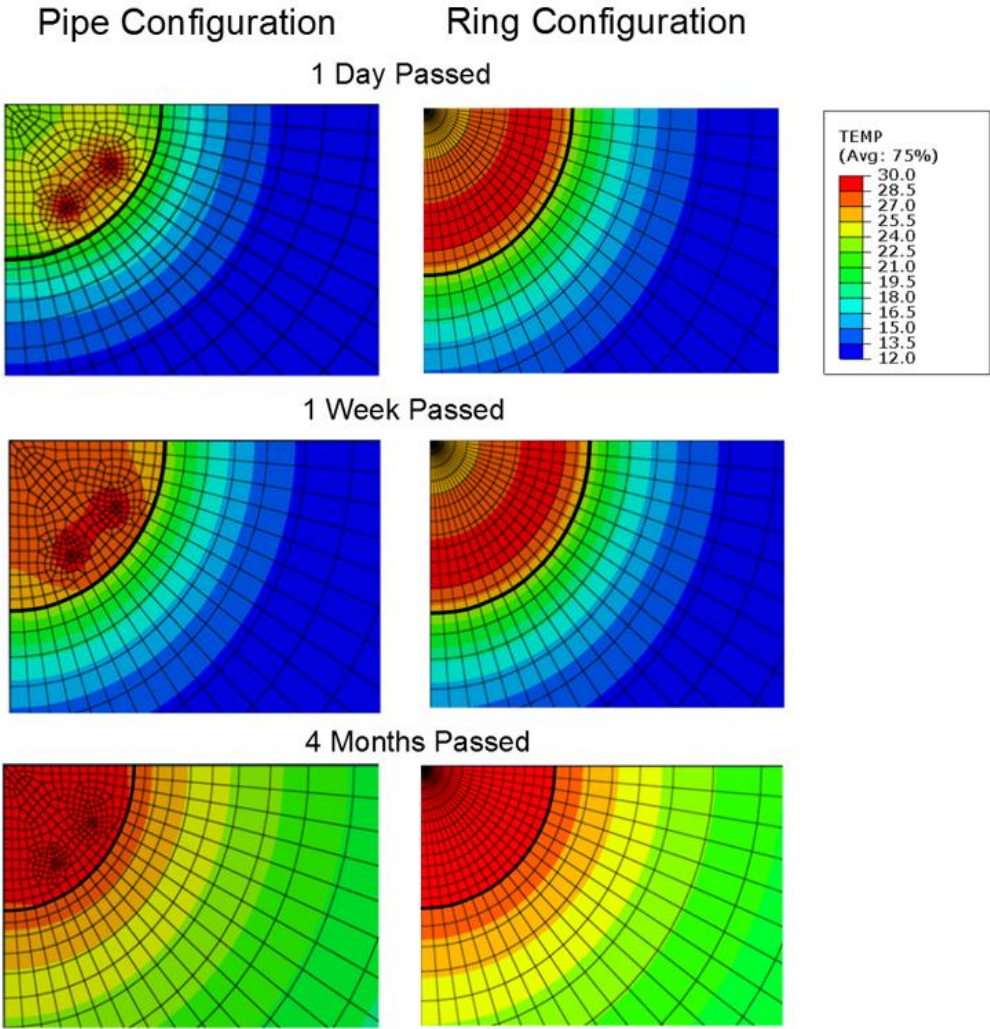


**Figure 5-13. Temperature fields through time for the two pile configurations (the bold black lines represent the pile-soil interface).**

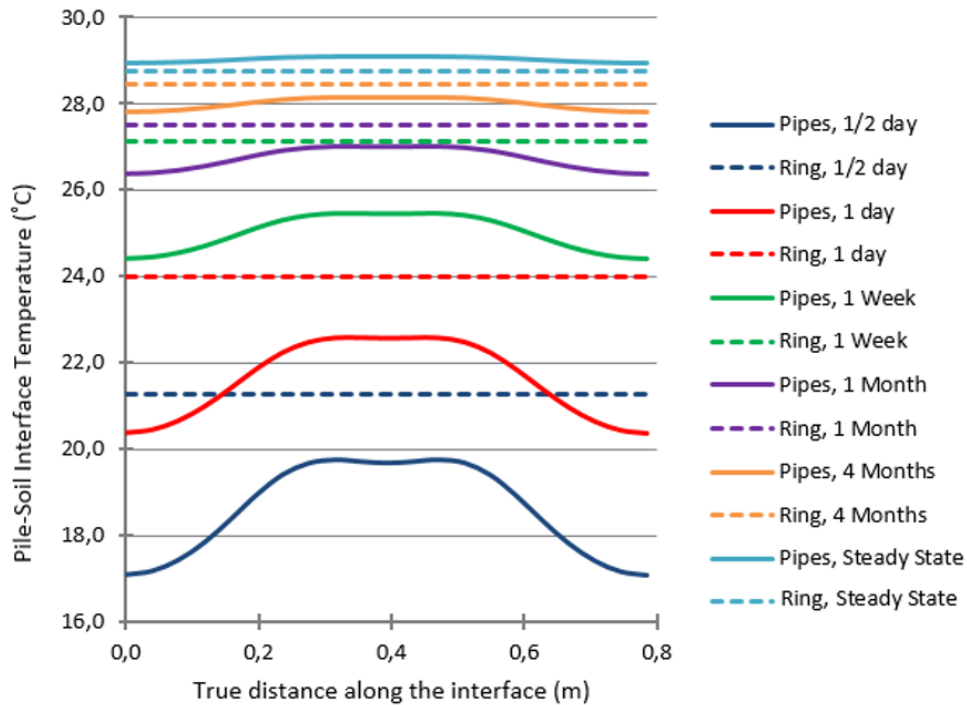


**Figure 5-14. Pile-soil interface temperature profiles around pile circumference through time and at the steady state.**

## 5.3 Thermal Loss through the Ground-Floor Slab and Ground Surface Temperature

Bodas Freitas et al., 2013, reported the significant influence of the ground surface temperature on the behaviour of a thermo-active pile in particular when the soil is more thermally expansive than the concrete. In a numerical simulation, the definition of the ground surface temperature will significantly affect the temperature of the soil, dictating how much it will expand or contract relative to the pile and therefore their thermo-mechanical response.

In this section we want to investigate what temperature values are to be expected at the ground surface below a building which is constructed in accordance with current regulations for thermal isolation. As part of a building's foundations, thermal piles are placed beneath it and the ground surface temperature will be conditioned by the heat flows incoming from both the building's interior and from the exterior environment. This study determined what values to adopt for the surface temperature in the thermo-mechanical numerical study presented in Chapter 6.

### 5.3.1 Numerical Model Implementation

An axisymmetric model consisting of a ground slab underlain by soil was developed using the finite element software Abaqus. The slab has a thickness of 0.4 m and a thermal conductivity of  $0.1 \text{ W/m.K}$  resulting in a U-value of  $0.25 \text{ W/m}^2\text{K}$ . The U-value of a construction element is defined as the ratio

between its thermal conductivity and its thickness and describes the amount of heat loss that occurs through this element (Eurima, 2011). The higher the U-value the worse are the insulation characteristics of the element and therefore the more energy heat is lost. Even though there is no current regulation on ground floor slabs U-values in Portugal, in the United Kingdom, for instance, the U-value for a ground floor slab must lie between  $0.20 \text{ W/m}^2\text{K}$  and  $0.25 \text{ W/m}^2\text{K}$  (Eurima, 2011).

Two slab radii were examined, 15 m and 30 m which considering the axisymmetry of the model correspond to a 30 m and 60 m diameter building respectively. The overall model dimensions are the same as indicated in section 5.2.1. The surface of the slab was maintained at a constant temperature of  $20^\circ\text{C}$ , which intended to recreate the fairly constant comfort temperature that we can expect inside a modern building environment.

The mesh geometry and thermal boundary conditions for the case of a 30 m slab are indicated in Figure 5-15, the mesh was made thinner at the top of the model and specially near the edge of the slab, where greater heat fluxes are expected, and gradually coarsens up as we get closer to the model boundaries where heat fluxes will be minimal. The model contains a total of 828 four node heat transfer elements which all have an initial temperature of  $12^\circ\text{C}$ . Soil properties are as previously indicated in Table 5-1.

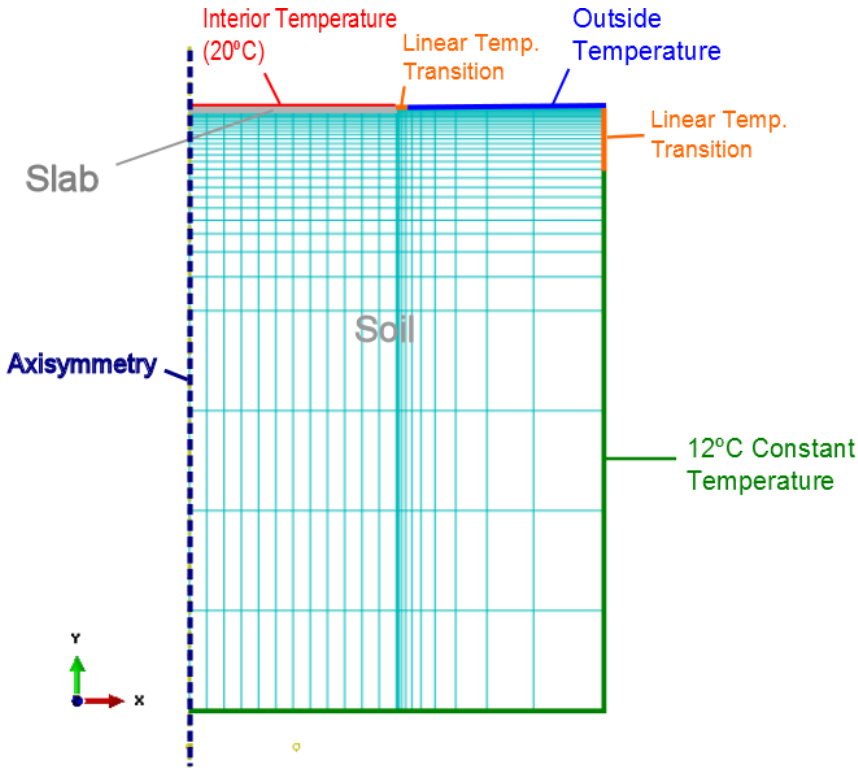


**Figure 5-15. 30m Slab numerical model: mesh and thermal boundary conditions.**

The model runs in two steps: an initial step where the initial temperature of all elements as well as the bottom and right side thermal boundary conditions are applied (Figure 5-15 in dark green), followed by a heat transfer step where the temperature of the slab and ground surface are applied. In order to avoid numerical difficulties due to the definition of two different temperature magnitudes at the same node, a

linear temperature transition is defined across a length of 0.5 m next to the slab edge, where the interior temperature linearly grows/decreases until it matches the outside temperature. The same principle of temperature linear transition was also applied at the right corner of the model across a length of 10m where the outside temperature linearly increases/decreases until it reaches 12°C.

### 5.3.2 Analysis Methodologies and Objectives

As previously mentioned, the aim of this model is to determine temperature levels at the ground surface (beneath the slab) and to assess how these are affected by heat flows coming from the building interior and from the outside. To do so, a steady state thermal analysis was carried for three different outside temperatures (0°C, 12°C and 25°C) which aim to recreate usual outdoor temperatures for Winter, Spring and Summer respectively and for the two different slab radii (15 m and 30 m). The upper surface of the slab is maintained at a constant temperature of 20°C.

### 5.3.3 Results and Discussion

Figures 5-16 and 5-17 illustrate temperature fields of the model at a steady state, for the outside temperatures of 0°C and 25°C respectively and for the case of the 30 m slab. Note that only the top half of the model is represented in these figures since we are only interested in the temperature field below the slab.

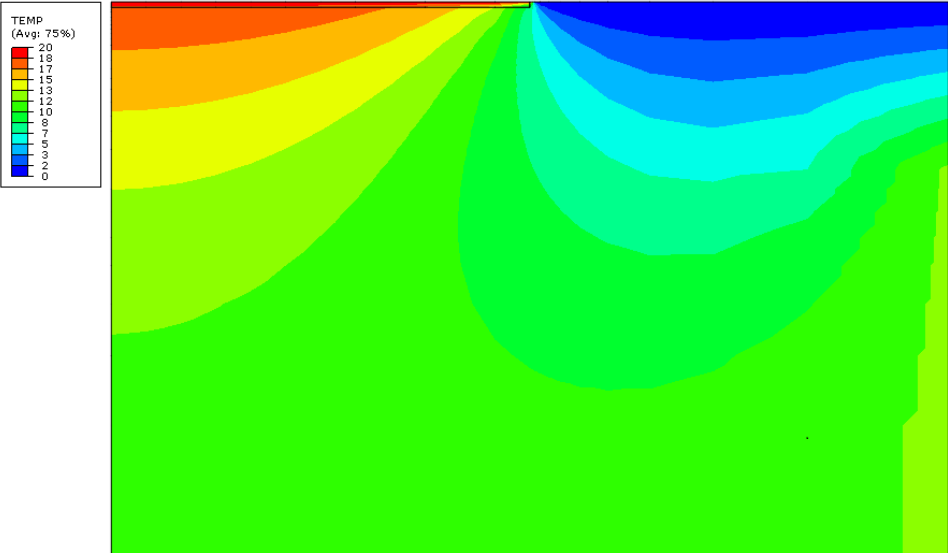
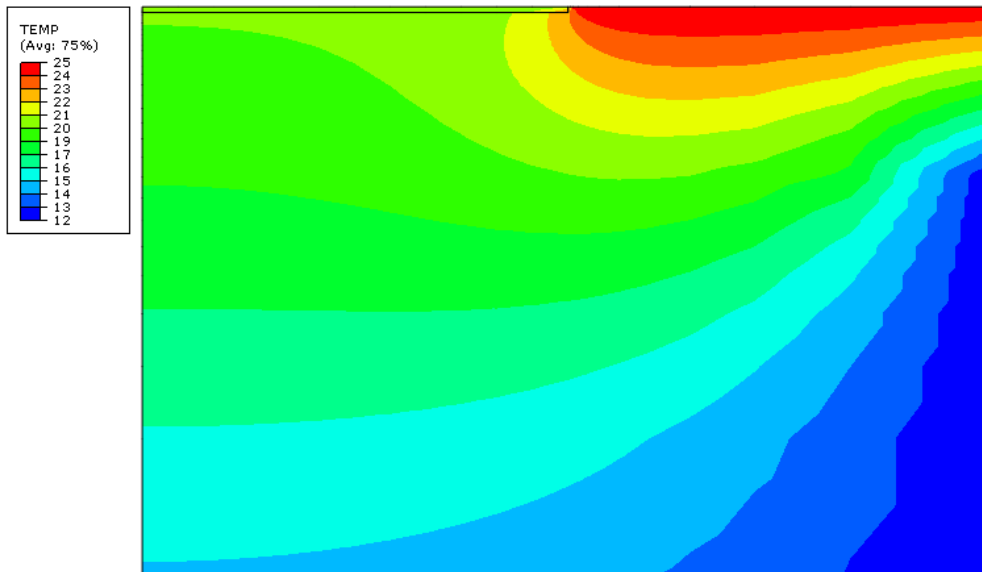


Figure 5-16. 30 m Slab model temperature field for an outside temperature of 0°C.



**Figure 5-17. 30 m Slab model temperature field for an outside temperature of 25°C.**

The model was able to recreate the expected behaviours. When outdoor temperatures were inferior to those indoors, the soil temperature below the slab lowers. This effect is naturally more significant the closer we are to the edge of the slab where heat fluxes due to the low outside temperature are higher. A similar behaviour was observed when the outside temperature was set at a higher value than the interior temperature, leading to an increase in the soil temperature below the slab. The effects of the outside temperature over the ground temperature were naturally more significant for the 15 m slab than for the 30 m slab model.

From Figure 5-16, it can clearly be seen the interaction between both the outside and the interior temperatures over the soil. The temperature of the soil beneath the slab is higher than in the remaining parts of the model as the heat flowing from the inside of the building opposes the heat flowing from the outside which can be seen in the temperature contours.

Figures 5-18 and 5-19 show the horizontal temperature profiles at a depth of 0.4 m (below the slab) for the 15 m and 30 m radius slabs respectively and for three different outside temperatures (25°C, 12°C and 0°C).

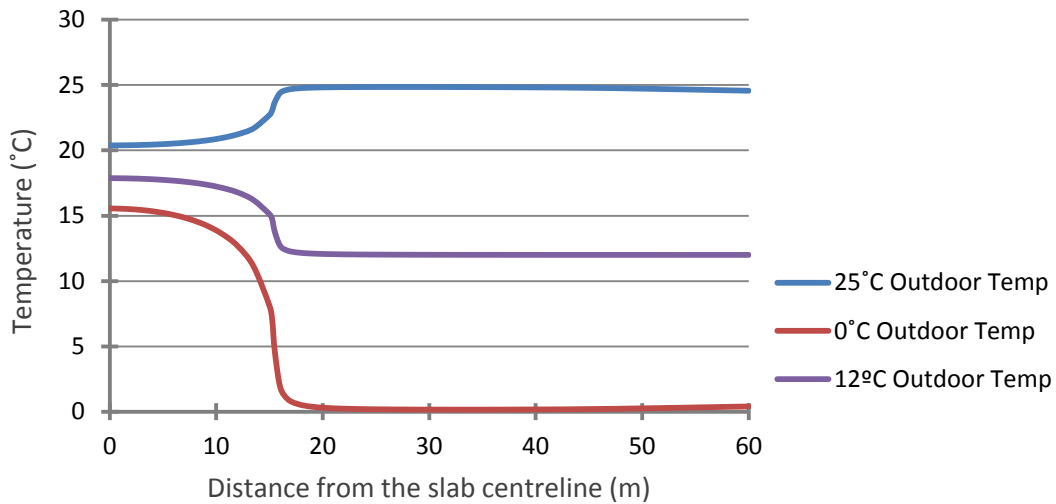


**Figure 5-18. Horizontal temperature profile below the 15m slab.**

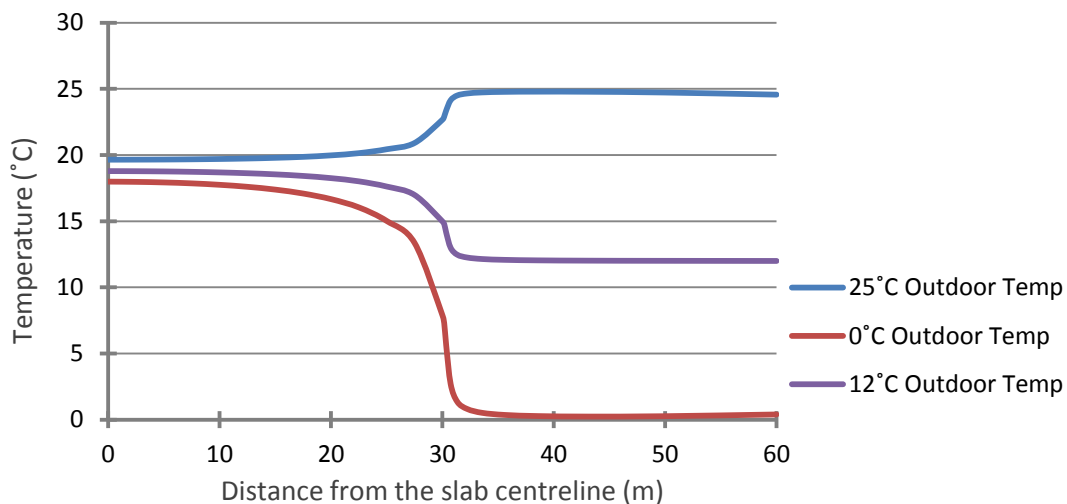


**Figure 5-19. Horizontal temperature profile below the 30m slab.**

For the 15 m slab case (Figure 5-18), results showed that for an outside temperature of 0°C (winter case) the ground surface temperature below the slab averaged 15.2°C over the first 7.5 m which then exponentially lowers as we get closer to its edge. When the outside temperature was set to 25°C (summer case) the same temperature value was 20.4°C but increasing as we get closer to the slab's edge. When the outside temperature was 12°C an intermediate case between the two previously described was verified.

Regarding the 30 m slab case (Figure 5-19), results showed for that for an outside temperature of 0°C (winter case) the ground surface temperature below the slab averaged 17.8°C over the first 15 m which then exponentially lowers as we get closer to its edge. When the outside temperature was set to 25°C (summer case) the same temperature value was 19.7°C which increases as we get closer to the slab's edge.

According to the results illustrated in Figures 5-18 and 5-19, and taking into consideration that a steady state analysis corresponds to an extreme case, we can conclude that the ground surface temperature below the central zone of a building constructed according to current European regulations for thermal insulation will be approximately that of the building's interior decreased by 2 to 5°C during winter or increased by 0 to 1°C during summer, depending on the dimensions of the building, the exact outdoor temperature and proximity to the building edge. It can also be concluded that larger buildings will be less affected in terms of temperature change beneath their ground floor slabs by the outside temperature, when compared to smaller buildings since the soil itself acts as thermal insulation to heat flowing from the building exterior.

Following these results and taking into consideration the model with the 30 m slab which is believed to better represent the large building dimensions where thermal active piled foundations are usually applied, a top temperature boundary condition of 18°C will be used as the base case for the thermal-mechanical model described in Section 6.2, the rather extreme values of 12°C and 24°C will also be tested. This range of ground surface temperatures is believed to cover all the possible ground surface temperatures that can be expected below the ground slab of any modern building. In effect, by simulating the temperature below the ground slab with a constant magnitude, the modelling that follows assumes that the pile is under the centre of a building of sufficient extent that heat flow from the building is essentially one-dimensional and that seasonal effects can be neglected.

It is also important to mention that in reality, steady state conditions are unlikely to develop given the seasonal nature of outdoor temperatures. Thomas & Rees (1999) present observations from a building that was monitored which showed that the effect of seasonal temperature fluctuations on ground temperatures are mainly seen only in the first few metres around the edges of the building.



# **Chapter 6**

## **Thermal-Mechanical Analyses**

In this chapter, the results of a series of thermal-mechanical numerical analyses of a thermo-active pile are presented and discussed.

## 6.1 Introduction

The thermal analysis performed in the previous section was of great importance to better understand the problem of a heat exchanger pile from a purely thermal point of view. It was also helpful to determine how certain modelling aspects such as the heating of the pile will affect the observed temperature fields and if those results correspond to what is observed in reality.

In this section, the mechanical aspect of the problem was also taken into consideration, in order to investigate how the thermal load affects the mechanical behaviour of the pile. Many of the conclusions and findings of the previous thermal analysis will be taken into consideration in the development of the thermal-mechanical model in this section. The impact of some thermal characteristics such as ground surface temperature over the mechanical response of the pile will also be further investigated.

The following aspects of the thermo-active pile problem were the objective of study in this section:

- The influence of the ground surface temperature;
- The effect of differing relative values for the concrete and the soil coefficient of thermal expansion;
- The influence of the pile length and therefore the length to diameter ratio.

In order to investigate these aspects, a thermal-mechanical numerical model of the thermally-activated pile problem was developed using the finite element software Abaqus. This model was used to run a series of steady state thermal-mechanical analyses whose results are reported and discussed.

## 6.2 Numerical Model Implementation

The axisymmetric thermal model previously developed in Section 5.2.1 (Figure 5-2) was adopted but was subject to some changes as the inclusion of the mechanical and thermal-mechanical effects added a lot of complexity to the problem. These changes and the overall characteristics of the thermal-mechanical model are discussed in the following sections.

### 6.2.1 Materials and material behaviour

Two materials were defined, concrete and soil. The same thermal properties used in the baseline thermal analysis were adopted (Table 5-1) while the mechanical and thermal-mechanical properties are indicated in Table 6-1.

The concrete linear coefficient of thermal expansion was assumed as  $1.0\text{E-}5$  m/m/K, according to data published in Tatro (2006) who reports values of concrete CTE between  $0.76\text{E-}5$  m/m/K and  $1.36\text{E-}5$  m/m/K, depending on the aggregate type used in its production. Although a soil linear coefficient of

thermal expansion of 2E-5 m/m/K was adopted for the baseline analysis, values of 0.5E-5 m/m/K and 4E-5 m/m/K were also tested. As previously discussed in section 3.2.2, these three values can be related to a lightly overconsolidated (OC), moderately OC and a heavily OC soil respectively. According to Cekerevac and Laloui (2004), soil thermal expansion will increase with an increase in its OCR, and highly OC soils can show a coefficient of thermal expansion several times higher than concrete.

Concrete was modelled as a purely elastic material while the soil was modelled as an elastic-perfectly plastic material with a Tresca failure criteria:  $\frac{1}{2}(\sigma_1 - \sigma_2) \leq \tau_u$ , where  $\sigma_1$  and  $\sigma_2$  are the principal stresses and  $\tau_u$  is the maximum shearing resistance of the soil. Plasticity was included in the soil model in order to assess if the thermal load in combination with the design mechanical load were enough to induce soil plasticity

	Soil	Concrete
Young Modulus, E (MPa)	30	30 000
Poisson's Coefficient, $\nu$	0.3	0.3
Maximum shearing resistance, $\tau_u$ (kPa)	75	-
Linear coefficient of thermal expansion, $\alpha$ (m/m/K)	2E-5	1E-5

**Table 6-1. Soil and concrete mechanical and thermal-mechanical properties.**

## 6.2.2 Geometry, Mesh, Boundary Conditions and Initial Conditions

### 6.2.2.1 Geometry and Finite Element Mesh

The geometry of the thermal-mechanical model remains identical to that of the thermal model described in Section 5.2.1. The pile in the baseline analysis has a diameter of 1 m and length of 30 m; piles of the same diameter but with lengths of 15 m and 45 m were also tested as one of the parameter variations.

The bottom and side boundaries of the model were set at a distance of 90 m (3L) and 60 m (2L) respectively. These boundary distances were proposed by Cruz Silva, 2012, who modelled a thermo-active pile with the same geometry using the software ADINA. These boundary distances were also tested using Abaqus and were found adequate to ensure the boundaries did not affect the pile response significantly.

With the addition of mechanical behaviour to the model, the mesh previously developed for the axisymmetric thermal model had to be reworked. In order to obtain adequate results, the thermal-mechanical analysis demanded thinner elements than a purely thermal analysis, especially those elements close to the pile which are responsible for dictating the development of its base and shear

resistance. Therefore, the mesh was refined, especially at the pile-soil interface and close to the pile. A total of 3569 heat transfer four node elements were created for the baseline model (30 m long pile) (Figure 6-1). The final mesh size was achieved through an iterative process, where the element size was decreased up to a final state where any further decrease would not produce significant changes in the result. Naturally, some mesh reworking was necessary when the pile length was changed to 15 m and 45 m but its overall geometry and element density remained the same.

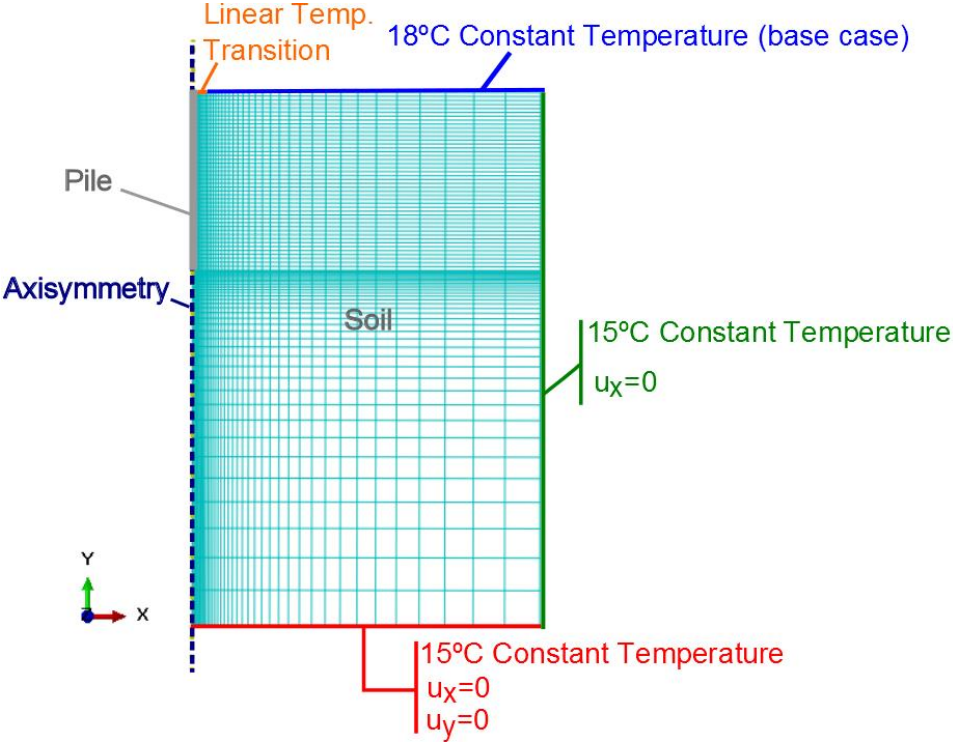


**Figure 6-1. Mesh and boundary conditions of the thermal-mechanical model for the baseline analysis.**

**6.2.2.2 Initial Conditions**

Initial vertical stresses corresponding to both the weight of soil and concrete were applied to all the elements of the model. The coefficient of lateral stress, K, was set to 1 meaning that the initial horizontal stresses were considered equal to the vertical ones. All the elements of the model also have an initial temperature of 15°C. This is an idealization of what will happen in reality; as illustrated in Figure 2-1, the temperature profile in the uppermost part of the soil profile will vary due to the actual climatic conditions at the surface. For these analyses the simplification was made to reduce the number of variables being considered.

**6.2.2.3 Boundary Conditions**

Following the results reported in Section 5.3, the thermal boundary condition on the top surface of the model was set to a constant temperature of 18°C for the baseline analysis. This was considered another key parameter for the study and values of 12°C and 24°C were also considered as one of the parameter

variations.

The bottom and right hand side thermal boundary conditions of the model were set to a constant temperature of 15°C. While in the thermal model a value of 12°C was used for these boundaries, it was decided to increase it to 15°C in the thermal-mechanical model so the results are somewhat comparable to those reported by Bodas Freitas et al., 2013 who also used a value of 15°C for these boundaries. According to Figure 2-1, the soil temperature after a depth of 10 m to 15 m will be situated in between 12°C to 15°C in most European regions, so either of these values is acceptable.

Following the conclusions of Section 5.2.1, where full body heating and edge heating were found to produce similar temperature fields at a steady state, and since the aim of the model was to recreate a thermal pile whose absorber pipes are placed close to its edges (Figure 5-1 (a)), the heating of the pile was simulated by applying an increase of 30°C to all the elements making up the pile (full body heating). While most of the analysis discussed in this thesis will only feature pile heating, a thermal cooling load of -15°C will also be tested. Since the heating thermal load will rise the pile temperature to 45°C while the ground surface will remain at 18°C in the baseline analysis, a linear temperature decrease from 45°C to 18°C at the ground surface next to the pile head was defined across a length of 0.5 m (Figure 6-1 in orange). The same principle of pile-soil linear temperature transition was also applied when the ground surface temperature was set to 12°C and 24°C. If this transition is not defined, calculation problems were expected due to the definition of two very different temperature magnitudes at the same node. Note that a temperature transition was not necessary to be defined at the upper right corner of the model as the temperature difference between right BC and ground surface BC is much lower and any small imprecision in the calculation of the temperature field in this zone will not affect the response of the pile.

Regarding the mechanical boundary conditions, the right boundary of the model is fixed in the horizontal direction while the bottom boundary is fixed in both directions. The left boundary of the model corresponds to the axis of symmetry.

Both thermal and mechanical boundary conditions are illustrated in Figure 6-1.

### 6.2.3 Pile-Soil Interface Behaviour

Initially, a perfectly rough pile-soil interface was assumed. However, this interface makes slippage between the pile and the soil impossible as the interface of both these bodies is “tied” together.

It was then decided to simulate pile-soil interface behaviour by the addition of a layer of zero-thickness interface elements whose tangential behaviour is modelled with an elastic-perfectly plastic constitutive model (Figure 6-2). The interface elements mobilize shear resistance depending on the relative displacement (slip) between the solid elements representing the soil and those representing the concrete; in this case, reaching a maximum shearing resistance of 75 kPa for a total slip of 0.0015 m (0.15%d).

The slip is measured as the vertical distance between nodes which initially, before any load is applied, are connected (slip = zero). The amount of relative displacement required to fully mobilize the interface resistance is not an intrinsic property and will depend on both the soil and the pile surface properties.

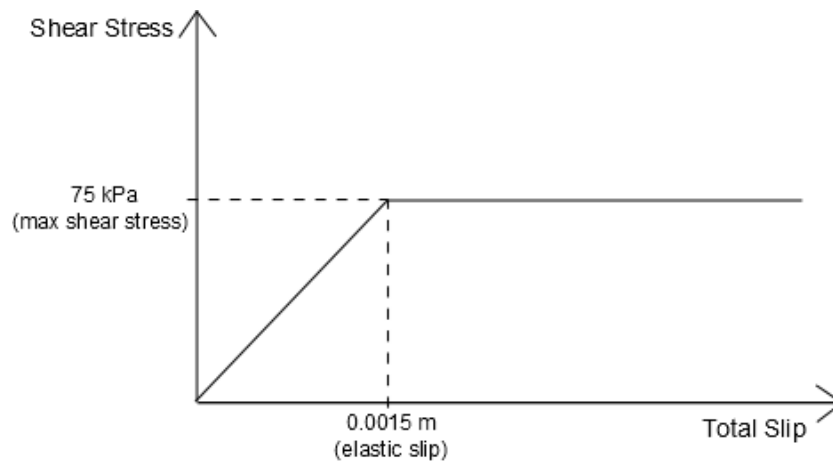


**Figure 6-2. Interface elements constitutive model: total slip versus shear stress.**

## 6.2.4 Model Validation

Unlike an elastic model, there are no analytical or numerical solutions available for the evaluation and comparison of the bearing capacity of a pile in an elastic-plastic medium. In this study, model validation was done through the analysis of the pile load-settlement curve in order to access if the model behaves coherently and as expected.

The pile was loaded incrementally through the imposition of a settlement at its head and the predicted load-settlement curve is plotted in Figure 6-3. The load was measured as the average axial stress at the top four nodes of the pile, which constitute the pile head. The mobilized interface shear stress for four different settlement values is plotted in Figure 6-4.

Two different pile behaviour phases can clearly be seen in Figure 6-3. Initially the pile has a stiffer behaviour as it mobilizes mostly lateral resistance. During this initial phase the load-settlement curve is approximately linear as both the soil and the interface are in an elastic state. At a settlement of about 18 mm, the pile lateral shearing resistance is fully mobilized which can be seen in Figure 6-3. Further loading will then lead to a different behaviour as only base resistance remains to be mobilized and therefore any load increment will lead to large settlement as the base resistance of the pile only accounts for about 10% of the total pile resistance. This “two phase behaviour” is generally seen in real load tests performed on piles placed in stiff clays, which work mainly through the mobilization of lateral shearing resistance. At 400 mm settlement (40%*d*), the pile reached an ultimate load of 9.8 MPa (about 7.7 MN).

The pile-soil interface behaved as intended reaching a maximum shearing resistance of 75 kPa which was obtained at a pile head settlement of about 18 mm. This means that for a settlement of 18mm the soil nodes at the pile-soil interface averaged a vertical deformation of about 16.5 mm (91.7% of the applied settlement) and the slip between the pile and soil was 1.5 mm, this being the maximum elastic slip defined for the interface behaviour (see Figure 6-2).

Some perturbation of the interface shear stress profile (Figure 6-4) can be seen at the pile’s foot due to

soil movement and deformation in this zone.

The pile reached a total base resistance of 651 kN which given a  $\tau_u$  value of 75 kPa results in a bearing capacity factor,  $N_c$ , of 11 which is an acceptable value for a stiff clay.

Given these results, it can be concluded that the model is capable of modelling the mechanical behaviour of a friction pile and produces sensible results.

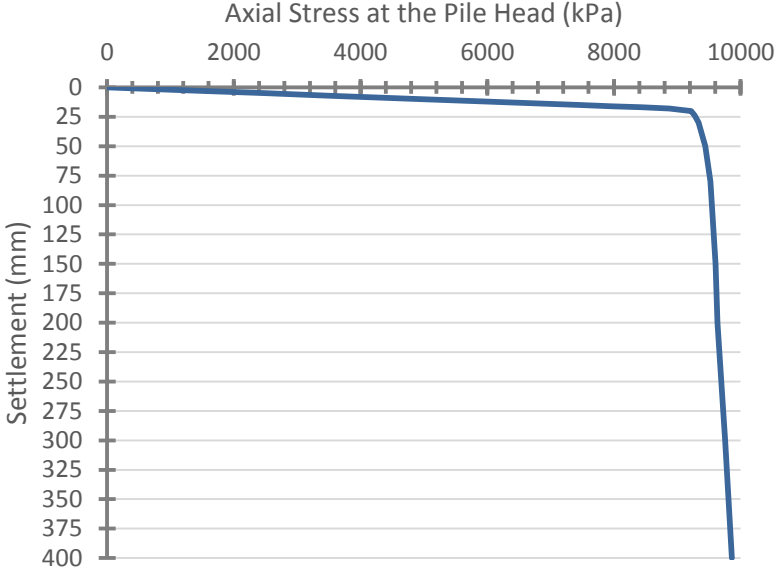


Figure 6-3. Pile load-settlement curve.

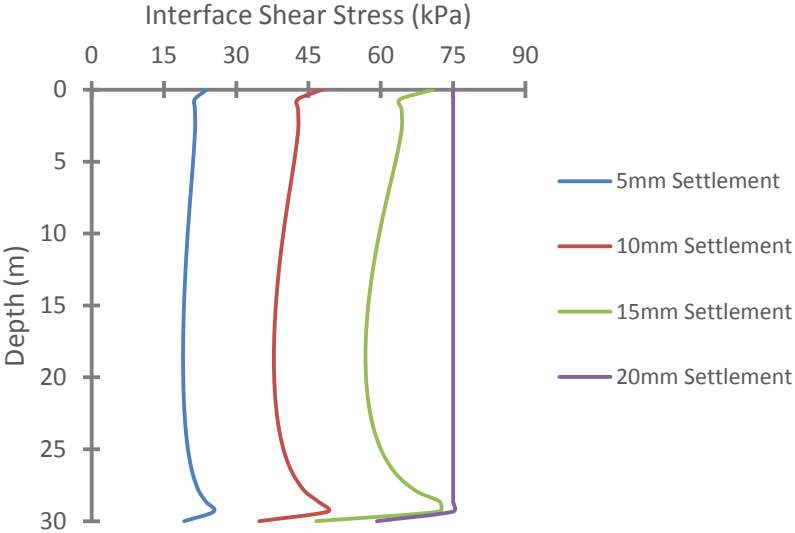


Figure 6-4. Mobilized pile-soil interface shear stress.

### 6.3 Analysis Methodology and Objectives

As previously mentioned, the aim of the thermal-mechanical analysis is to assess the influence of the following aspects on the thermal-mechanical behaviour of the pile: the ground surface temperature boundary condition of the model; the ratio between pile length and diameter; the ratio between soil and concrete thermal expansion values.

Regarding the ground surface thermal boundary condition, three different temperatures were considered: 12°C; 18°C and 24°C. This range of values covers the temperature levels that can be expected at the ground surface below a building.

Concerning the soil and concrete coefficient of thermal expansion values, three situations were considered:

1. Soil half as thermally expansive as the concrete;
2. Soil two times more thermally expansive than concrete;
3. Soil four times more thermally expansive than concrete.

As previously mentioned, these three situations aim to simulate a lightly overconsolidated (OC), moderately OC and heavily OC soil respectively. The coefficient of thermal expansion is a very important parameter to analyse as a wide range of soil thermal expansion values can be seen in reality, depending on the soil mineralogical and grading properties as well as consolidation levels. Bodas Freitas et al. (2013) and Cruz Silva (2012) highlighted the likely importance of this parameter in the thermal-mechanical behaviour of piles.

While the pile diameter is always 1 m, three different pile lengths were also considered (15 m, 30 m and 45 m), i.e. L/d ratios in the range of 15 to 45 which cover the values usually adopted for piles.

A total of 27 analyses were undertaken which correspond to all the possible combinations of the parameters summarised above and in Table 6-2, where the central column (in green) represents the parameter set used in what is considered to be the baseline analysis.

Top Thermal Boundary Condition	12°C	18°C	24°C
Soil and Concrete CTE, m/m/K	$\alpha_c = 1E^{-5}$ ; $\alpha_s = 0.5E^{-5}$ (concrete 2 times more expansive than soil)	$\alpha_c = 1E^{-5}$ ; $\alpha_s = 2E^{-5}$ (soil 2 times more expansive than concrete)	$\alpha_c = 1E^{-5}$ ; $\alpha_s = 4E^{-5}$ (soil 4 times more expansive than concrete)
Pile length-diameter ratio, L/d	15 (pile 15m)	30 (pile 30m)	45 (pile 45m)

**Table 6-2. Parameter changes applied to the model.**



The thermal-mechanical analysis is run in three steps (geostatic, static and temperature-displacement) and at a steady state. The three steps are performed in sequence where the results of one step become the initial conditions of the following one. After the analysis is complete, not only the results of the final step are available but also the results of the previous ones. Each of the three steps has the following purpose:

1. **Geostatic Step:** The geostatic step is the initial step for most geotechnical studies performed in Abaqus. In this step, the initial stresses corresponding to the weight of both the pile and the soil are applied to the model. An initial temperature of 15°C is also applied to all elements of the model. In the geostatic step, Abaqus checks if the introduced stresses are in equilibrium and if all the elements remain at an elastic state or not.

2. **Static Step:** In the static step the mechanical load is applied to the pile;

The mechanical load on the pile is applied as a uniform pressure at its head. A uniform pressure load was preferred to a settlement load since the pile head must be able to move freely when the thermal load is applied. Specifying a fixed displacement would not allow the pile head to freely deform and would greatly affect the development of the thermally induced stresses.

The applied mechanical load value was calculated as the design load of the pile according to the European regulation for geotechnical design (NP EN 1997-1). To obtain the design resistance, the partial coefficients for resistance ( $\gamma_b = 1.6$ ;  $\gamma_s = 1.3$ ) and the correlation factor ( $\xi_3 = \xi_4 = 1.4$ ) were applied to both the shaft and the base resistances of the pile.

Regarding the base case (30 m pile), the calculated ultimate shaft resistance was 7069 kN and the ultimate base resistance was 651 kN. By applying the appropriate partial factors from NP EN 1997-1 to these values a pile design compression resistance of 4175 kN is obtained. Given the pile diameter of 1 m, this translates into a uniform pressure of about 5.3 MPa. The same methodology was applied in order to determine the mechanical load applied to both the 15 m and 45 m piles which resulted in uniform pressures of 2.8 MPa and 7.8 MPa respectively.

3. **Temperature-Displacement Step:** In this last step the thermal load is applied to the pile.

The thermal load is applied as a “full body heat” (Figure 5-3 (a)), where the temperature of all the pile elements was uniformly raised to 45°C from the initial temperature of 15°C ( $\Delta T = +30^\circ\text{C}$ ). While an increase of 30°C in the pile temperature is somewhat of an extreme value, field tests performed in the past showed that it can happen in hot summers when the cooling demand is very high. This value was chosen as we wanted to assess the maximum effect due to the thermal load that we can expect in a thermally activated pile. The effect of a cooling thermal load ( $\Delta T = -15^\circ\text{C}$ ) was also tested, however, in order not to excessively increase the number of analyses performed, the parameter study discussed in Section 6.4.2 considers only a heating thermal load.

## 6.4 Results and Discussion

### 6.4.1 Baseline Analysis

As previously mentioned, the baseline analysis or base case corresponds to a 30 m long pile, an 18°C top thermal boundary condition and a soil with a coefficient of thermal expansion ( $2E-5$  m/m/K) twice that of the concrete ( $1E-5$  m/m/K).

#### 6.4.1.1 Baseline Analysis: Heating

Axial normal stresses in the pile, Figure 6-5 (a), and the pile-soil interface shear stresses, Figure 6-5 (b), show the effect of the mechanical load only, the thermal load only (temperature increase of 30°C) and the combined effect of both these loads. Note that in Abaqus, positive axial stress values mean tensile stress while negative values mean compressive stress.

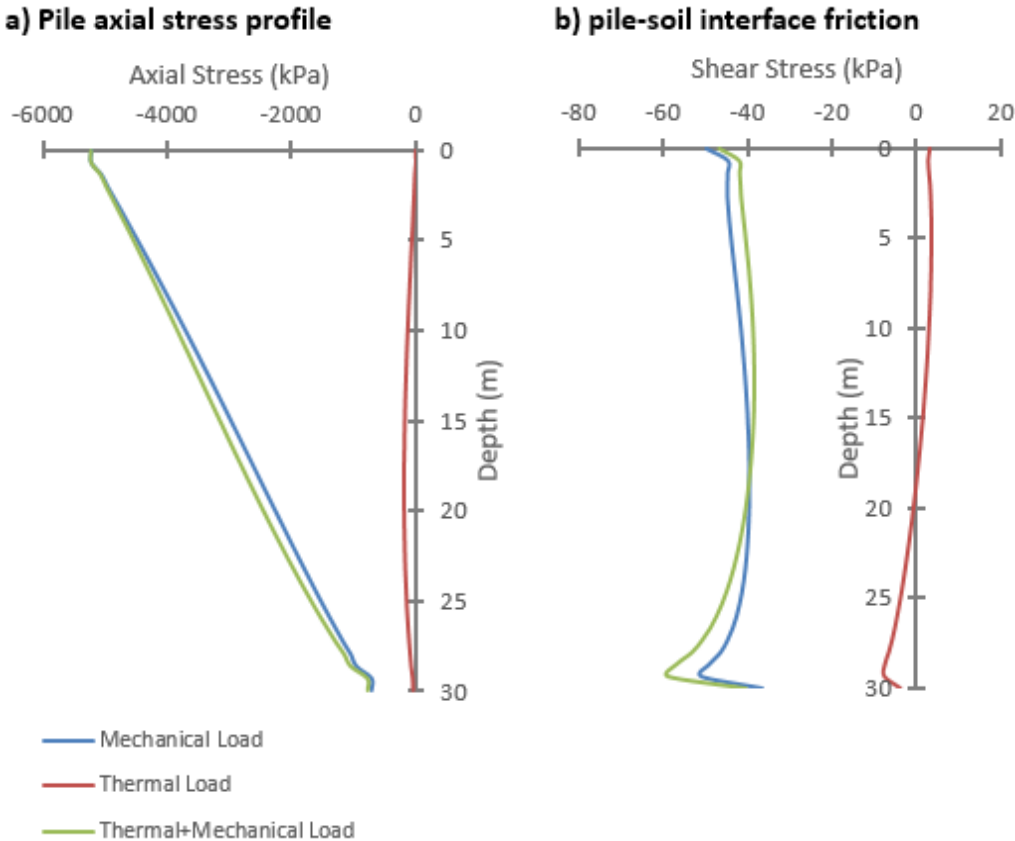


Figure 6-5. Stresses in the pile and in the pile-soil interface.

Similar behaviours to those described in Section 4.1 were verified. The thermal load increased the axial compressive load in the pile. The maximum thermally induced axial stress was 182.2 kPa and occurred at a depth of 18.7 m which corresponds to the point where the strain restraint was highest. If the pile was symmetrically restrained this point would be located at 15 m depth (middle of the pile) however, in

this case, the lower half of the pile presents higher restraint than the upper half due to the presence of the soil at the pile base while the pile head is free to move. For this reason, it is expected that the point of maximum strain restraint will be located closer to the base which was indeed verified in the results.

The interface shear stress profile due to the thermal load (Figure 6-5 (b)) was also as expected. By inducing relative motion between pile and soil, the thermal load led to a reduction of shear stress above a depth of 18.7 m due to the pile expanding upwards and an increase of shear stress below this depth due to the pile expanding downwards. Naturally, the thermal load induced an equilibrated shear stress profile with a null value at the 18.7 m section which corresponds to the section of maximum strain restraint.

Figure 6-6 shows the effect of the mechanical load only, the thermal load only and the combined effect of both these loads in terms of pile vertical displacements. As expected, the mechanical and thermal load induced opposite effects. While the mechanical load induces a downwards movement in the pile leading to a settlement of -10.5 mm at the pile head, the thermal load makes the pile and soil expand and induces an upwards movement returning the pile head almost to the initial position by inducing a vertical displacement of 9.1 mm, i.e. a resultant settlement of -1.4 mm. Notably, the displacement at the base of the pile is virtually unchanged however when other parameter combinations were evaluated (see Section 6.4.2 below) this was found to be a consequence of the parameter set being considered in this particular case. According to Equations 4-1 and 4-2, if no restraint is applied in the pile, the maximum length change it can experience due to a thermal load of +30°C is 9mm. In the baseline analysis case the pile length change due to the thermal load was 8.7 mm, meaning that the restraint applied to the pile by the soil is very low which explains the low magnitude of the thermally induced stresses observed in Figure 6-6 (about 2% of the stress change implied by perfect restraint (Equation 4-3)).

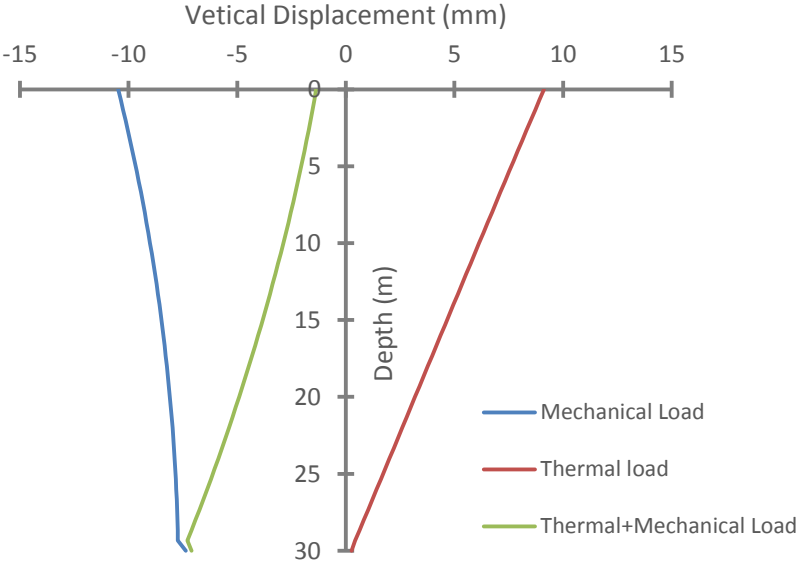


**Figure 6-6. Pile vertical displacement.**

While a “standard” thermal pile behaviour was observed for the baseline case, in reality the thermally induced stresses are highly dependent on the relationship between pile and soil coefficients of thermal expansion as well as the temperature field in the ground, as will be verified and discussed in the following sections.

**6.4.1.2 Baseline Analysis: Cooling**

If thermal piles are used for heating a building instead of cooling, their temperature will reduce. In this section the effects of a cooling thermal load ( $\Delta T = -15^\circ\text{C}$ ) are discussed and compared to the effects of the heating thermal load previously analysed.

The effect of the heating and cooling thermal loads on the pile axial stress and pile-soil interface shear stress are shown in Figure 6-7 (a) and Figure 6-7 (b) respectively.

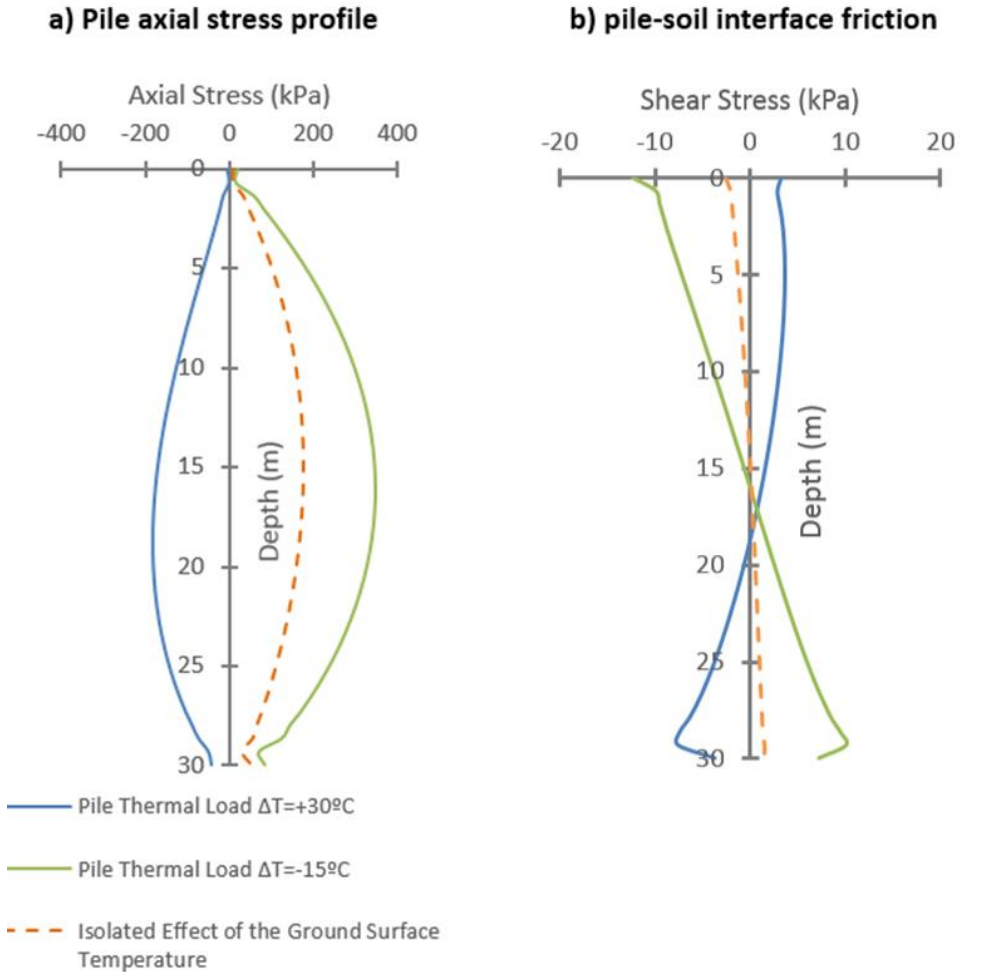


**Figure 6-7. Thermally induced stresses (heating and cooling thermal loads).**

As expected, when the pile was cooled ( $\Delta T = -15^\circ\text{C}$ ) an opposite behaviour to the one previously described for the heating thermal load ( $\Delta T = +30^\circ\text{C}$ ) was verified. As the pile is cooled it will tend to

contract, however, due to the restraint imposed in the pile by the soil, this contraction will be partially prevented leading to the development of tensile stresses on the pile. For the case of  $\Delta T = +30^\circ\text{C}$ , it can be seen that the point of maximum restraint, which is the point of maximum axial stress, occurs at a greater depth than for the case of  $\Delta T = -15^\circ\text{C}$ , this phenomena is believed to be caused by a reduction of the foot restraint. When the pile is cooled, the soil will also be cooled and tend to contract instead of expand which is believed to lead to reduced restraint at the pile foot. Because the foot restraint reduces the pile becomes more symmetrically restrained and the section of maximum strain restraint will get closer to the middle of the pile.

While intuitively it would be expected that the thermally induced stresses in the pile would be proportional to the thermal load, in fact, the results show that cooling apparently led to higher stress changes, even though the temperature change was half that used for heating. This behaviour is related to the influence of the ground surface temperature and to the fact that the soil is more thermally expansive than concrete. In order to better explain these effects, a supplementary analysis was undertaken whereby only the surface temperature was applied to the model (orange dashed line in Figure 6-7). In this supplementary analysis, the change in axial stress was tensile with a value of about 180 kPa which is due to the warming of the surface from the initial value of  $15^\circ\text{C}$  to  $18^\circ\text{C}$  and the associated soil expansion relative to that of the pile. Now, when the change in axial stress due to the change in pile temperature is re-examined, the change due to heating of  $+30^\circ\text{C}$  is approximately twice that of cooling by  $-15^\circ\text{C}$ . It is also interesting to note that for the set of parameters used in this analysis, the thermal induced stresses in the pile due to the sole increase in the ground surface temperature by  $3^\circ\text{C}$  were of the same magnitude as those induced by a pile heating of  $30^\circ\text{C}$ . The effect of the relationship between soil and concrete thermal expansion values and the ground surface temperature over the thermally induced stresses in the pile is further studied in Sections 6.4.2.1 and 6.4.2.2 respectively.

Note that the effect of the surface temperature has not been decoupled as it was considered that the two forms of thermal loading are likely to occur more-or-less simultaneously, i.e. the building will come to some long-term temperature equilibrium at the same time that the foundation piles are being used for heating and cooling. It is interesting to note however that the effect on the pile response due to the surface temperature alone is of a similar magnitude to that seen for the temperature changes applied to the pile.

In order to not excessively increase the number of numerical analyses performed in the parameter study presented in Section 6.4.2, the pile was only subjected to heating ( $\Delta T = +30^\circ\text{C}$ ) and cooling was not considered.

## 6.4.2 Parameter Study

### 6.4.2.1 *Soil and concrete coefficient of thermal expansion*

Figure 6-8 (a) and (b) illustrate the axial stress and interface shear stress changes developed due to the heating thermal load ( $\Delta T = +30^\circ\text{C}$ ) for the three combinations of soil and concrete thermal expansion

values previously detailed. All the remaining model parameters remained the same as in the baseline analysis.

These figures clearly show the influence of the relative values of the concrete and soil thermal expansion coefficients with respect to the changes in axial stress and shear stress during thermal loading, confirming the results reported by Bodas Freitas et al, (2013). In fact, this relationship is responsible for dictating not only the magnitude of the thermally induced stresses but also their direction.

When soil is half as thermally expansive as concrete (blue lines in Figure 6-8) similar behaviour to what was previously described in the heating baseline analysis (Section 6.4.1.1) was observed, however the magnitude of the developed stresses was considerably higher. This happens because the soil has a lower tendency to expand; the relative movement between the soil and the pile is greater and therefore the change in shear stress in the interface is larger. This results in greater restraint of the pile and consequently, the development of larger magnitude thermally induced axial stress.

When the soil is four times more expansive than concrete, the pile goes into tension. In this case, because the soil is considerably more thermally expansive than concrete, it will expand more than the pile, which leads to the development of tensile stresses.

When the soil is two times more expansive than concrete (the base case), we are in a situation in between the two previously described. As the soil is more expansive than the concrete, tensile stresses would be expected in response to heating, this doesn't happen because the pile is at a higher temperature than the soil. For the combination of parameters used in this case, the resultant effect is for the pile to expand slightly more than the soil does and the two effects, soil and pile expansion, end up opposing each other and resulting in low magnitude thermally induced compressive stresses.

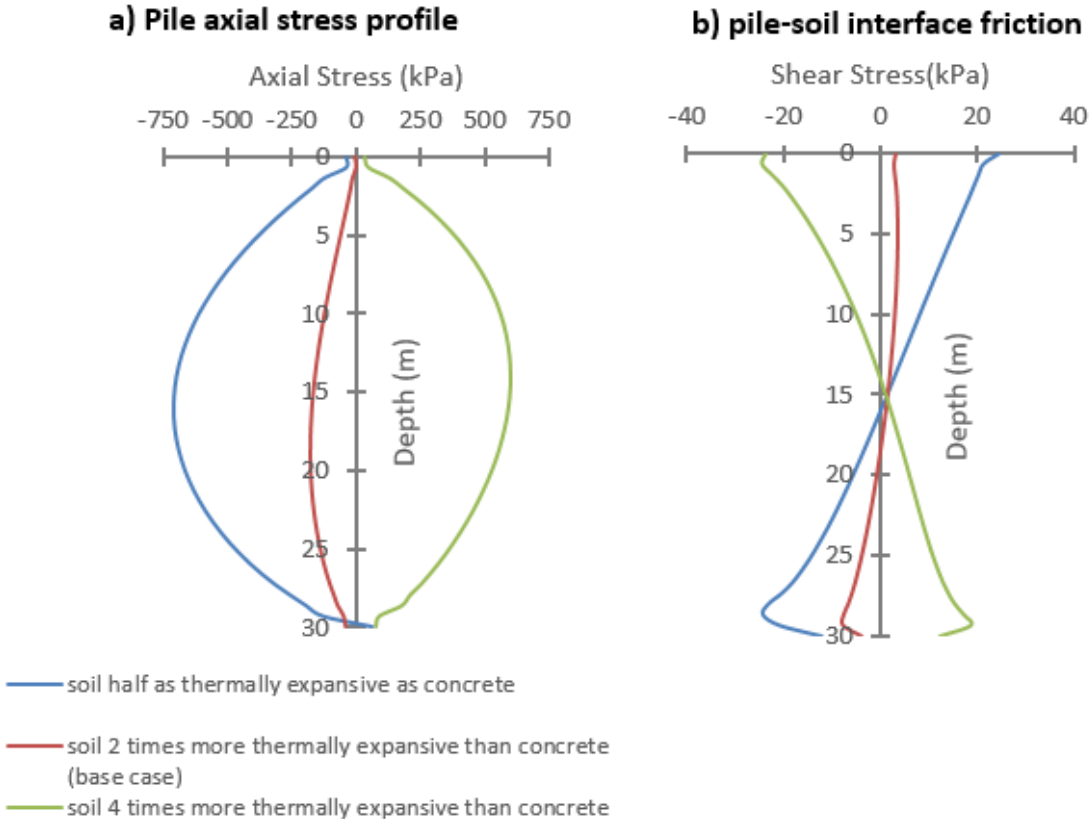


**Figure 6-8. Thermally induced stresses for three cases of soil and concrete thermal expansion values.**

The change in pile vertical displacements due to the thermal load is plotted in Figure 6-9. It can be seen that as we increase the coefficient of thermal expansion of the soil, the more the pile moves upwards due to the thermal load. This is due to the added increase in volume the soil experiences which “pushes” the pile upwards. Comparing the results from the cases when the soil is 2 times and 4 times more expansive than concrete, it can also be seen that the pile is also slightly stretched due to the high tensile stresses the soil imposes over it. In fact, according to Equations 4-1 and 4-2, if the effect of soil expansion is ignored, the maximum length change the pile can experience due to a thermal load of +30°C is 9mm, while for the case when the soil was 4 times more thermally expansive than concrete, this length change was 9.4mm, proving the stretching effect the soil has over the pile.

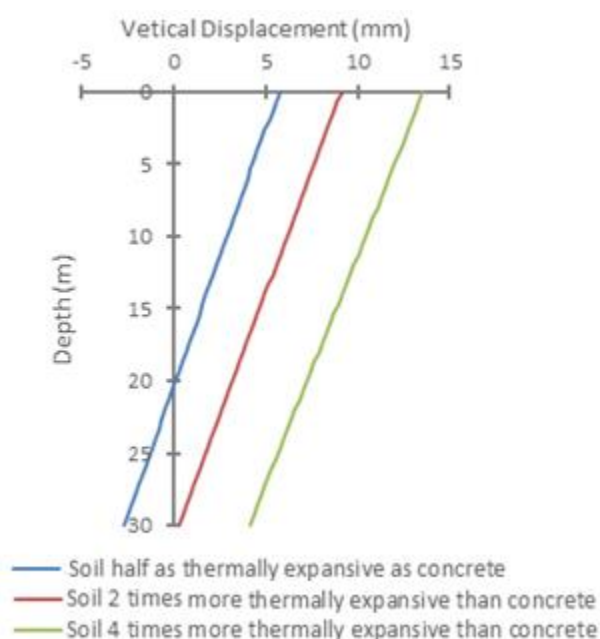


**Figure 6-9. Thermally induced vertical displacements in the pile for three cases of soil and concrete thermal expansion values.**

#### 6.4.2.2 Ground Surface Temperature

Figures 6-10 (a) and (b) illustrate the thermally induced stresses in the pile and interface for three different ground surface temperature boundary conditions: 12°C; 18°C (base case) and 24°C. These boundary conditions aim to recreate the range of ground surface temperature that can be expected below a building’s ground slab. Naturally, these boundary conditions will have a great effect over the soil temperature field especially in the upper part of the model and therefore affect how much it will try to expand or contract, and how it will interact with the pile.

Because all the elements forming the pile are heated to a constant temperature of 45°C, a change in the ground surface thermal boundary condition will only affect the temperature of the soil and therefore

how much it expands or contracts. Besides the ground surface temperature, all the other model parameters remained the same as in the baseline analysis.

Figures 6-10 (a) and (b) show a clear influence of ground surface temperature over both the magnitude and direction of the thermally induced stresses in the pile. In comparison to the base case (red line), an increase in ground surface temperature changed the thermally induced axial stresses from compressive to tensile and the direction of the interface shear stresses. To understand this behaviour it is important to remember that in this analysis, the soil is twice as thermally expansive as the pile; therefore, any increase in temperature will lead to a significant expansion of the soil. By increasing the ground surface temperature, we also increase the average temperature of the soil mass beneath it, which will lead to expansion and the development of tensile stresses in the pile, as the soil will expand more than the pile.

The opposite phenomenon happens when we decrease the ground surface temperature. Reducing the temperature of the soil below the initial state will lead to contraction and the development of larger compressive stresses in the pile. In this case, even though the pile is less expansive than the soil, because it is subjected to considerably higher temperatures it will still show a tendency to expand more than the soil which will lead to compressive thermally induced stresses.

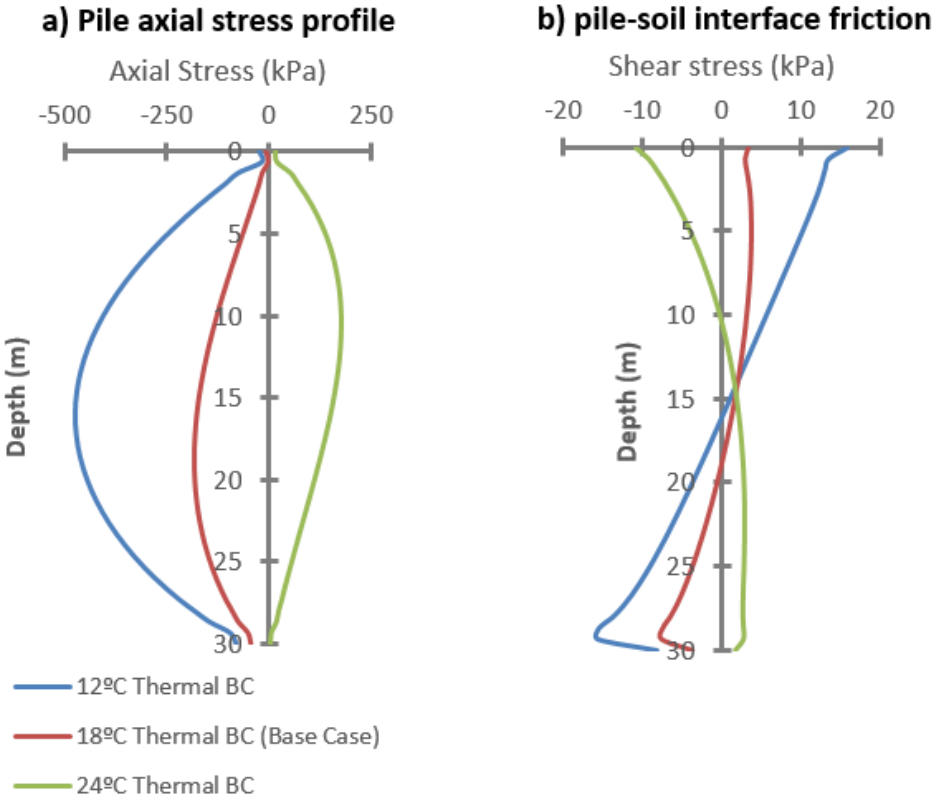


**Figure 6-10. Thermally induced stresses for three different ground surface temperatures.**

The change in pile vertical displacements due to the ground surface temperature is plotted in Figure 6-11. From this figure it can be seen that as we increase the ground surface temperature the more pile moves upwards. This behaviour is due to the added soil expansion, especially at the upper part of the model, caused by an increase in the ground surface temperature. As the soil tends to expand against the pile, it will induce tension in the pile and lift it. For instance, for the case of a 24°C thermal BC, the



pile total length change due to the thermal load was 9.1mm, while Equations 4-1 and 4-2, which don't take into consideration the effect of the soil expansion, predict a maximum pile length change of 9mm.

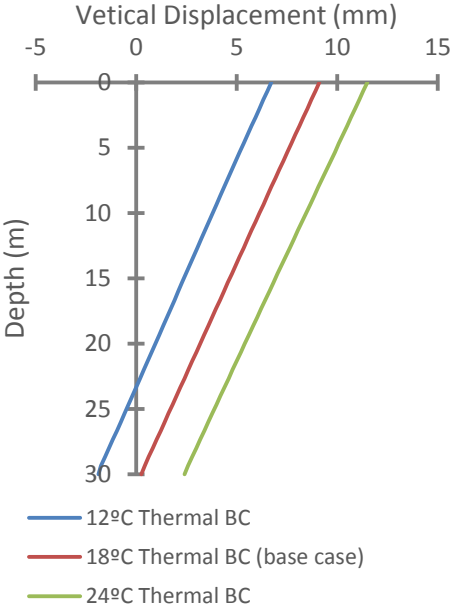


**Figure 6-11. Thermally induced vertical displacements for three different ground surface temperatures.**

**6.4.2.3 Pile diameter-length ratio**

Figures 6-12 (a) and (b) illustrate the thermally induced stresses in the pile and pile-soil interface for three different pile lengths: 15 m; 30 m (base case) and 45 m. The pile diameter is 1 m for the three cases, the soil is two times more expansive than concrete, and all the remaining model parameters are those of the baseline analysis.

While a change in the pile length didn't induce any behaviour changes in the pile, i.e. the resultant effect was compressive thermally induced stresses in all three cases, the magnitude of the developed stresses was clearly affected by this change as the longer the pile (larger the ratio, L/d), the larger were the mobilized pile axial normal stresses and the pile-soil interface shear stresses (Figures 6-12(a) and (b)). Two phenomena are believed to be the cause of this increase in thermally induced stresses:

1. The main cause derives from the fact that the longer the pile is, the more it will expand or contract when subjected to a temperature change and therefore the higher the shear stresses mobilized at the pile-soil interface will be. This mobilization of shear stress will induce strain restraint in the pile and thermally induced stresses are directly proportional to the amount of strain restraint (Equation 4-3). If the soil and the interface remain elastic, the increase in thermally induced stress due to the increase in strain restraint with pile length is believed to be a linear effect.
2. A second cause of this behaviour, while perhaps less important than that described above, is the variation of the soil temperature field with depth. In fact, in the baseline analysis, the top boundary

of the model is kept at 18°C while the bottom at 15°C, This means that temperature field around the 15 m pile will be generally warmer than that of say the 45 m pile and therefore, in the former case, the effect of the temperature change in the pile on the soil temperature will be less. If the temperature change is less, then the relative movement on the pile-soil interface will be smaller leading to lower changes in shear stress and pile restraint.

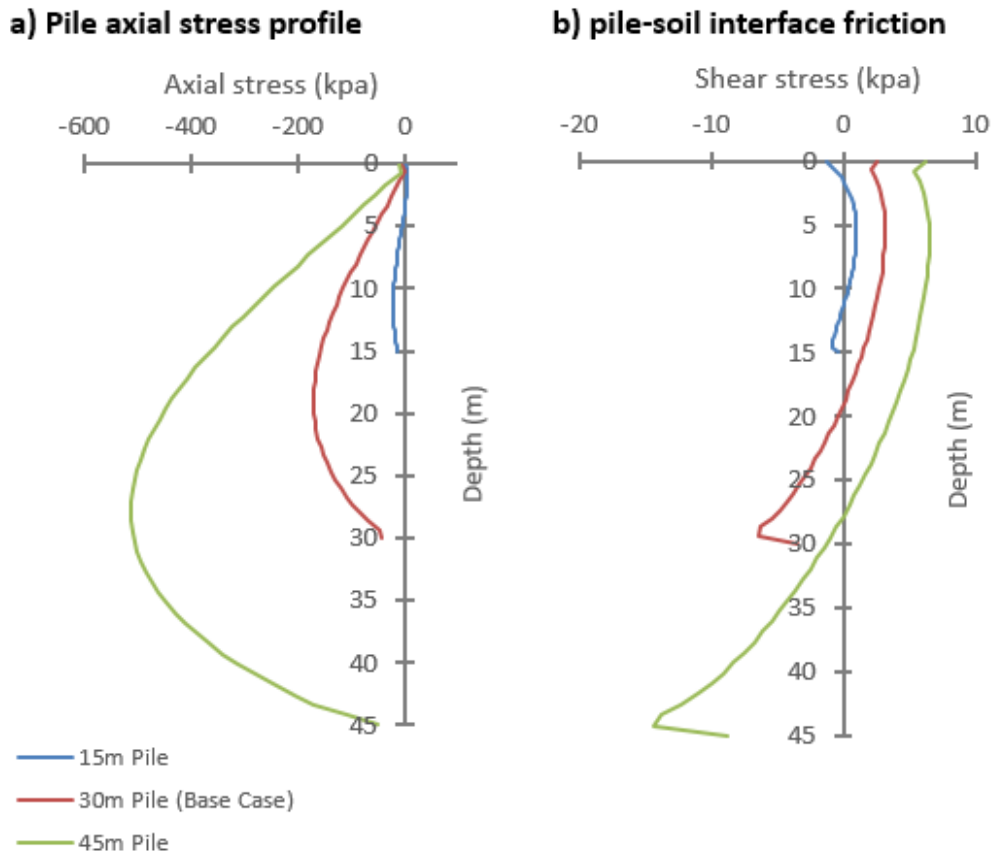


Figure 6-12. Thermally induced stresses for three different pile lengths.

#### 6.4.2.4 Result summary and interaction between the studied parameters

Figures 6-13, 6-14 and 6-15 illustrate the maximum thermally induced axial load in the pile as a function of the ground surface temperature for the three pile lengths and the three ratios of soil to concrete coefficients of thermal expansion previously considered. Each figure corresponds to a fixed pile length (15 m, 30 m and 45 m). As noted previously, in these figures, positive axial load values represent tensile stress and negative values, compressive stress.

These figures show a strong influence of the ground surface temperature over the thermally induced axial load on the pile, as previously assessed in Section 6.4.2.2. A clear connection between this influence and the relationship between soil and concrete coefficients of thermal expansion can be seen. In fact, the effect of the ground surface temperature will greatly increase with an increase of the coefficient of thermal expansion of the soil and the thermally induced stresses will become increasingly tensile. This behaviour can be explained as the higher the soil coefficient of thermal expansion is, the

more it will tend to expand relative to the pile for the same temperature change and therefore the more tensile the stresses it will induce.

As discussed in Section 6.4.2.3, the longer the pile, the higher the thermally induced stresses will be due to the increase in the pile restraint.

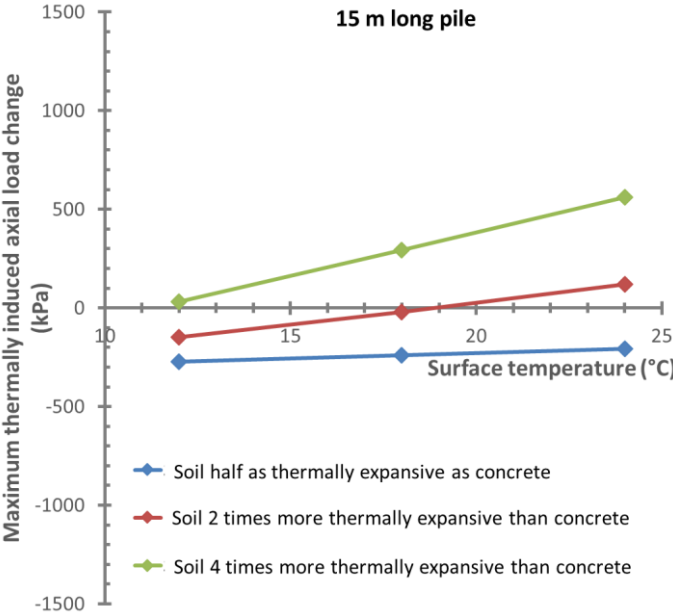


**Figure 6-13. Maximum thermally induced axial stress in the pile as a function of the ground surface temperature (15m pile).**

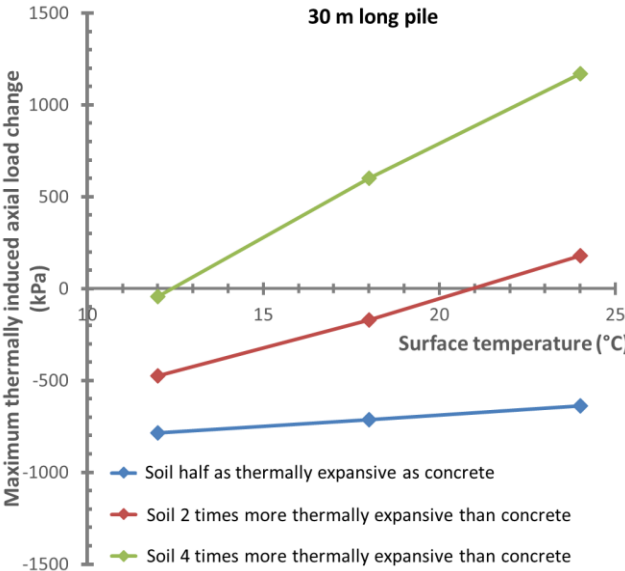


**Figure 6-14. Maximum thermally induced axial stress in the pile as a function of the ground surface temperature (30m pile).**

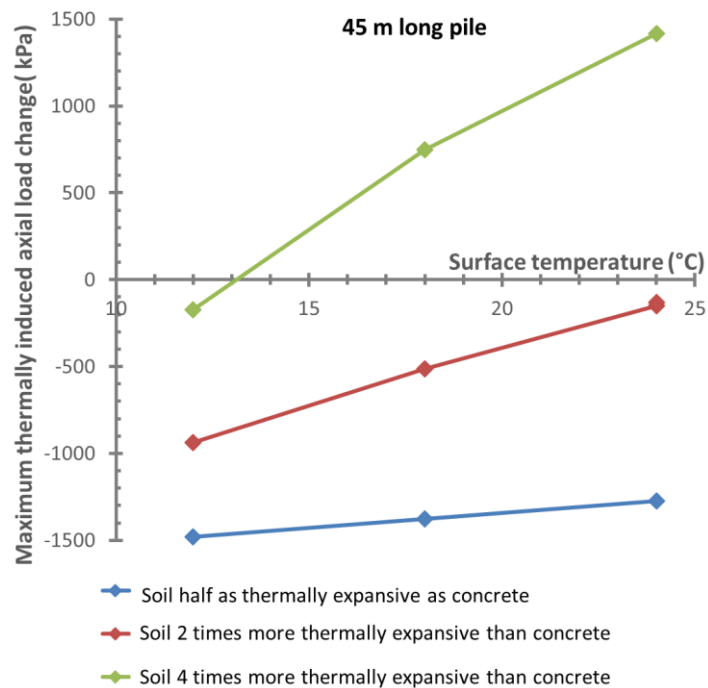


**Figure 6-15. Maximum thermally induced axial stress in the pile as a function of the ground surface temperature (45m pile).**

The same data set is re-visualised in Figures 6-16, 6-17 and 6-18 however in this case each figure corresponds to a fixed value of the ratio between the soil and concrete coefficient of thermal expansion. Once again, positive axial load values represent tensile stress while negative values compressive stress.

When the soil is less thermally expansive than concrete (Figure 6-16), the ground surface temperature has a minimal impact over the thermally induced stresses in a pile of a particular length, and the stress changes are always compressive. Since in this case the concrete is more expansive than soil and since the pile will be at a higher temperature than the soil independently of the ground surface temperature adopted, it is natural that a variation of the ground surface temperature won't induce significant change as the pile will always expand considerably more than the soil. However, as we increase the soil' coefficient of thermal expansion (Figures 6-17 and 6-18), the ground surface temperature becomes increasingly important and thermally induced stresses become increasingly tensile.

When the soil is two times more expansive than the concrete (Figure 6-17), this complex and interesting interaction between pile and soil can clearly be seen. In this case, even though the soil coefficient of thermal expansion is higher than the concrete, for the low ground surface temperatures we still verify compressive stresses because the pile temperature is considerably higher than that of the soil, and the pile will expand more than the soil does. However, as we increase the ground surface temperature and therefore the soil temperature, this behaviour starts to reverse and the compressive stresses start reducing and eventually, the thermally induced stresses on the pile become tensile. The surface temperature at which this transition occurs can be seen to vary with the pile length.

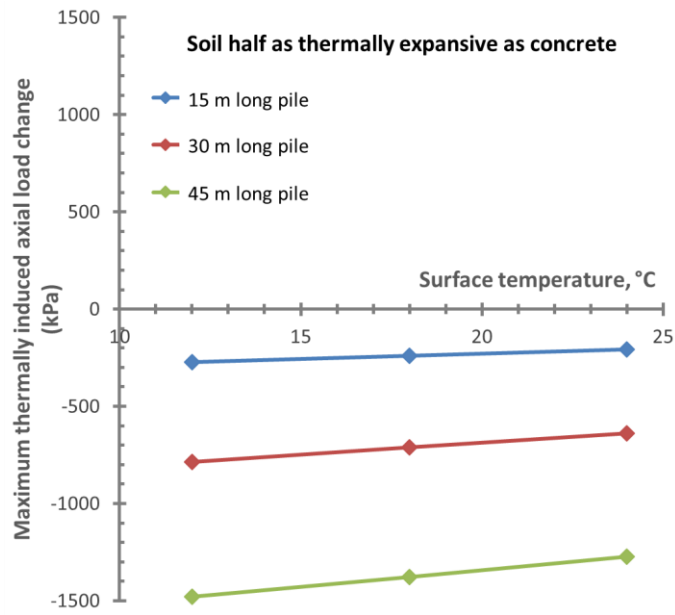


**Figure 6-16. Maximum thermally induced axial stress in the pile as a function of the ground surface temperature (soil half as thermally expansive as concrete).**

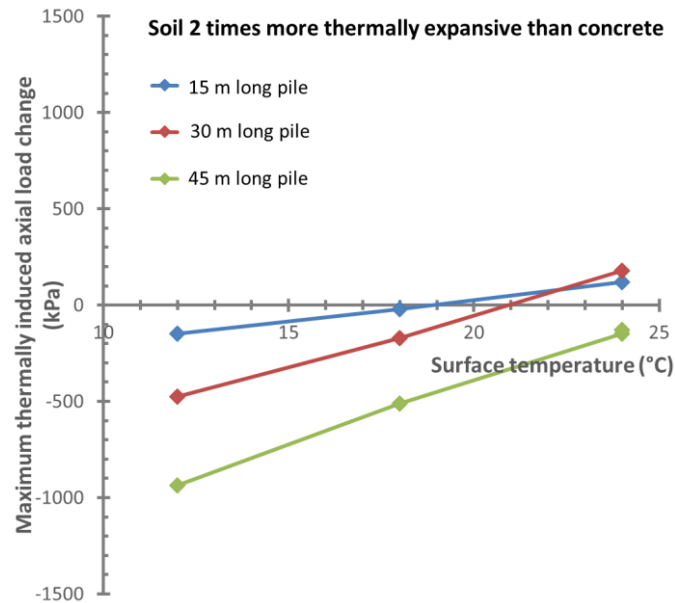


**Figure 6-17. Maximum thermally induced axial stress in the pile as a function of the ground surface temperature (soil two times more thermally expansive than concrete).**

When the soil is four times more expansive than the concrete (Figure 6-18), the soil tendency to expand will always surpass that of the concrete if the ground surface temperature is 13°C or higher. In this case, thermally induced compressive stresses will only develop in the pile for very low ground surface temperatures (<12°C), which is when the pile will start expanding more than the soil.

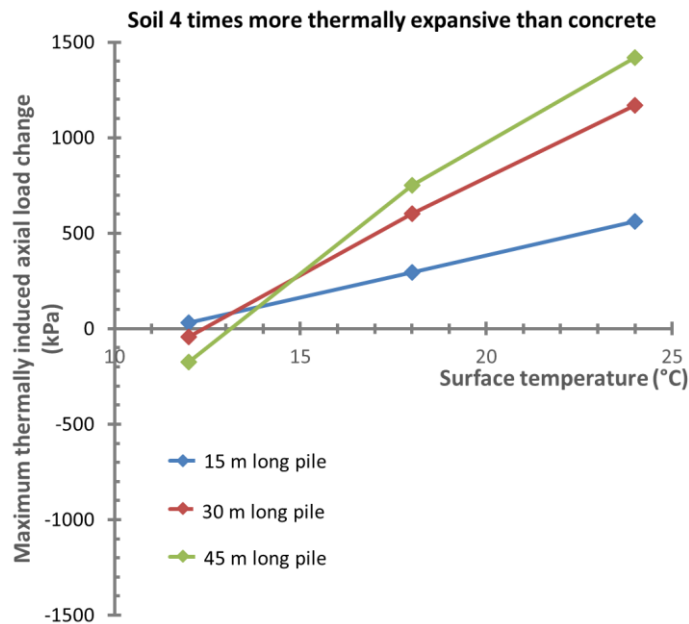


**Figure 6-18. Maximum thermally induced axial stress in the pile as a function of the ground surface temperature (soil four times more thermally expansive than concrete).**

Figure 6-19 shows the same data set redrawn yet again with the thermally induced axial stresses expressed as a function of the ratio between soil and concrete coefficient of thermal expansion ( $\alpha_{\text{soil}}$  and  $\alpha_{\text{conc}}$ ) and for a pile length of 30 m. Once again, the significant influence of the ground surface temperature over the thermally developed stresses is clearly seen. However and as expected, these lines converge to the same value for the case of a soil with a coefficient of thermal expansion of zero. In fact, when the soil coefficient of thermal expansion is zero, a change of the ground surface temperature won't produce any effect because the soil becomes "immune" in terms of volumetric changes to any thermal load and the pile temperature is unaffected by the ground surface temperature as it was modelled to heat uniformly to 45°C and to remain at this temperature.

When the ratio of soil to concrete coefficient of thermal expansion is equal to zero, the maximum thermally induced axial stress in the 30 m pile in Figure 6-22 is about 900 kN; in the 15 m long pile it was about 300 kN and the 45 m pile, 1600 kN. In relation to the length of the pile, the thermally induced stress in the pile when the ratio of soil to concrete coefficient of thermal expansion is equal to zero, is approximately linear.

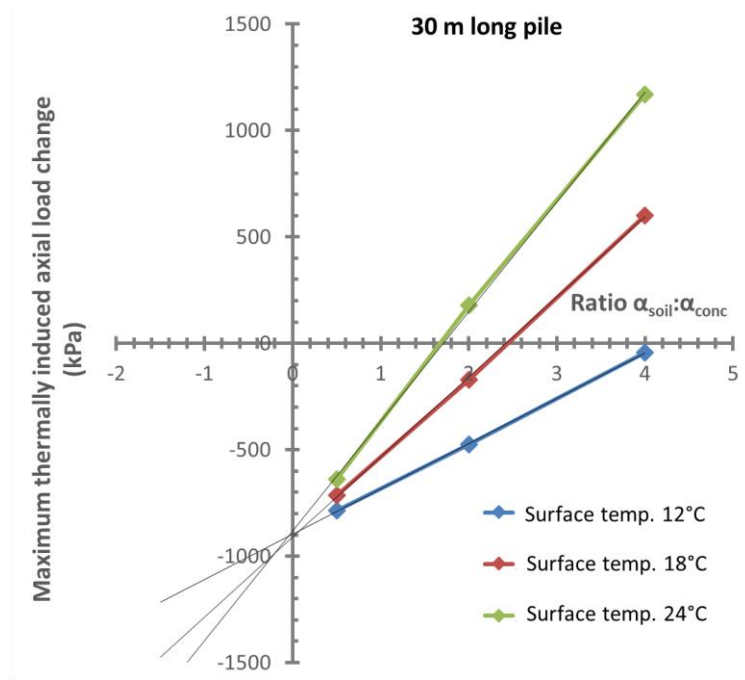


Figure 6-19. Maximum thermally induced axial stress on the pile as a function of the ratio between soil and concrete thermal expansion coefficients (30m Pile).





# **Chapter 7**

## **Conclusions**

The current thesis intended to analyse in a systematic way the thermal-mechanical behaviour of thermo-active piles. Thermal and thermal-mechanical numerical analyses were conducted whose main results and conclusions are summarized in this chapter.

## 7.1 Conclusions and Results Summary

Thermal and thermal-mechanical numerical analyses of a thermally activated pile were performed in this thesis using the finite element software Abaqus. It is believed that these analyses produced important and interesting results which will definitely contribute to improving our current knowledge regarding the thermal-mechanical behaviour of energy foundations. Some of the reported findings may also help in the future development of numerical models as a number of simulation hypotheses and simplifications were studied in order to investigate their legitimacy.

Regarding the thermal analysis, the most significant results were the following:

- At a steady state, full body and edge heating produced similar temperature fields; however those obtained from centreline heating showed considerably lower temperatures especially at the pile-soil interface (Figure 5-6). Consequently, if the energy pile being simulated has its heat exchange pipes placed close to the centreline, full body heating or edge heating are not appropriate and centreline heating should be adopted.
- The pipe layout and ring heating produced similar temperature fields at a steady state; however a transient analysis showed that the temperature fields differed considerably during the first weeks of heating (Figure 5-14). If a transient analysis of an energy pile is required, it is recommended that the pipe layout is modelled.
- The ground surface temperature below the central zone of a building constructed according to current European regulations for thermal insulation will be approximately that of the building's interior decreased by 2 to 5°C during winter or increased by 0 to 1°C during summer, depending on the dimensions of the building, the exact outdoor temperature and proximity to the building edge. As thermally activated piles are generally placed beneath the building, these results can be used to determine an approximate value for the ground surface temperature which can be applied to a numerical simulation.

Regarding the thermal-mechanical analysis, the most significant results were the following:

- The relative values of the coefficient of thermal expansion for the soil and the concrete play a key role in dictating the direction and the magnitudes of the developed stresses in a pile subjected to thermal loading. Results showed that even for the same thermal load, this ratio can dictate if the thermally induced stresses in the pile will be compressive or tensile.
- If the soil is more thermally expansive than concrete, the ground surface temperature has a very important influence over the thermally induced stresses developed in the pile. This effect was however considerably less significant if the concrete is more expansive than soil. It is therefore

recommended that numerical simulations of energy piles pay close attention to the correct definition of the ground surface temperature.

- For the same pile diameter, the longer the pile, the larger the thermally induced stresses will be. This phenomenon is believed to be caused mainly by the increased shear stress mobilized at the pile-soil interface which increases restraint on the pile. To a lesser extent, the variation of the ground temperature with depth may also affect the development of thermally induced stresses for piles with different lengths, especially when soil presents a higher thermal expansion coefficient than concrete.

## 7.2 Future Developments

Following the thermal mechanical analysis performed in this thesis, it was determined that the relationship between the coefficient of thermal expansion of concrete and soil has a vital influence over the observed thermal-mechanical behaviour of an energy pile. While a homogenous soil was admitted in this study, in reality, soils are generally heterogeneous and different soil layers, whose thermal-mechanical properties are not the same, can usually be identified in most construction sites. Therefore, it would be important to run a similar study as the one presented in this thesis but where two or more different soil layers are modelled and whose coefficients of thermal expansion, in particular, vary. This change is expected to produce considerable changes in the thermally induced stresses in the pile which will be the result of the complex interaction between the soil layers and the pile. The understanding of this interaction would be an important step in achieving a complete understanding of the effects of the thermal load over a foundation pile.

While an isolated thermo-active pile was considered in this thesis, in reality, a number of piles are required to effectively heat/cool a building and therefore these piles are usually placed in groups. The addition of one or more piles to the model will lead to changes in its temperature field which, as discussed in this thesis, will lead to significant stress changes in the piles, especially if the soil is more thermally expansive than concrete. It would be of great interest to assess how significant these stress changes would be in order to better understand if the thermo-active pile problem can be studied from a single pile perspective or if the modelling of the pile group is required.

Other possible developments to the analyses discussed in this thesis are:

- Studying the behaviour of the thermo-active pile through time by adopting a cyclic thermal load, according to the heating/cooling seasons, instead of a constant temperature increase/decrease. This study will also require a change from a steady state to a transient thermal-mechanical analysis and the development of a 3D pile model with a pipe layout;
- Addressing the influence of the soil and pile-soil interface stiffness to the observed thermal-mechanical response of the pile.



# References

- Amis, T. (2011) Energy foundation in the UK. UK Ground Source Heat Pump Association conference, Ground Source Live, Petersborough ([http://www.gshp.org.uk/Ground\\_Source\\_Live\\_2011.html](http://www.gshp.org.uk/Ground_Source_Live_2011.html)).
- ASHRAE (2009). ASHRAE Handbook—Fundamentals (SI), American Society of Heating, Refrigerating and Air-Conditioning.
- Bodas Freitas, T. M., Cruz Silva, F. and Bourne-Webb, P.J. (2013). The response of energy foundations under thermo-mechanical loading, Accepted for publication in the Proc. 18<sup>th</sup> ICSMFE, Paris, 4 pages.
- Bourne-Webb, P. J., Amatya, B., Soga, K., Amis, T., Davidson, T. & Payne, P. (2009) Energy pile test at Lambeth College, London: geotechnical and thermodynamic aspects of pile response to heat cycles, *Geotechnique*, 59 (3), 237-248.
- Bourne-Webb, P., Amatya, B. & Soga, K. (2013) A framework for understanding energy pile behaviour., *Proceedings of the Institution of Civil Engineers Geotechnical Engineering*.
- Bourne-Webb, P. (2014) A framework for understanding energy pile behaviour. Presented to British Geotechnical Association evening meeting.
- Brandl, H. (2006) Energy foundations and other thermo active ground structures, *Geotechnique*, 56 (2), 81 – 122.
- Baldi G, Hueckel T, Pelegrini R. Thermal volume changes of the mineral-water system in low-porosity clay soils. *Canadian Geotechnical Journal* 1988; 25:807–825.
- Cekerevac C and Laloui L (2004) Experimental study of thermal effects on the mechanical behaviour of a clay. *International Journal for Numerical and Analytical Methods in Geomechanics* 28(3): 209–228.
- Cruz Silva F. 2012. Load-displacement behaviour of thermo-active piles. MSc Thesis, Instituto Superior Técnico, Lisboa, Portugal, 105 pages.
- Di Donna, A., Dupray, F., & Laloui, L. (2013). Effect of thermo-plasticity of soils on the design of energy piles, *Proc. European Geothermal Conference, EGC 2013, Pisa, Italy*, 1-8.
- Eurima, 2011. U-values in Europe. European Insulation Manufacturer Association (<http://www.eurima.org/index.php?page=u-values-in-europe>).
- Farouki, O. T. (1986) *Thermal Properties of Soils*, Series on Rock and Soil Mechanics Volume 11, Trans Tech Publications, Germany.
- Hiraiwa, Y. & Kasubuchi, Y. (2000) Temperature dependence of thermal conductivity of soil over a wide range of temperatures (5-75oC), *European Journal of Soil Science*, 51, 211-218.

- Laloui, L., Nuth, M. & Vulliet, L. (2006) Experimental and numerical investigations of the behaviour of heat exchanger pile, *International Journal for Numerical and Analytical Methods in Geomechanics*, 30, 763-781.
- Loveridge, F. (2012). *The Thermal Performance of Foundation Piles used as Heat Exchangers in Ground Energy Systems*. PhD thesis. University of Southampton, Southampton, United Kingdom, 179 pages.
- Neville, A.M., 1995. *Properties of concrete*, 4th edition. Longman, London.
- Perry, J., Loveridge, F. & Bourne-Webb, P. (2011). Ground Sourced Energy, *Evolution*, Winter 2011, 20-23.
- Powrie, W., & Loveridge, F. (2013). Pile heat exchangers: thermal behaviour and interactions. *Proceedings of the ICE – Geotechnical Engineering*, 166(2), 178-196.
- Rees, S. W., Adjali, M. H., Zhou, Z., Davies, M. & Thomas, H. R. (2000) Ground heat transfer effects on thermal performance of earth contact structures, *Renewable and Sustainable Energy Reviews*, 4, 213-265.
- Rees, S. W., & Thomas, H. R. (2009). Measured and simulated heat transfer to foundation soils. *Géotechnique*, 59(4), 365–375.
- Surayatriyastuti, M., Mroueh, H, and Burlon, S. (2013). Numerical analysis of a thermo-active pile under cyclic thermal loads, *Proc. European Geothermal Conference, EGC 2013, Pisa, Italy*, 1-8.
- Sultan, N., Delage, P. & Cui, Y. J. (2002). Temperature effects on the volume change behaviour of Boom clay. *Engineering Geology* 64, 135-145.
- Tatro S.B., (2006). Thermal properties, in – STP169D Significance of tests and properties of concrete and concrete-making materials, Lamond and Pielert eds., ASTM International, USA, p. 226-237.
- Thomas H. R., Rees S. W. (1999). The thermal performance of ground floor slabs – a full scale in-situ experiment. *Building and Environment* 34 (1999). Pp 139 – 164.